

https://dspace.org/

Towards a safe mining environment: the development of a framework to model and manage the risk of flyrock

Carpenter, Ernest Benjamen Mahoney

2025-08
University of the Witwatersrand, Johannesburg
https://hdl.handle.net/10539/49637
Carpenter, Ernest Benjamen Mahoney. (2025). Towards a safe mining environment: the development of a framework to model and manage the risk of flyrock. [Master's dissertation, University of the Witwatersrand, Johannesburg]. WIReDSpace. https://hdl.handle.net/10539/49637

Downloaded from a DSpace repository. https://dspace.org/

School of Mining Engineering



UNIVERSITY OF THE
WITWATERSRAND,
JOHANNESBURG

TOWARDS A SAFE MINING ENVIRONMENT: THE DEVELOPMENT OF A FRAMEWORK TO MODEL AND MANAGE THE RISK OF FLYROCK

Ernest BM Carpenter

(Student Number: 0510027D)

Supervisors: Ms. Matsobane Nong and Dr. Mpoyi J. Kanda

I declare that this is my own unaided work. It is being submitted to the Faculty of Engineering and the Built Environment, University of the Witwatersrand, in partial fulfilment of the requirements for the degree of Master of Science in Engineering.

Johannesburg, 2025

DECLARATION

I have familiarised myself with the University of the Witwatersrand Student Academic Misconduct Policy (SAMP). I hereby declare that the work I am submitting for assessment is my original work. I affirm that I have not plagiarised, misrepresented, or colluded with any other person or source. I have properly acknowledged, cited, and referenced all the sources that I have used in my work. I also declare that where I have used artificial intelligence (AI) tools it has only been as a means of guidance. The ideas and arguments presented in my work are my original thoughts and interpretations. I acknowledge that any academic misconduct, such as plagiarism or collusion will result in serious consequences. According to the SAMP, these consequences may include a reduced grade, a fail mark, or disciplinary action. The Faculty of Engineering and the University of the Witwatersrand have my consent to investigate any potential academic misconduct in my work. This investigation may include the use of similarity and AI detection software to check the originality of my work. I undertake to abide by the decision of any such investigation.



28/08/2025

Signature of Candidate Date

“If I have seen further, it is by standing on the shoulders of giants”

Sir Isaac Newton, 1675

ABSTRACT

Flyrock incidents at Anglo American Plc operations, as well as across the broader mining industry, have highlighted the significant safety risks associated with flyrock. These incidents pose a serious threat to personnel, while also causing potential damage to equipment and infrastructure. More than half of the observed flyrock exceedances are not reported nor investigated. The underlying issue is not a lack of blasting standards but rather a failure to systematically capture and address flyrock risks throughout the drill and blast process.

To overcome these challenges, this research aimed to develop a framework for modelling, monitoring, measuring, and reporting the risks associated with flyrock occurrences to enhance risk management strategies. The study sought to determine whether the current models used for flyrock prediction are effective in identifying risks and explore techniques for monitoring flyrock occurrences.

To answer the research questions and achieve the aim of the study, historic incident reports, blast videos, and drill and blast data from various Anglo American Plc operations were analysed. Furthermore, the flyrock monitoring strategies currently used at the mines were reviewed to identify shortfalls and areas of improvement through the establishment of guidelines. The study identified gaps in the drill and blast process to assess the risk of flyrock. As a result, the process was ammended so that the risk can be verified and validated at various stages.

The prediction models utilised in commercial drill and blast software were reviewed. The study confirmed that the current predictive model in use at Anglo American Plc operations, sufficiently identified flyrock risk. A flyrock risk reporting dashboard was also developed and implemented as part of the study to proactively raise flyrock risk awareness for every blast.

The occurrence of flyrock is not as a result of ‘pressing the button’ to initiate the blast, but in most cases it is the consequence of a decision or action taken earlier in the drill and blast process and the establishment of the framework will help address the lack of risk awareness of flyrock.

Recommendations out of this study also include amendment of the drill and blast process flow to cater for flyrock prediction modelling at various stages in the process, ultimately using the latest blast hole charging status. It is also recommended for future work to extend this framework to include secondary blasting and cater for fragment rebound distances in the estimations and monitoring.

ACKNOWLEDGMENTS

My wife, Arinda, for her support, encouragement and above all, patience.

TABLE OF CONTENTS

DECLARATION i

ABSTRACT iii

ACKNOWLEDGMENTS v

LIST OF FIGURES ix

LIST OF TABLES xii

LIST OF EQUATIONS xiii

LIST OF ABBREVIATIONS AND SYMBOLS xiv

1 INTRODUCTION 1

1.1 Research Background and Context 1

1.2 Problem Statement 10

1.3 Justification and Significance of the Research 10

1.4 Research Questions 10

1.5 Research Aim and Objectives 11

1.6 Structure of the Research Report 11

2 LITERATURE REVIEW 13

2.1 Introduction 13

2.2 Understanding Flyrock in Surface Mining Operations 13

2.3 Flyrock Framework to Manage Risk 16

2.4 Flyrock Modelling: Past and Present Approaches 18

2.5 Flyrock Modelling: Current Commercial Drill and Blast Applications 21

2.6 Flyrock Modelling: Components of Prediction Methods Used 26

2.7 Flyrock Modelling: Discussion of Reviewed Models Used in the Project 48

2.8 Flyrock Monitoring and Measuring Techniques 49

2.9 Chapter Summary 54

3 RESEARCH METHODS 56

3.1 Introduction 56

3.2 Research Approach 56

3.3 Data Collection 56

3.4 Data Validation Process 59

3.5 Data Analysis Approach 60

3.6 Chapter Summary 68

4 RESULTS AND ANALYSIS 69

4.1 Introduction 69

4.2 Improved Flyrock Footprint Calculation 69

4.3 Data from Video Analysis and Observations 73

4.4 Observed Flyrock Mechanisms and Ranges 78

4.5 Vertical Displacement Factor 79

4.6 Flyrock Exceedances 81

4.7 BlastVision® Trials 87

4.8 Video Capturing Guideline 92

4.9 Chapter Summary 97

5 CONCLUSIONS AND RECOMMENDATIONS 99

5.1 Introduction 99

5.2 Summary of Chapters 99

5.3 Research Observations 99

5.4 Research Contributions 100

5.5 Research Limitations 103

5.6 Recommendations for Future Research Work 104

REFERENCE LIST 108

APPENDIX A. Data for Graph 34 (Flyrock Footprint Calculation)..... 122

APPENDIX B. Data for Graph 35 (Modified Flyrock Footprint Calculation)..... 145

APPENDIX C. Flyrock Calculator..... 169

APPENDIX D. Flyrock Risk Reporting Dashboard 171

LIST OF FIGURES

Figure 1: Global map of Anglo American Plc's operations 1
Figure 2: Anglo American Plc flyrock definition 3
Figure 3: Cumulative number of publications with reference to flyrock in the title 5
Figure 4: Sample gap analysis (reported vs video analysis) 7
Figure 5: Five examples of flyrock incidents reported in study period 8
Figure 6: Importance of flyrock evaluation as part of blast clearance criteria 9
Figure 7: Three key mechanisms for flyrock 14
Figure 8: Flyrock framework components 16
Figure 9: Paradigm flyrock calculator 22
Figure 10: Maptek's BlastLogic process overview 23
Figure 11: BlastLogic's flyrock module 24
Figure 12: BlastLogic's estimation approach for face burst 25
Figure 13: Flyrock trajectory components 26
Figure 14: SDOB calculation 28
Figure 15: SDOB categories 28
Figure 16: Comparison of predictability of flyrock distance models 32
Figure 17: The complexity of flyrock and its prediction 38
Figure 18: Oblique-angled system of co-ordinates 41
Figure 19: Chudinov's trajectory components 45
Figure 20: Maximum throw vs boulder size and borehole diameter 46
Figure 21: Flyrock footprint related to personnel clearance criteria 47
Figure 22: Comparison of maximum flyrock distances from blasted muckpile 48
Figure 23: A report generated by the blast video analysis (BVA) system 52
Figure 24: Workflow progress of BlastVision® and types of visualisations 53
Figure 25: Methodology used in study for analysis 57
Figure 26: Various types of cameras used to capture footage of blasts 58
Figure 27: Review blast video 60
Figure 28: Identify projectile impact point 61
Figure 29: Holes plot of a drill pattern 62
Figure 30: Charged plot of a drill pattern 62
Figure 31: Stemming plot of a pattern 63

Figure 32: Data flow for the flyrock risk reporting dashboard 64
Figure 33: Flyrock footprint graph 65
Figure 34: SDOB plot 66
Figure 35: Drone configuration requirement 67
Figure 36: Range comparison graph with error 70
Figure 37: Adjusted range comparison graph 71
Figure 38: Trajectory comparison before change in Equation 33 72
Figure 39: Trajectory comparison after change in Equation 33 72
Figure 40: Observation distribution per site 74
Figure 41: Density vs UCS plot 75
Figure 42: Cratering vs Face burst 78
Figure 43: Actual vs Predicted (BlastLogic) Ranges 79
Figure 44: SDOB vs VDF 80
Figure 45: VDF vs range 81
Figure 46: Predicted and actual ranges compared to the exclusion boundary 82
Figure 47: Predicted vs actual range 83
Figure 48: Flyrock risk reporting for incident E/Blast 1 - (A) Footprint, (B) Trajectory 84
Figure 49: Adjusted Flyrock risk reporting for incident E/Blast 1 - (A) Footprint, (B) Trajectory 85
Figure 50: Section of Anglo American Plc drill and blast process flow 86
Figure 51: BlastVision® analysis of trial 1 87
Figure 52: BlastVision® snapshot of flyrock trajectories (trial 1) 88
Figure 53: BlastVision® details of flyrock trajectories (trial 1) 88
Figure 54: BlastVision® analysis of trial 2 89
Figure 55: BlastVision® snapshot of flyrock impacts (trial 2) 90
Figure 56: BlastVision® details of flyrock trajectories (trial 2) 90
Figure 57: Independent manual analysis results 91
Figure 58: BlastVision® follow-up review (trial 2) 92
Figure 59: Example of camera placement based on purpose 94
Figure 60: Example of a Camera Placement Request 95
Figure 61: One pager of blast video camera placement, capturing and analysis guideline 97
Figure 62: Amended Anglo American Plc drill and blast process flow 102

Figure 63: Flyrock from secondary blasting..... 103
Figure 64: Trajectory analysis considerations 104
Figure 65: 2D Statistical Analysis in RocFall2 105
Figure 66: Parameter sensitivity impact on Fmax..... 106
Figure 67: Initial boulder drill and blast design and risk evaluation proposal 107
Figure 68: Snapshot of the input and output sheets of the flyrock calculator 169
Figure 69: Example of flyrock risk reporting dashboard..... 171
Figure 70: Alternative view of the trajectory plot..... 172

LIST OF TABLES

Table 1: Some definitions of flyrock as used by different researchers 2
Table 2: Anglo American Plc's risk matrix adapted from MIL-STD-882B 4
Table 3: Flyrock accident statistics cited by authors 6
Table 4: Details of reported flyrock impacts in study period 8
Table 5: Factors contributing to flyrock occurrence 15
Table 6: Recent published flyrock prediction techniques 19
Table 7: Commercial software and the implemented flyrock model 21
Table 8: Violence factor selection criteria 50
Table 9: Adjusted table for VDF 51
Table 10: Data gathered for analysis 58
Table 11: Percentage variances in trajectory comparison 73
Table 12: Captured data 76
Table 13: Flyrock footprint calculation data 122
Table 14: Adjusted flyrock footprint calculation data 145

LIST OF EQUATIONS

Equation 1: Lundborg flyrock range 27
Equation 2: Chiapetta's flyrock range 27
Equation 3: Chiapetta's SDOB 27
Equation 4: Roth's flyrock range 29
Equation 5: Richards & Moore's flyrock range from face burst 29
Equation 6: Richards & Moore's flyrock range from stemming ejection 29
Equation 7: Richards & Moore's flyrock range from cratering 30
Equation 8: Chernigovskii's flyrock range 30
Equation 9: McKenzie's flyrock range (2009) 31
Equation 10: McKenzie's flyrock range (2022) 31
Equation 11: Lundborg's velocity 32
Equation 12: Roth's velocity 33
Equation 13: Nguyen's velocity 33
Equation 14: Chiapetta's velocity 34
Equation 15: Richards & Moore's velocity 34
Equation 16: Gibson & George's velocity 35
Equation 17: McKenzie's velocity coefficient 35
Equation 18: McKenzie's velocity 35
Equation 19: Blair's velocity 36
Equation 20: Lundborg's fragment size 36
Equation 21: Chernigovskii's fragment size 37
Equation 22: Chernigovskii's fragment mass 37
Equation 23: McKenzie's fragment size (2009) 37
Equation 24: McKenzie's fragment size (2022) 38
Equation 25: Drag force 39
Equation 26: Drag coefficient 39
Equation 27: Chernigovskii’s drag factor 40
Equation 28: Chernigovskii’s trajectory 41
Equation 29: Stojadinovic's trajectory 42
Equation 30: Stojadinovic's trajectory (cont.) 42
Equation 31: Chudinov's proportionality factor 43
Equation 32: Chudinov's trajectory 43
Equation 33: Adjusted proportionality factor 70

LIST OF ABBREVIATIONS AND SYMBOLS

In order of appearance

Abbreviation	Definition
Fmax	Flyrock Maximum Range
HPH	High Potential Hazard
BEZ	Blast Exclusion Zone
FOS	Factor of Safety
HPI	High Potential Incident
PUE	Priority Unwanted Event
FFTA	Fuzzy Fault Tree Analysis
MCDM	Multi-Criteria Decision-Making
DMRE	Department of Minerals Resources and Energy
RES	Rock Engineering System
ANN	Artificial Neural Network
ANFIS	Adaptive Neuro-Fuzzy Inference System
SDOB	Scaled Depth of Burial
VOD	Velocity of Detonation
RK4	Fourth-order Runge-Kutta
VDF	Vertical Displacement Factor
RADAR	Radio Detection and Ranging
LiDAR	Light Detection and Ranging
ViDAR	Visual Detection and Ranging
SHE	Safety, Health and Environmental
DTM	Digital Terrain Model
BLIS	BlastLogic Integrated Server
UCS	Uniaxial Compressive Strength

Symbol	Description	Units
Rmax	Maximum flyrock range	m
d	Drill hole diameter	mm, in
V_o	Initial launch velocity	$m.s^{-1}$
g	Gravitational acceleration	$m.s^{-2}$
θ	Launch angle	°
D	Distance from the surface to the centre of defined crater charge	m
W	Weight of explosives occupied only in top of the explosive column	kg
m	Charged mass per metre	kg/m
B	Burden	m
SH	Stemming height	M
β	Drill hole angle	°
α	Burden breakout angle	°
φ	Slope angle of floor	°
Sf	Shape factor	
P_r	Rock density	kg/m^3
Xf	Fragment size	mm
E	Explosive energy	$kcal.m^{-1}$
P_e	Density of explosives	g/cc
Δt	Length of time of the impulse	ms
K_v	Velocity coefficient	
VOD	Velocity of detonation	$m.s^{-1}$
D_f	Drag Force	N
C_d	Drag coefficient	
S	Cross sectional area of the fragment	m^2
M	Mass of fragment	kg
V_T	Terminal velocity	$m.s^{-1}$
P_{air}	Density of air	kg/m^3
b_d	Drag factor	m^{-1}
k	Proportionality factor	
H	Trajectory apex height	m
T	Time of flight	sec
V_a	Velocity at apex	$m.s^{-1}$
L	Horizontal range	m
t_a	Time to apex	sec
x_a	Horizontal distance to apex	m
$Θ_i$	Impact angle	°
V_i	Impact velocity	$m.s^{-1}$
S_{air}	Coefficient characterising the retarding of air	
V_m	Mass of material per unit length	kg/m
Vf	True volume of the fragment	m^3

t	Time component	sec

1 INTRODUCTION

The purpose of this chapter is to introduce and provide an overview of the research study, which is focused on flyrock incidents experienced at Anglo American Plc operations and the global surface mining industry. The research context and background, problem statement, research aim, and objectives are presented. The structure of the report is also described in this chapter.

1.1 Research Background and Context

This study is based at Anglo American Plc, a globally diversified mining company with operations located in 15 regions across the globe (Anglo American Plc, 2024). Figure 1 shows all the Anglo American Plc operations across the world.

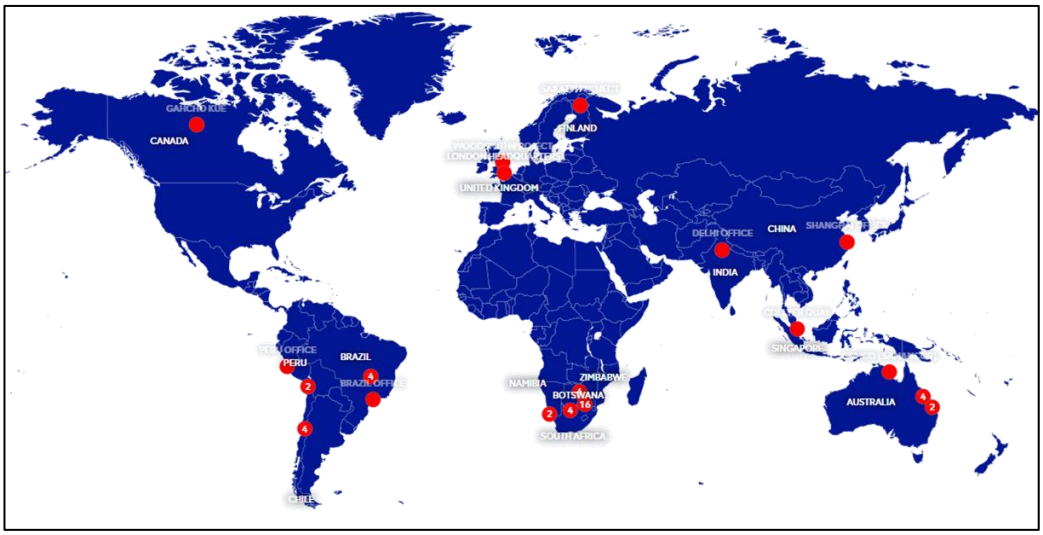

Figure 1: Global map of Anglo American Plc's operations (Anglo American Plc, 2024)

Each region has its own unique blasting challenges, but all surface operations commonly experience risks associated with flyrock. There are various definitions of flyrock found in literature. Table 1 is a summary compiled by Raina (2023) depicting various definitions of flyrock used by different researchers.

Table 1: Some definitions of flyrock as used by different researchers (Raina, 2023)

Author (s)	Definition	Comments
Fletcher and D'Andrea (1986)	Flyrock is the rock that is propelled through the air during mine blasting	Is a good yet not complete definition of flyrock as the term rock in the context of flyrock should have been used as a fragment
Davies (1995)	Flyrock, is essentially the product of uncontrolled venting of the gases that are developed when a charge is initiated	Explains mechanism of flyrock but does not give a proper definition
Gibson and George (2001)	Flyrock can be described essentially as the unexpected and undesirable projection of rock fragments during detonation of a blast	Is a good definition
Little (2007)	Flyrock—the undesired propulsion of rock fragments through the air or along the ground beyond the blast zone by the force of the explosion that is contained within the blast clearance (exclusion) zone	Qualifies the flyrock with respect to its desirability and relates it to blast danger zone. The "propulsion of rock fragments" cannot be a flyrock
Lwin and Aung (2019)	Flyrock refers to the uncontrolled dispersion of rock fragments from blast areas caused by explosive energy	"Uncontrolled dispersion of rock fragments" is not a correct definition

In some cases, flyrock risk is defined not in terms of a distance travelled but rather as a probability of occurring (Raina & Bhatawdekar, 2022). From Table 1 the more appropriate description of flyrock is generally defined as fragments of rock that are ejected from a blast face and travel beyond a stipulated distance. Anglo American Plc describes flyrock according to the company's explosive handling standard. In this standard flyrock is defined as rock fragments projected beyond the maximum

predicted range (this horizontal range is referred to as Fmax) during blasting (Anglo American Plc, 2020). Figure 2 shows a rock fragment's trajectory and classification based on the distance it travels from the source.

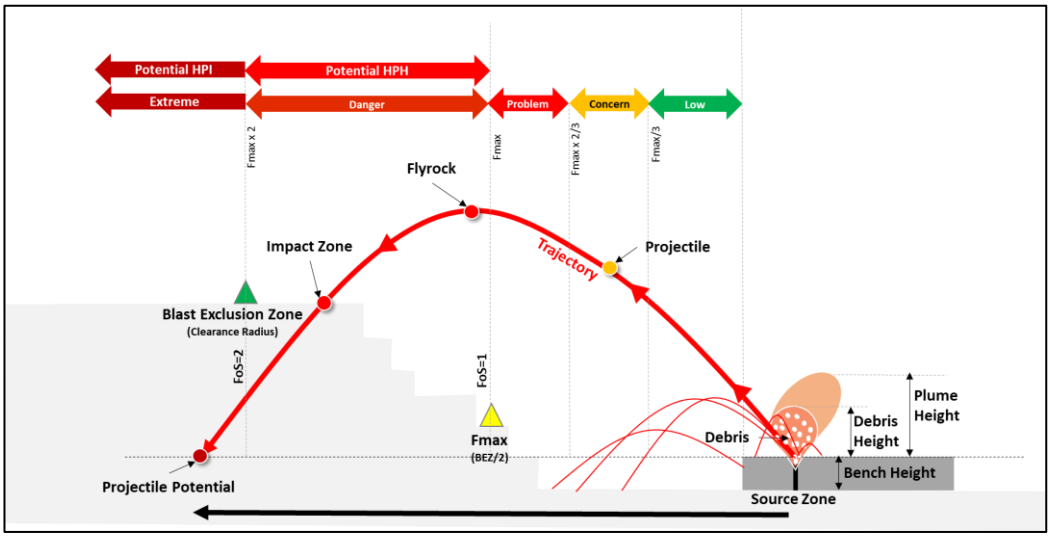

Figure 2: Anglo American Plc flyrock definition (Anglo American Plc, 2020)

Figure 2 indicates that if a projectile is launched from a blast and travels beyond Fmax, it is referred to as flyrock. The incident is then also classified as a High Potential Hazard (HPH). The incident will be classified as a High Potential Incident (HPI) if the projectile travels further than the blast exclusion zone (BEZ), which is defined as double the Fmax distance due to the application of a factor of safety (FOS) of two. Therefore, based on the standard, flyrock must trigger an appropriate response as either HPH or HPI.

Flyrock is considered a Priority Unwanted Event (PUE), due to the high-risk levels associated with it (Anglo American Plc, 2020). Flyrock has the potential to negatively impact personnel, structures, and damage equipment in and around surface mines (Anglo American Plc, 2020). A PUE is any event with a maximum consequence rating of either four or five (high and major) on the Operational Risk Management matrix as depicted in Table 2. An event with a rating of four or five has the potential to cause a single or multiple fatalities.

Table 2: Anglo American Plc's risk matrix adapted from MIL-STD-882B (Kovačević, et al., 2019)

Event Risk Rating/ Priority (1)					
Consequence / Likelihood	1 Minor	2 Low	3 Medium	4 High	5 Major
5 Almost Certain	Medium (11)	Significant (16)	Significant (20)	High (23)	High (25)
4 Likely	Medium (7)	Medium (12)	Significant (17)	High (21)	High (24)
3 Possible	Low (4)	Medium (8)	Significant (13)	Significant (18)	High (22)
2 Unlikely	Low (2)	Low (5)	Medium (9)	Significant (14)	Significant (19)
1 Rare	Low (1)	Low (3)	Medium (6)	Medium (10)	Significant (15)

During blasting events, rock projectiles ejected from a blast are often overlooked unless they cause injuries, equipment damage, infrastructure destruction, or fatalities (Gibson & George, 2001). In rare cases, observed at Anglo American operations, flyrock incidents are reported as "near misses" when they nearly harm people or damage infrastructure. Consequently, from the author's experienced, most flyrock events at Anglo American Plc sites are not officially recorded, resulting in a lack of comprehensive data and limited information for research and model development to improve outcomes.

Historically, predicting flyrock was challenging (Raina, 2023). However, with more rigorous investigations over time, and technological advancements, the scientific understanding of flyrock has significantly improved in recent years. Figure 3 shows flyrock publications between 1960 and 2021.

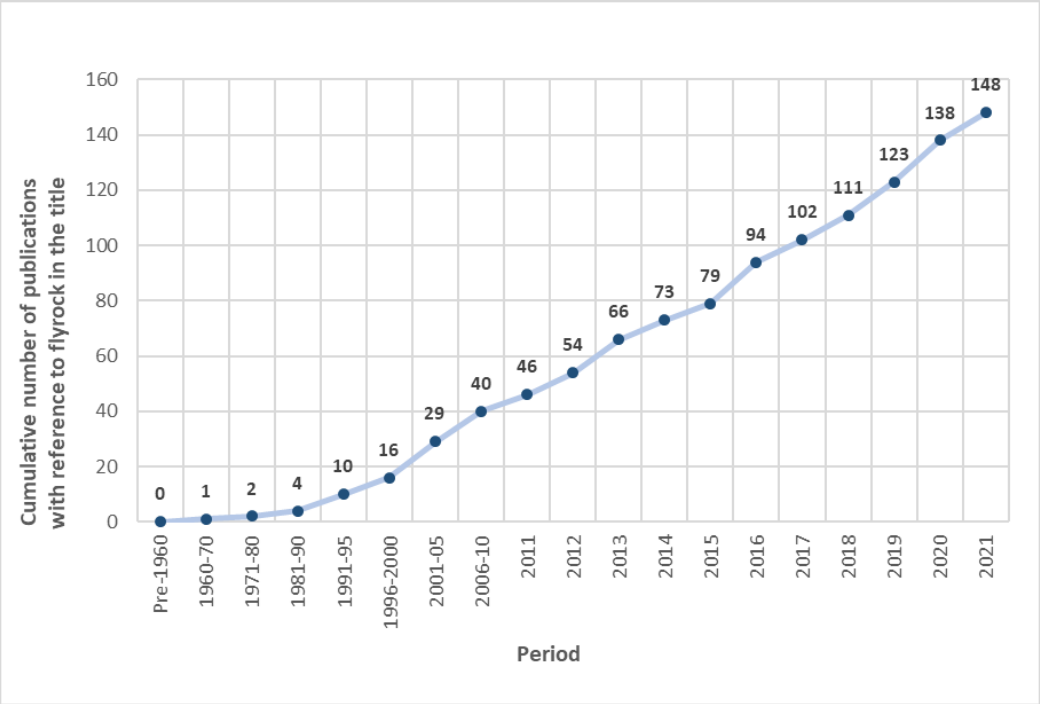

Figure 3: Cumulative number of publications with reference to flyrock in the title (Redrawn from Raina, 2023)

Raina (2023) developed Figure 3 using data obtained through searches with variations of the spelling of flyrock in the title. The figure shows that scientific research on flyrock has significantly increased over the years with 148 papers on the subject from 1960 to 2021. Although research in flyrock has increased, their occurrence has not reduced (Sevelka, 2025).

In comparison with other unwanted blasting outcomes such as ground vibration and air overpressure, flyrock is the least understood (Szendrei & Tose, 2022). The occurrence of flyrock is still present because of poor designs, compliance during execution and human error (Fletcher, 1983). Riana, et al. (2015) compiled a summary of worldwide blasting accidents from 1978 to 2011. The summary is shown in Table 3.

Table 3: Flyrock accident statistics cited by authors (Raina, et al., 2015)

Author (s)	Date Range	Reported Blasting Injuries	Percentage of Injuries related to flyrock
Bajpayee, et al. (2004)	1978 – 1998	281	41%
Little (2007)	1978 – 1998	412	68%
Kecojevic and Radomsky (2005)	1978 – 2001	195	28%
Verakis and Lobb (2007)	1994 – 2005	168	19%
Mishra and Mallick (2012)	1996 – 2004	30	24%
Verakis (2011)	2010 – 2011	18	38%
Adhikari (1999)	-	-	20%

The inconsistent and lack of reporting of flyrock events and the associated risks have been and are still a global concern (Sevelka, 2022). When incident statistics are underreported, the available data becomes incomplete and misleading. This incomplete picture fails to capture the true frequency and potential consequences of flyrock events. Consequently, decision-makers and stakeholders perceive the risk as less severe than it is. More recent published studies summarising flyrock-related accidents are limited with individual events published mostly in media reports or summarised in forensic/litigation appraisal literature (InterVal, 2024).

Extracting data from one of the appraisal literatures indicates potentially 27 incidents from 2010 to 2019 (InterVal, 2024). Sevelka (2024) commented in the analysis that as of August 2024, there were 240 documented flyrock incidents, resulting in 49 deaths and 49 injuries globally.

Anglo American Plc Safety, Health and Environment (SHE) records show that between April 2023 and May 2024, six flyrock incidents were reported from across all operations. A review of videos of the blasts concerned, as well as other blast events from the operations showed that from all the blasts initiated during the period, flyrock exceedances (rock fragments traveling further than set Fmax for the blast) were experienced in 70% of the blasts as shown in Figure 4.

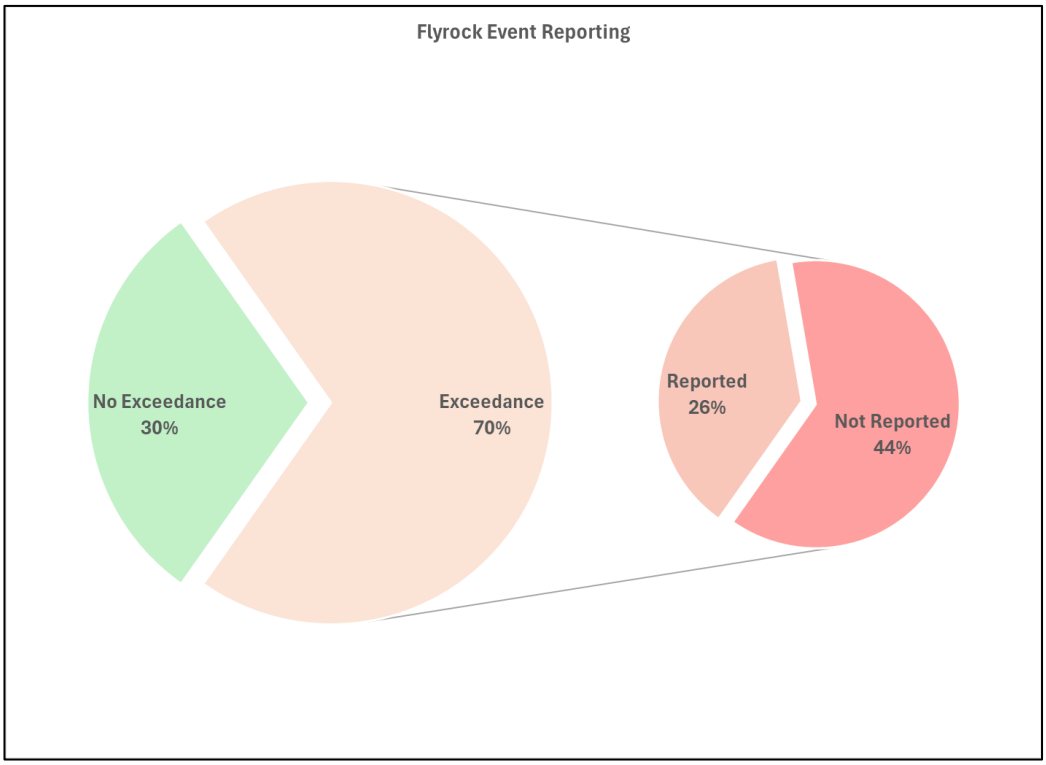

Figure 4: Sample gap analysis (reported vs video analysis)

A review of the 70% of blasts where the limits were exceeded, indicated that only 26% were reported. The analysis of the reported exceedances was not representative of all the exceedances. Figure 5 depicts the impact locations of five of the six flyrock events reported at various Anglo American Plc operations. The details of which are summarised in Table 4.

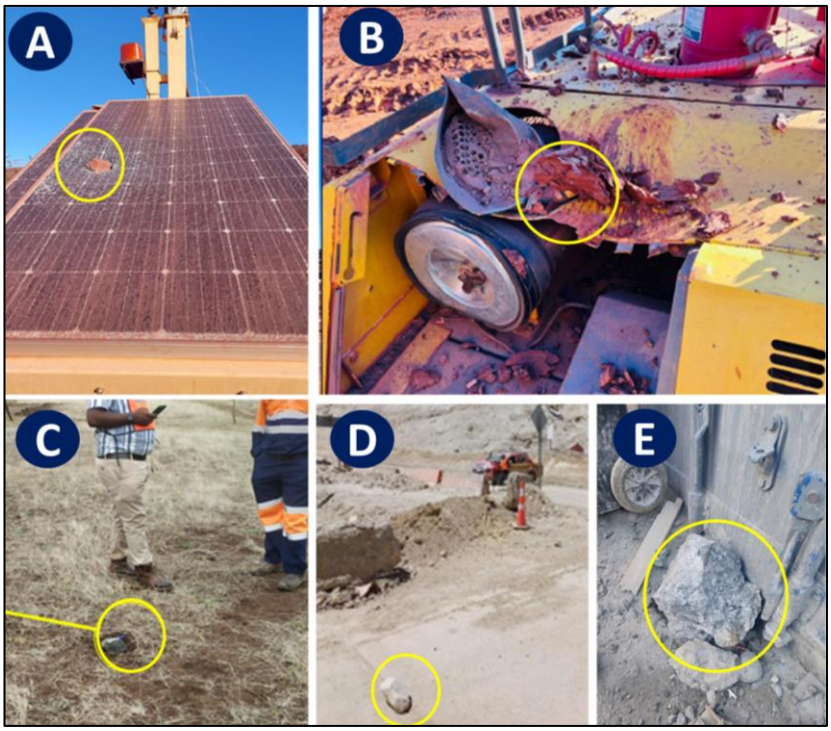

Figure 5: Five examples of flyrock incidents reported in study period

Table 4: Details of reported flyrock impacts in study period

Flyrock event	Horizontal distance (m)	Projectile size (kg)	Risk Rating	Description
A	Not specified	Not specified	HPH	A projectile impacted a solar panel of a radio repeater that was situated outside the blast exclusion zone
B	Not specified	Not specified	HPH	A fragment from a face burst impacted on the top of a front-end loader that was found inside the blast exclusion zone
C	522	2.7	HPI	The final position of a fragment propelled from a blast and landed close to the position of the blast guards
D	460	4.5	HPI	A rock fragment that was launched during a blast from the bottom of a pit and landed close to the position of the blast guards
E	745	22.5	HPI	A portion of the rock fragment that was ejected from a blast and landed close to workers outside the exclusion zone

Of the six reported incidents, three were classified as High Potential Incidents (HPI's), while the remaining three were categorized as High Potential Hazards (HPH's). As illustrated in Figure 5, these incidents led to equipment damage and production stoppages. The incident reports from various Anglo American Plc surface operations clearly indicate that rock fragments were being propelled beyond acceptable ranges, highlighting the ongoing risk associated with flyrock events.

In managing risks associated with flyrock and enforcing compliance to the set blast exclusion zone, Anglo American Plc has explored various potential technology solutions to monitor proximity of people and equipment to the blast exclusion zone. Figure 6 shows the components of the blast clearance technology system.

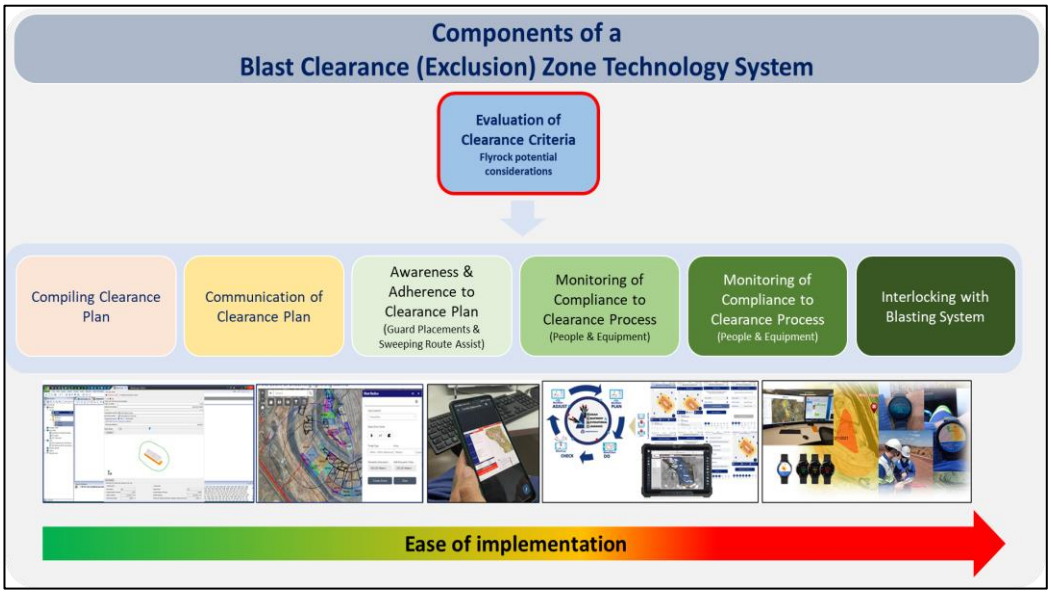

Figure 6: Importance of flyrock evaluation as part of blast clearance criteria (Carpenter, 2022)

Primary input to the potential technological solution is the blast exclusion zone criteria. To establish the BEZ, the potential range of flyrock need to be taken into consideration. The remaining components in the system utilise or are measured against the flyrock risk evaluated BEZ. This again highlights another important reason for a framework to model and manage the risk of flyrock.

1.2 Problem Statement

The lack of proper reporting of flyrock incidents can lead to complacency, increasing the risk of serious consequences, including single or multiple fatalities. This issue does not stem from an absence of standards and procedures for blast design and execution but rather from a gap in the process needed to facilitate the awareness and prediction of flyrock. Additionally, there is a lack of systematic processes for reporting and mitigating flyrock risks at every stage of the drill and blast process, including proactive modelling and monitoring of potential exceedances. Depending on the severity of a flyrock incident, regulatory penalties, equipment damage, and, in the worst case, fatalities can result in production stoppages, leading to significant revenue losses.

1.3 Justification and Significance of the Research

This research will be focused on the development of a framework that will drive the flyrock risk awareness, and give guidance on identifying, modelling, and reporting the risks at surface mining operations. This research is motivated by a clear need to improve flyrock alertness throughout the drill and blast process flow. Flyrock incidents have a safety, but also financial implication to the operations through cost of damages and production losses due to incident stoppages. As a result, the development of a flyrock framework to manage risk, also reduces potential financial losses.

Furthermore, the framework will also assist with embedding a scheme to monitor actual blasts for flyrock and measure projectiles with the purpose to improve blasting outcomes and safety. Although this work is done for blasting at Anglo American Plc's operations, it is envisaged to be applicable to all surface mining operations.

1.4 Research Questions

To guide the focus of this study, the research will answer the following questions:

- Are the current models used for predicting flyrock effective in highlighting its risk?

- What methods and/or techniques can be deployed to efficiently monitor flyrock; and
- How can mines proactively report on potential flyrock risks?

1.5 Research Aim and Objectives

In answering the questions posed in the study, the research is geared towards developing a framework for modelling, monitoring, measuring and reporting the risks associated with flyrock occurrences to enhance risk management strategies. To achieve this, the objectives of the study are therefore to:

- Conduct literature review on flyrock and evaluate current flyrock predictive models.
- Conduct a flyrock predictive model verification to confirm if the current used predictive model is appropriate in highlighting the risk.
- Develop a flyrock framework that encompasses a guideline for optimal methods to monitor and measure actual flyrock during blasting for compliance monitoring and, continuous model validation; and
- Develop a flyrock risk reporting dashboard to improve awareness.

1.6 Structure of the Research Report

This research report consists of five chapters. The first chapter introduces the research study covering the research background and context of flyrock concerns in the mining industry, the problem statement related to flyrock occurrences at Anglo American Plc surface operations. It also covers the justification for the research based on the flyrock exceedances observed, and the research objective to establish a flyrock framework.

The second chapter is an in-depth literature review covering flyrock theory and prediction models. In this chapter, key concepts and theories relating to flyrock are discussed.

Chapter three covers the approach adopted for the research in this study. After addressing the research design criteria, the approach to collecting flyrock related

data, as well as the process to validate and analyse the flyrock data obtained in the study is elaborated on.

Chapter four presents the data obtained using the methodology discussed in chapter three. Evaluating actual data against the model predicted data is critical in the process of establishing a framework. This chapter also presents an analysis of the data from the sources previously stipulated. The findings from this analysis are also discussed in detail.

The conclusions and recommendations are discussed in chapter five. In this chapter, the research report chapters are summarised, and observations, contributions and limitations are highlighted. Finally, recommendations for future work are mentioned.

2 LITERATURE REVIEW

2.1 Introduction

The literature review chapter serves as a background on previous work done related to the research topic. The chapter will cover key concepts and arguments related to flyrock evaluation in the industry. Previous work on flyrock modelling and monitoring techniques will also be discussed which will serve as the basis for establishing the proposed framework.

2.2 Understanding Flyrock in Surface Mining Operations

The persistent threat of flyrock in surface mines continues to captivate the mining community, despite advancements in blasting technology (Raina, 2023; Van Der Walt and Spiteri, 2023; Sevelka, 2025). Historically, flyrock incidents were often overlooked due to mines being located far from communities, which has changed with expanding mine operations which encroach human settlements, and historically less stringent blasting regulations (Raina, 2023). As a result, any flyrock incidences affect urbanisation, infrastructure development, etc.

The main objective of blasting in mining is to break and fragment rock into smaller pieces, making it easier to excavate, extract and process the minerals (Ghasemi, et al., 2012). This fragmentation process results in internal ballistics when the explosive charge detonates, releasing a massive amount of energy in a very short time (Chernigovskii, 1985). The explosion sends out a very fast shockwave from the blast hole, moving faster than the speed of sound (Johnson, 2018). The shockwave compresses the rock, causing it to deform and creating a zone of crushed rock around the blasthole (Dotto & Pourrahimian, 2024). As the shockwave propagates and is reflected from the free face in the form of a tension wave, it creates tensile stresses in the rock, which leads to the formation of fractures (Shadabfar, et al., 2021; Dotto and Pourrahimian, 2024; Blast Training International, 2015). The fractures propagate through the rock, driven by the tensile stresses as well as the gas pressure remaining in the blast hole which opens the fractures and increases the rate of fracture acceleration (Blast Training International, 2015). The rock breaks into smaller fragments as the fractures

intersect and the rock is torn apart. The fragments are ejected from the blast (external ballistics), often at high velocities, up to 250 m/s, and can travel long distances more than a 1000m (Szendrei & Tose, 2024). These velocities are directly impacted by the degree of confinement (amount of intact material between a free face and explosive charge) and the amount of energy released from the explosives (Lundborg, 1974; Richards and Moore, 2002; McKenzie, 2009).

In general, three key mechanisms describing the sources of flyrock are illustrated in Figure 7.

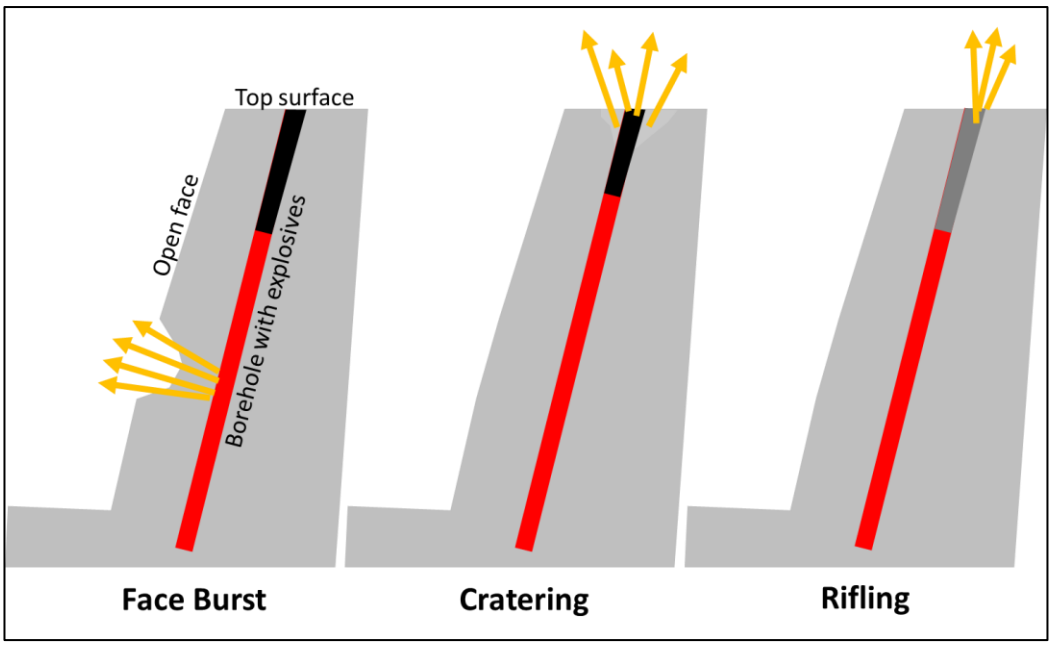

Figure 7: Three key mechanisms for flyrock (Richards & Moore, 2002)

The three mechanisms Richards and Moore (2002); Szendrei and Tose (2023); Rawnaq, et al. (2024) are:

i. Face burst – where the fragments are propelled from the open face due to the lack of burden in front of the blast hole.
ii. Rifling – where the fragments are ejected (almost vertically) out of the top of the blast hole in most cases due to lack of stemming (sometimes referred to as stemming ejection); and
iii. Cratering – where the fragments are ejected from the crater region formed at the top of the hole because of insufficient confinement (stemming).

In order to develop a framework for flyrock, it is important to understand the causes of flyrock as a result of blasting. The causes are divided into controllable and uncontrollable factors during blasting (Masir, et al., 2020). Raina (2023) summarised some of the factors as shown in Table 5.

Table 5: Factors contributing to flyrock occurrence (Raina, 2023)

Uncontrollable factors	**Controllable factors**
Rock strength/ Density	Drill diameter
Joint properties and characteristics	Burden
Presence of weak zones	Spacing
Presence of voids	Stemming length
	Charge length

Table 5 indicates that the controllable factors are mainly associated with the pattern design criteria, while the uncontrollable factors are related to the uncertainty linked to the rock mass properties and geological structures.

This also agrees with the views of Szendrei and Tose (2023) who grouped the causes of flyrock into five categories, namely:

i. The geometrical/design factors of the pattern leading to insufficient confinement of the explosive charge.
ii. Design factors leading to inadequate stemming design, again resulting in insufficient confinement.
iii. Explosive loading deviations resulting in overcharging.
iv. Delay timing resulting in insufficient burden relief; and
v. Rock mass and structural quality resulting in rock defects and anomalies.

Van Der Walt and Spiteri (2020) highlighted the causative input parameters that drives the various flyrock predictive models. The controllable factors from Table 4 are predominately used in the estimation of flyrock ranges with the key influential parameters being powder factor (which is related to the burden, spacing and charge length) and stemming length (Van Der Walt & Spiteri, 2020).

2.3 Flyrock Framework to Manage Risk

In general, a risk management framework is a structured process that helps operations identify, assess, and reduce risks (International Organization for Standardization, 2023).

A risk management framework typically consists of several key components, examples are:

- Risk identification covering the processes and tools used to identify potential risks, including threats, vulnerabilities, and opportunities.
- Risk assessment methods to evaluate and prioritise identified risks, considering likelihood, impact, and other factors.
- Risk mitigation strategies and controls to reduce or eliminate identified risks, such as avoidance, transfer, or mitigation.
- Risk monitoring processes to track and review risks, ensuring that mitigation strategies remain effective.
- Risk communication mechanisms to share risk-related information with stakeholders, including reporting and escalation procedures.

In the context of the study, a complete flyrock framework is thus a structured process to manage the risk of flyrock. As indicated in Figure 8, this structured process covers components of modelling, monitoring and measuring flyrock occurrences.

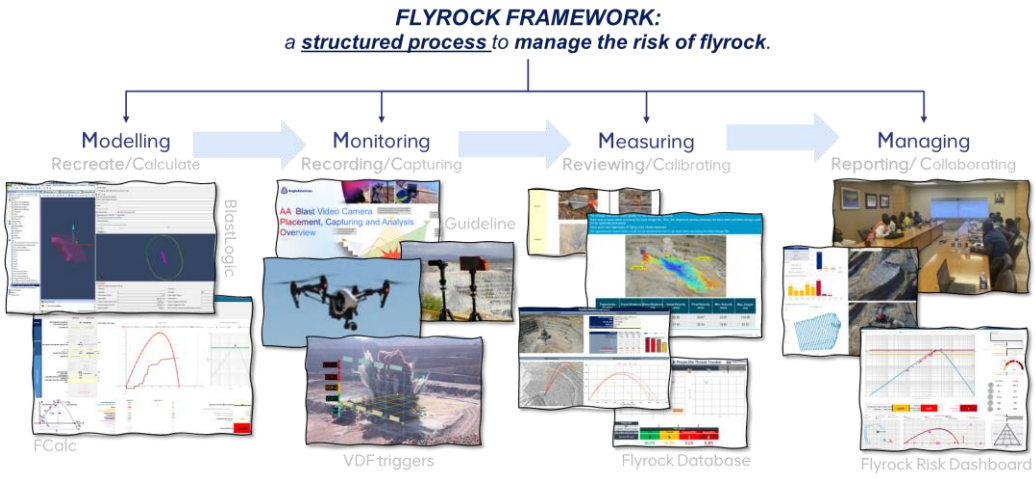

Figure 8: Flyrock framework components

Having a platform to report and discuss flyrock risk is also a vital component that is depicted in Figure 8.

Scovira (2012) presented a flyrock elimination program that was initiated as a result of an increase in the frequency and severity of flyrock incidents in a North America quarry and construction business.

During an analysis of the incidents by Scovira (2012), three gaps were identified, namely:

I. There was no standard applied to how design tools were consistently utilised in the whole business.
II. There was no proper evaluation of face burdens was conducted; and
III. There was a skill shortage to capture data and conduct proper analysis.

Scovira (2012) established a corporate driven framework to address the gaps. The process covered the standardisation of blast design equipment and usage policies, revision of the blasting safety guidelines of the company, introduction of 3D photogrammetry and borehole deviation tools to properly evaluate the risk for flyrock from face bursts and employing field engineers to do required measurements. The implementation of this framework reduced the frequency of flyrock incidents because of improved awareness on the risk of flyrock (Scovira, 2012).

The framework proposed by Masir, et al. (2020), focus on the assessment of flyrock risk. The main aim of this framework is to calculate a risk number with the aim of minimising flyrock risk. The critical step in this process uses fuzzy fault tree analysis (FFTA) and multi-criteria decision-making (MCDM) to determine if the occurrence of flyrock is a design error, human error or natural error. The flyrock risk assessment performed in this systematic approach is then used to manage the risk of flyrock occurrence.

In general, a framework for flyrock represents a structured process with components or steps that identifies the risk associated with flyrock through predicting the occurrence and assess the likelihood of exceeding set limits. The modelling of potential flyrock ranges during various stages of the drill and blast

process, allows sites to apply mitigation strategies such as adjusting the design or increasing the blast exclusion zone (Raina, 2023). Monitoring and measuring actual flyrock is another key part of the framework, helping confirm that blasting activities meet compliance requirements.

2.4 Flyrock Modelling: Past and Present Approaches

Accurately predicting potential flyrock enables organisations to:

- Ensure compliance with regulatory standards and legal obligations (South African Government, 2024).
- Enhance operational safety by defining appropriate blast clearance zones (Anglo American Plc, 2020).
- Minimise equipment damage by preventing improper placement relative to the blast area; and
- Minimised downtimes by allowing smaller blast clearance zones, meaning equipment and personnel can return to the site sooner after blasting. Less idle time results in more productive hours (Li, et al., 2023).

Based on the factors and mechanisms that causes flyrock, various techniques have been developed to predict flyrock occurrences (Raina, 2023). Some of the techniques are rock engineering related, empirical, ballistic, statistical (Van Der Walt & Spiteri, 2023).

The Rock Engineering Principles (RES) approach involves understanding the core principles of rock mechanics and engineering to predict flyrock (Faramarzi, et al., 2014). It takes into account factors such as rock properties, blast design, and energy distribution. This method provides insight into the underlying mechanisms and allows for adjustment based on site-specific parameters. However, this approach is site specific and cannot be generalised (Hasanipanah, et al., 2018; Van Der Walt & Spiteri, 2020).

Statistical models use data analysis techniques to identify patterns and correlations in flyrock data (Babaeian, et al., 2023). These models can include regression analysis (Armaghani, et al., 2016), machine learning (Hudaverdi & Agan, 2023), and probabilistic models (Blair, 2022). Statistical models can handle large datasets

and complex relationships, providing probabilistic predictions with confidence intervals. However, they require extensive data for training and validation and may be less intuitive and harder to interpret (BoganaVijaykumar, 2024).

Empirical models predict flyrock using historical data and observations (Raina, 2023). These models often involve developing regression equations or charts based on past blasting events. They are relatively simple and quick to apply, making them useful for preliminary assessments. However, they may not be accurate for new or unique conditions and rely heavily on the quality and quantity of historical data.

Ballistic method applies the principles of projectile motion to predict the trajectory and distance of flyrock (Stojadinović, et al., 2011). It considers factors such as initial velocity, angle of projection, and air resistance. This method provides a clear physical and mathematical basis for predictions and can be used to simulate different blasting scenarios. However, it requires accurate input data for reliable predictions and may not account for all variables affecting flyrock behaviour.

Table 6 is a summary, compiled by Van Der Walt and Spiteri (2020), showing the broad flyrock prediction technique categories and how much of publications between 2010 and 2019 were allocated to these categories.

Table 6: Recent published flyrock prediction techniques (Van Der Walt & Spiteri, 2020)

Flyrock Prediction Technique Category	Allocation in Recent Publications
Rock Engineering Principles (RES)	6%
Empirical Analysis	23%
Statistical Analysis	6%
Artificial Computational Systems (ANN, ANFIS, etc.)	53%
Ballistics Principles	12%

Table 6 shows that recently a vast amount of time is spent on techniques related to artificial intelligence methods. This is not surprising as this is the trend not just

in blasting but mining in general. Zhou, et al. (2024) compiled a summary of some of the recent publications with associated machine learning and optimisation algorithm techniques. Based on the summary, it is shown that machine learning and optimisation algorithm methods do have potential in predicting and managing flyrock and other environmental effects of blasting.

However, when it comes to commercial drill and blast packages, the vast majority still employs non-artificial intelligence methods. The limited use of machine learning and optimisation techniques for flyrock modelling in commercial drill and blast software applications could be due to several limitations:

- Data quality and availability where high-quality, comprehensive datasets are essential for training effective machine learning models. In many cases, the available data may be insufficient or of poor quality, limiting the model's accuracy and reliability (Szendrei & Tose, 2022).
- Generalisation issues where machine learning models trained on specific datasets may not generalise well to different sites or conditions. This can lead to inaccurate predictions when applied to new environments (Noble Desktop, 2024).
- Advanced machine learning models, especially those involving deep learning, require significant computational resources for training and optimisation. This can be a barrier for some drill and blast commercial software applications (Zhou, et al., 2024).
- Integrating machine learning models with existing operations and systems can be challenging (Kitameraki, 2023). Ensuring compatibility and seamless operation requires substantial effort and expertise.

Despite these limitations, ongoing research and advancements in machine learning and optimisation techniques hold promise for improving the accuracy and applicability of flyrock modelling. The advantage of a flyrock framework is its ability to support comprehensive data capturing. This includes inputs from video analysis, field measurements, and charging data recorded in the drill and blast management system. These data sources can then be used to expand training datasets, which helps improve flyrock prediction techniques and methods.

2.5 Flyrock Modelling: Current Commercial Drill and Blast Applications

A number of commercially available drill and blast software applications now allows for the prediction of flyrock distances. To align with the objectives of this study and expand on the models listed in Table 7, the focus of the remaining literature review will be on some of these non-artificial intelligence methods and techniques.

Table 7: Commercial software and the implemented flyrock model

Drill and Blast Software	Flyrock Model
Maptek's BlastLogic	Richards & Moore or McKenzie
Orica's SHOTPlus	Richards & Moore
O-Pitblast	Richards & Moore
Maxam Rioblast	Richards & Moore
Paradigm	McKenzie
MineExcellence's BLADES	Richards & Moore
BMI's BlastPlan II	McKenzie
Datamine's DataBlast	McKenzie

2.5.1 Orica's SHOTPlus

The Exclusion Zone Tool embedded in SHOTPlus uses an empirical calculator that produces a BEZ based on predicted flyrock distances (Orica Digital Solutions, 2024). The tool is based on the work by Richards and Moore (2002).

2.5.2 O-Pitblast

O-Pitblast utilises also the equations produced by Richards and Moore (2002) to estimate the clearance criteria. The application uses the equations for all three flyrock mechanisms to predict the distance and then utilises the largest distance to establish the BEZ (O-Pitblast, 2023).

2.5.3 Austin Powder’s Paradigm

The Paradigm flyrock model provides a method for assessing and visualizing the potential risks associated with a given blast design (Austin Powder, 2024). By calculating a flyrock footprint for each hole in the pattern, the worst-case scenario flyrock distances are used to construct the BEZ. This comprehensive model takes

into account various factors, including free face ejections, safety factors, terrain, and even allows for the application of a fixed distance clearance footprint by incorporating a factor of safety. Paradigm flyrock model is based on the work of McKenzie (2009, 2022). Paradigm also provides a simplified standalone flyrock calculator depicted in Figure 9.

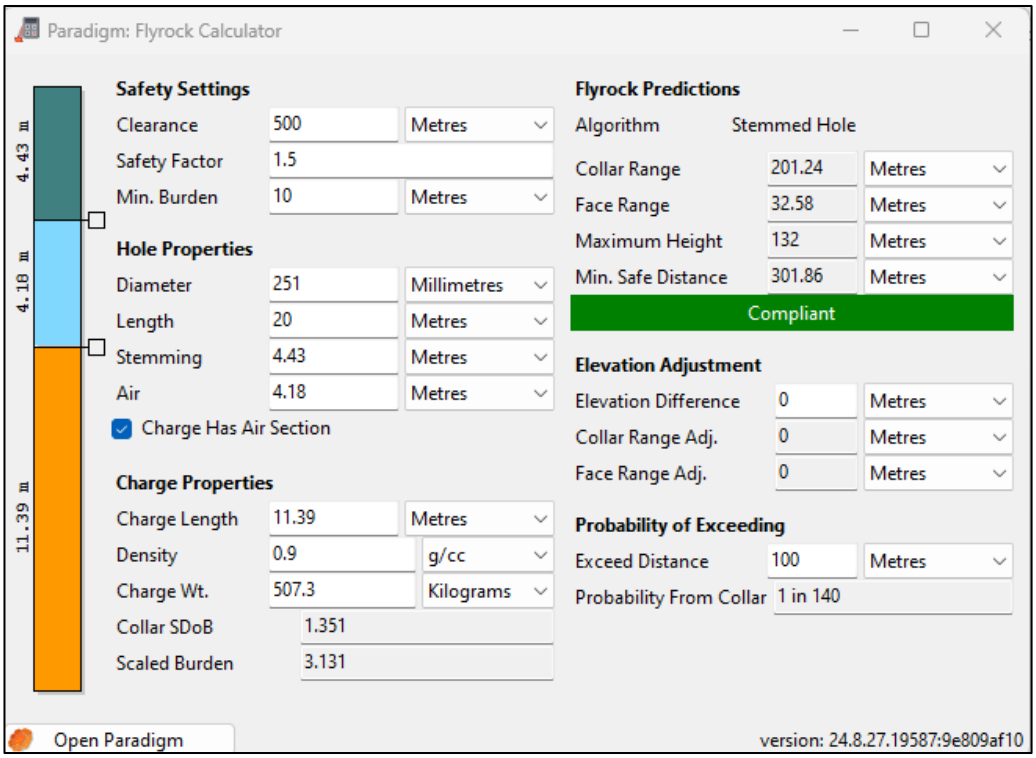

Figure 9: Paradigm flyrock calculator (Austin Powder, 2024)

The Paradigm flyrock calculator provides an easy and quick way of doing flyrock predictions taking various parameters into consideration. The calculator also provides a probability of exceedance estimation.

2.5.4 Maptek's BlastLogic

Anglo American Plc surface operations use Maptek's BlastLogic as the current preferred drill and blast management application (Tordoir & Roberts, 2019). It is also one of the main tools used in this study and hence is discussed in more detail. Figure 10 depicts the process flow covered by the BlastLogic software application (Maptek, 2024).

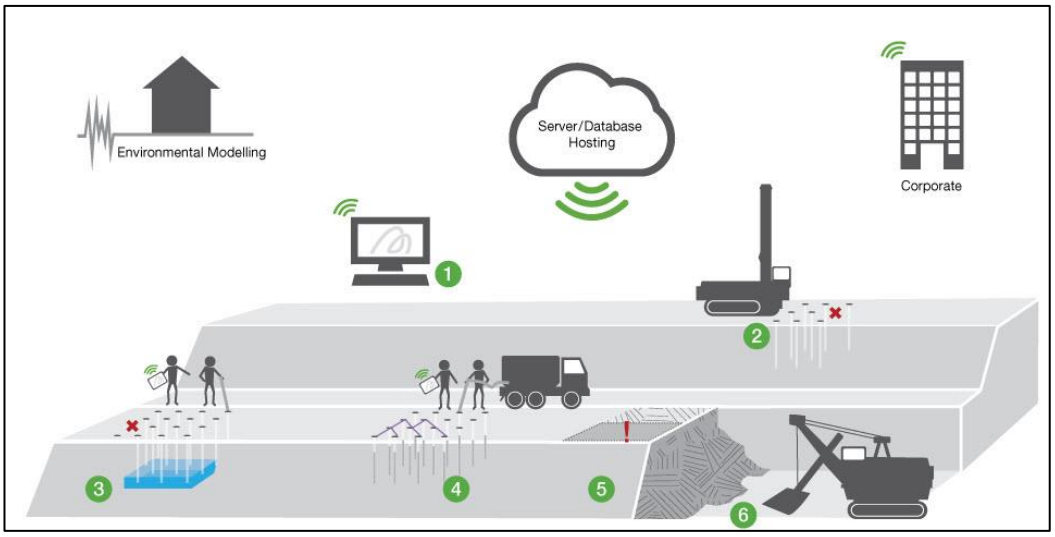

Figure 10: Maptek's BlastLogic process overview (Maptek, 2024)

The key steps from Figure 10 are:

1. Desktop application where the blast is designed.
2. Drill holes monitored and validated during drilling via tablet or desktop.
3. Post drilling measurements (dipping) of holes for quality assurance using remote tablets and validated on desktop.
4. Execution of charging plan. Recording of actual quantities using on bench tablets.
5. Review of blast performance and results; and
6. Reconcile and correlate blast outcomes with production data.

BlastLogic's flyrock module (Figure 11) presents a means to estimate a maximum horizontal distance of flyrock based on input criteria. The resulting polygon may be used to assist with recognising the potential extent of flyrock movement and establishing blast exclusion zones (Maptek, 2024). The flyrock module gives access to two flyrock predictive models, namely McKenzie (2009) as well as Richards and Moore (2002). Note Anglo American Plc adopted using the McKenzie (2009) option.

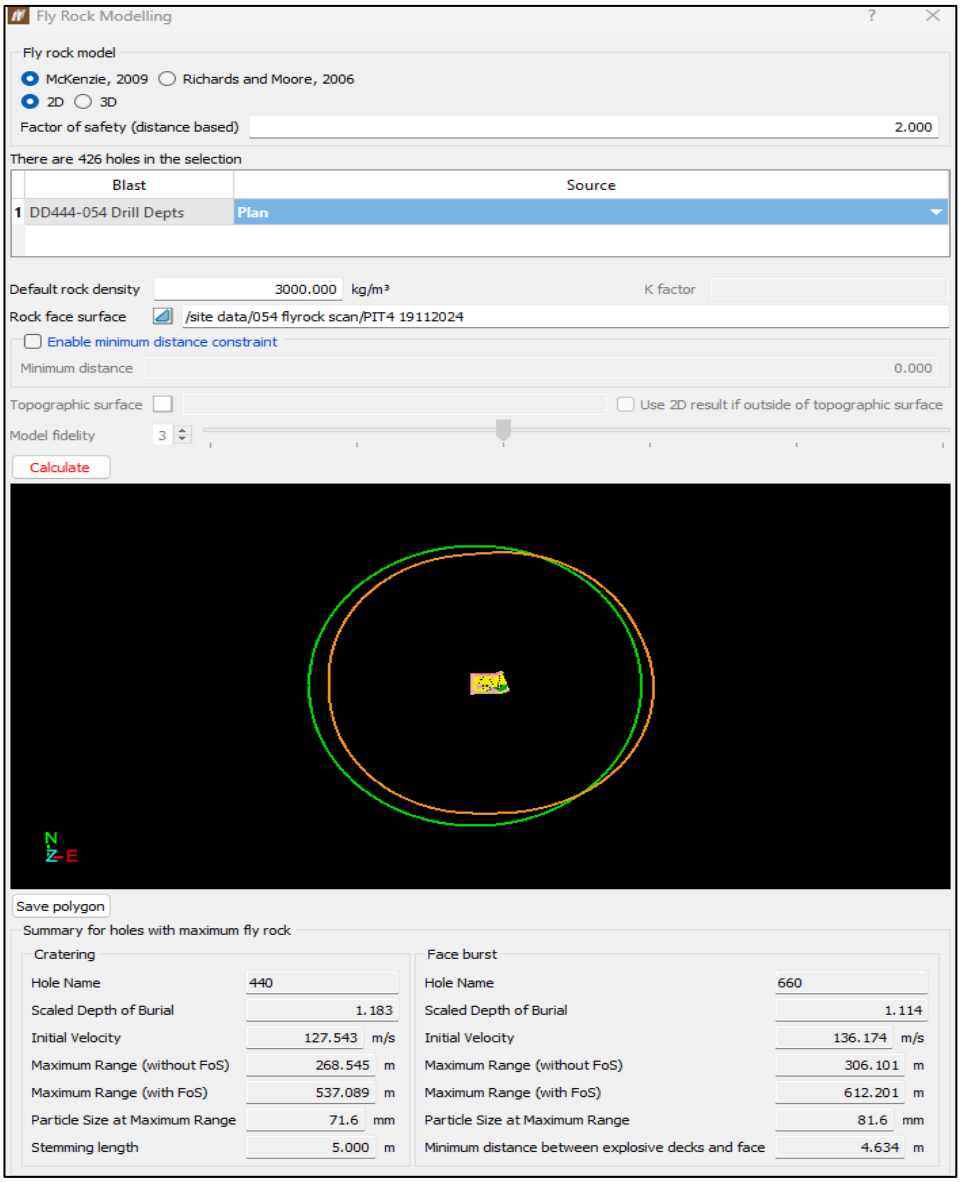

Figure 11: BlastLogic's flyrock module (Maptek, 2024)

For both models the application offers two types of modelling options, namely 2D and 3D (Figure 11). Both options use a projectile launch velocity. The velocity is determined from the predictive model that is selected. The launch velocity for the same blast may be different in the two models. This difference is due to the input parameters used by the two models. McKenzie (2009) model incorporates also rock fragment criteria such as rock density, shape factors and aerodynamic coefficients together with stemming and explosive quantities. On the other hand, Richards and Moore (2002) uses hole geometry, associated stemming as well as explosive quantities and a site-specific factor to estimate the velocity.

One of the main general differences between the two models is that McKenzie (2009) takes into consideration the effect of drag on rock fragments and Richards and Moore (2002) do not. In the 2D option, a simplified assumption is made that the topographic surface is flat, resulting in a maximum trajectory angle of 45 degrees. The flyrock trajectory path determined by the launch velocity, angle and resisting forces is then used to calculate the impact point with this theoretical surface.

The model accounts for two primary mechanisms of flyrock, namely cratering and face burst. In the 3D option, the velocity of the rock is used to determine the intersection point between the rock's trajectory and the surrounding topography. This calculation is repeated for multiple vertical angles to identify the maximum horizontal distance for a given orientation. The process is repeated for various orientations, creating a boundary around each blasthole. Once individual hole boundaries are established, a comprehensive boundary polygon is generated to encompass the entire blasting area (Maptek, 2024). The approach BlastLogic implements for determining face burst is demonstrated in Figure 12.

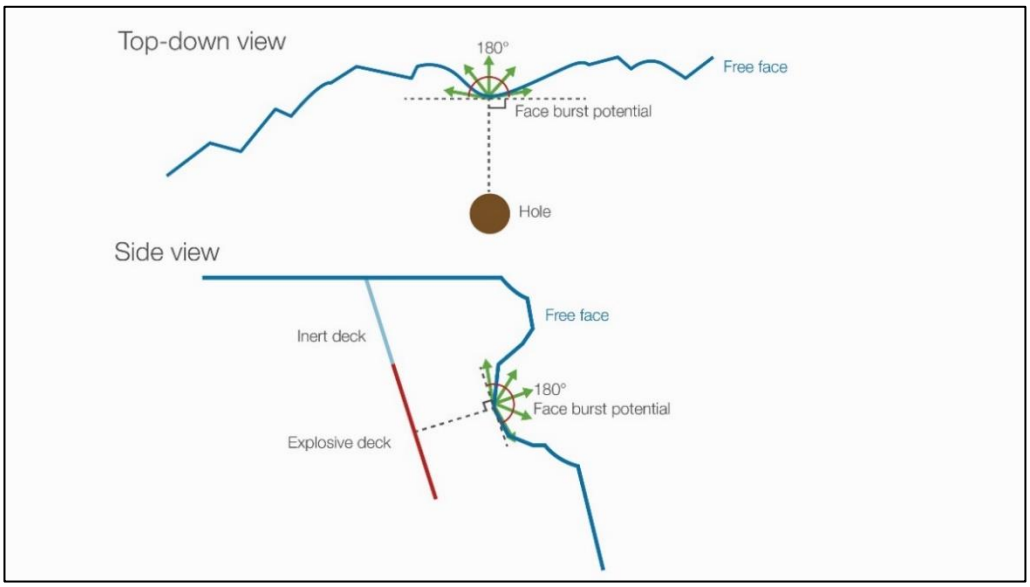

Figure 12: BlastLogic's estimation approach for face burst (Maptek, 2024)

BlastLogic calculates the shortest distance vector between explosive charge and the free face and then simulates the potential for face burst in a 180-degree arc. This arc is centred on the line perpendicular to the vector connecting the explosive

charge to the face. In cases where a single hole has multiple points near the face, BlastLogic prioritises the closest point for assessment (Maptek, 2024).

2.6 Flyrock Modelling: Components of Prediction Methods Used

The breakdown of the flyrock prediction models, some used in the packages discussed, will be categorised into the components shown in Figure 13, namely:

A. Flyrock range estimation.
B. Projectile launch velocity and angle approximation.
C. Fragment size prediction.
D. Forces impacting fragment in flight; and
E. Trajectory representation.

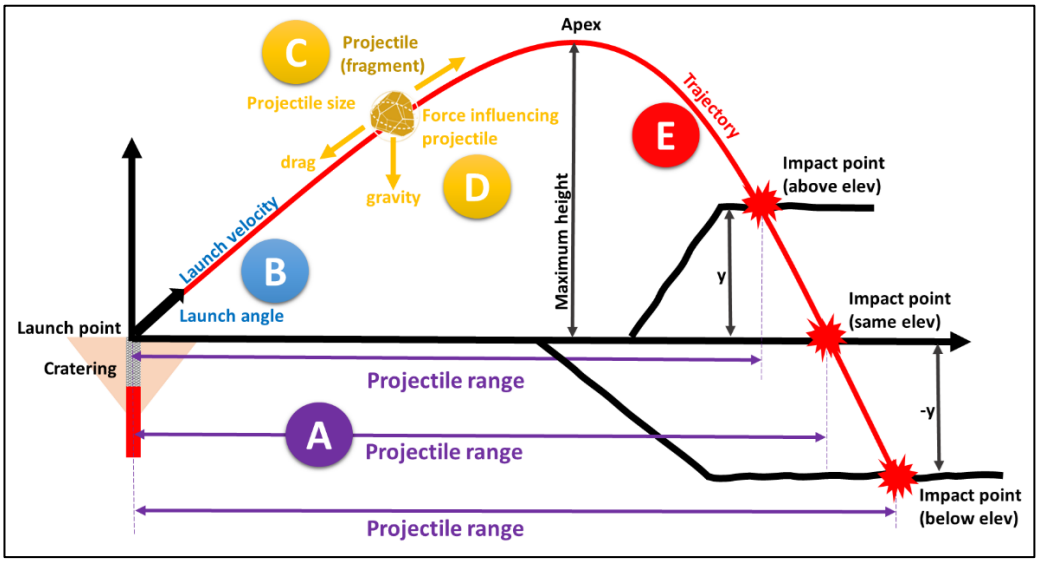

Figure 13: Flyrock trajectory components

2.6.1 Flyrock Range Estimation

Lundburg (1974), developed a model that relates maximum flyrock traveling distance from crater blast with drill hole diameter and the relationship is formulated in Equation 1.

Max Range (Rmax):

$$Rmax = 260 \times d^{\frac{2}{3}}$$ *Equation 1*

Where: *Rmax* is the maximum range of the flyrock (m).
d is the drill hole diameter (in).

Szendrei and Tose (2022) highlighted that Lundborg's approach was seen as too conservative due to outdated knowledge of blast wave properties. This in most cases results in overprediction of ranges. Chiapetta, et al. (1983) formulated Equation 2 for the estimation of the throw of a projectile during blasting.

Range (Rmax):

$$Rmax = \frac{V_o \times \cos(V_o \times \sin(\theta) + 2 \times V_o \times \sin(\theta) + 2 \times g \times H)}{g}$$ *Equation 2*

Where: *Rmax* is the range of the flyrock (m).
V_o is the initial launch velocity ($m.s^{-1}$).
θ is the launch angle of the fragment (°).
H is the launch height above the floor (m).
g is the gravitational acceleration (9.81 m/s^2).

This formulation was mainly focused on flyrock emanating from face bursts. Further work by Chiappetta, et al. (1998) led to the categorisation of flyrock risk using the scaled depth of burial (SDOB) as a metric captured in Equation 3.

SDOB:

$$SDOB = \frac{D}{W^{\frac{1}{3}}}$$ *Equation 3*

Where: *SDOB* is the scaled depth of burial.
D is the distance from the surface to the centre of the defined crater charge (m).
W is the mass of the explosive occupied only in the top part (Figure 14) of the explosive column (kg).

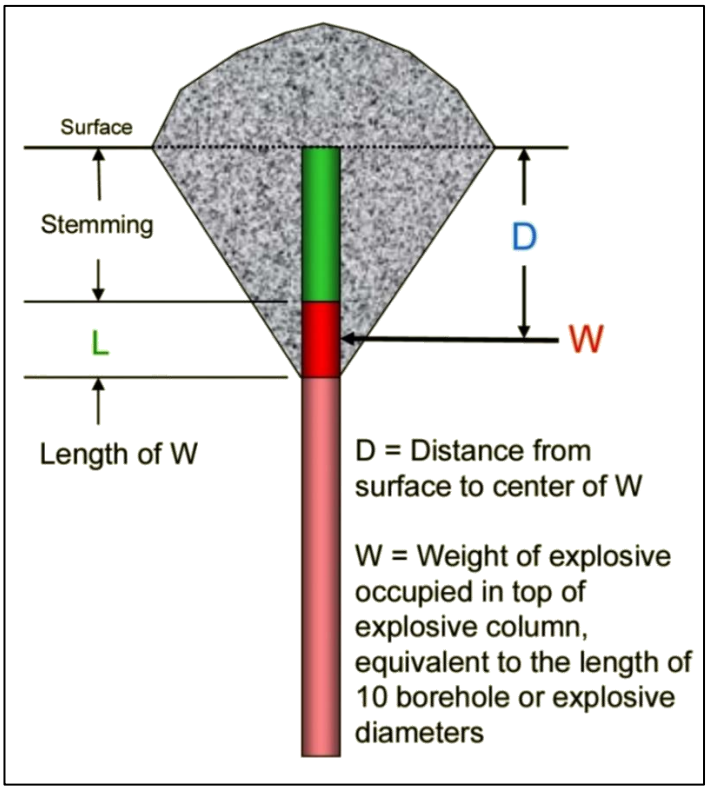

Figure 14: SDOB calculation (Chiappetta, et al., 1998)

The SDOB is an empirical measure of blast energy confinement. It is defined as the ratio of stemming material to explosive charge, measured within a distance equivalent to ten times the blasthole diameter (Tobin, 2013). The value of the SDOB is categorised as depicted in Figure 15.

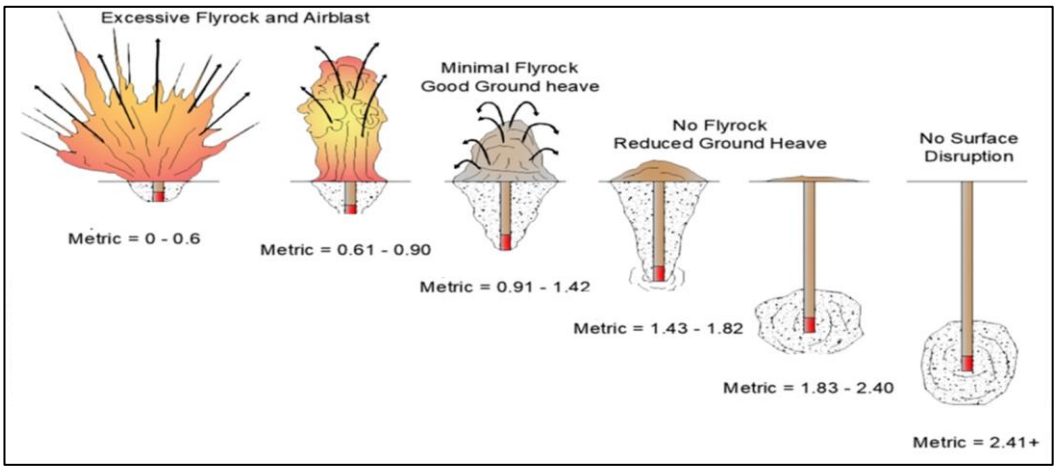

Figure 15: SDOB categories (based on Chiappetta, et al., 1998)

Figure 15 shows that the lower the value of the SDOB is the higher the likelihood for the occurrence of flyrock. A higher SDOB results in the reduction of potential cratering due to energy dissipation into the increased confinement.

In establishing his flyrock model, Roth (1979) used Equation 4 to estimate the travel distance. A similar approach using simple projectile motion equations was taken by Workman and Calder (1994).

Range (Rmax):

$$Rmax = {V_o}^2 \times \frac{\sin 2\theta}{g} \qquad \textit{Equation 4}$$

Where: *Rmax* is the range of the flyrock (m).
V_o is the initial launch velocity ($m.s^{-1}$).
θ is the launch angle of the fragment (°).
g is the gravitational acceleration ($m.s^{-2}$).

A more popular method, as alluded to in Table 7, is that of Richards and Moore (2002). This approach is an extension of work done by Workman and Calder (1994) and introduced an estimation formula (Equation 5, 6, 7) for each of the mechanisms illustrated in Figure 7.

Face burst:

$$Rmax = \frac{k^2}{g} \times \left(\frac{\sqrt{m}}{B}\right)^{2.6} \qquad \textit{Equation 5}$$

Rifling:

$$Rmax = \frac{k^2}{g} \times \left(\frac{\sqrt{m}}{SH}\right)^{2.6} \times \sin 2\beta \qquad \textit{Equation 6}$$

Cratering:

$$Rmax = \frac{k^2}{g} \times \left(\frac{\sqrt{m}}{SH}\right)^{2.6}$$ *Equation 7*

Where: *Rmax* is the range of the flyrock (m).
k is a constant.
β is the drill hole angle of the fragment (°).
B is the front burden (m).
SH is the stemming height (m).
m is the charged mass per metre (kg/m).
g is the gravitational acceleration (m.s^{-2}).

Although all the above prediction methods are based on a kinematic methodology, they do only consider the effect of gravity on the projectile (Szendrei & Tose, 2022). Gibson and George (2001) also built on the kinematic approach however, introduced the effect other forces (such as drag force) have on the projectile and not just gravity. Gibson and George (2001) estimated the range by using mathematical software to solve numerically the second-order non-linear ordinary differential equations.

Chernigovskii (1985) also supplied a simplified expression to estimate the horizontal distance an ejected projectile will travel (Equation 8).

Range (Rmax):

$$Rmax = S_{air}(f, \theta_0) \times \frac{2 \times {V_o}^2}{g} \times (\tan\varphi + \tan\theta) \times cos^2\,\theta$$ *Equation 8*

Where: *Rmax* is the range of the flyrock (m).
V_o is the initial launch velocity (m.s^{-1}).
θ is the launch angle (°).
φ is the slope angle of the floor (°).
g is the gravitational acceleration (m.s^{-2}).
$S_{air}(f, \theta_0)$ is derived from graphs specified by Chernigovskii (1985).

McKenzie (2009) used the foundation laid by Lundborg (1974) and the trajectory equations for motion that were formulated by Chernigovskii (1985). Similar to Gibson and George (2001), this approach started to consider the influence of air resistance on the flyrock range prediction. McKenzie (2009) also incorporated the SDOB into the range prediction using empirical correlation methods. Ultimately Equation 9 was compiled to estimate the maximum range.

Range (Rmax):

$$Rmax = 11 \times SDOB^{-2.167} \times \left(\frac{d}{Sf}\right)^{0.667} \qquad \textit{Equation 9}$$

Where: *Rmax* is the maximum range of the flyrock (m).
d is the drill hole diameter (mm).
Sf is the shape factor (1.2 is used mostly).

Note that in a more recent publication, based on more available blast data to refine the empirical equation, McKenzie (2022) slightly altered the coefficient of the equations as follows:

Range (Rmax):

$$Rmax = 9.47 \times SDOB^{-2.167} \times (d)^{0.667} \qquad \textit{Equation 10}$$

As the work of McKenzie (2009, 2022) is based on Lundborg (1974), the ranges estimated can be overestimated and referred to by McKenzie (2022) as worst-case or maximum ranges.

Drawing on measured flyrock data, Raina (2023) conducted a comparative evaluation of selected predictive models for estimating flyrock range. Figure 16 indicates the findings.

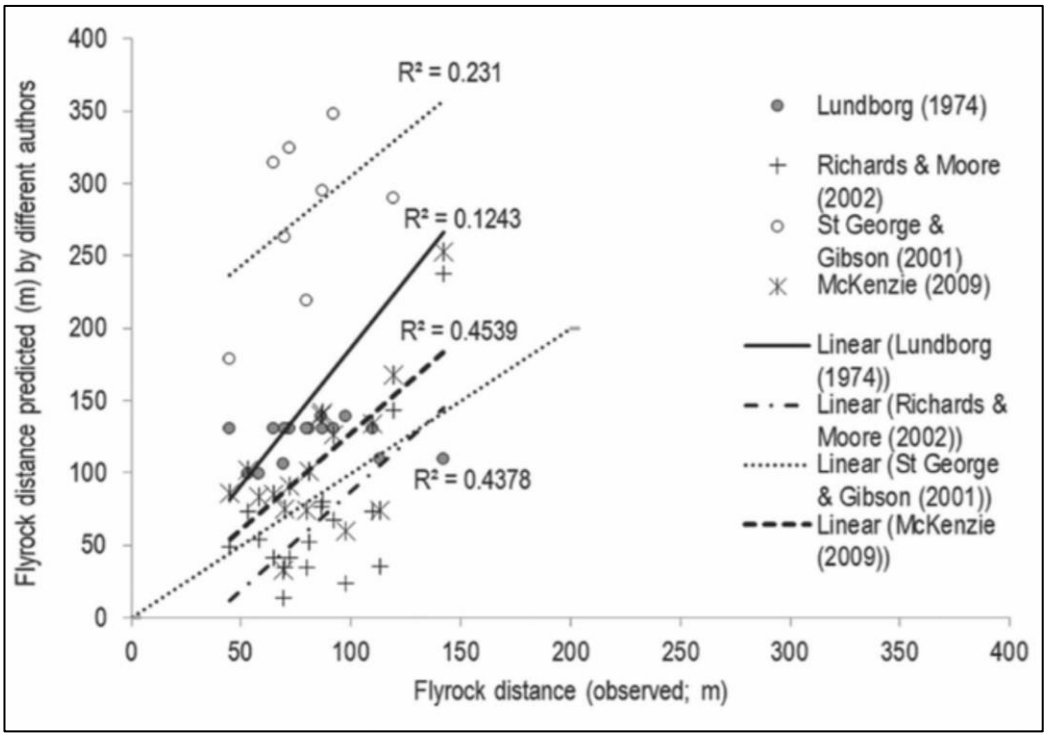

Figure 16: Comparison of predictability of flyrock distance models (Raina, 2023)

Based on the evaluation presented in Figure 16, the correlation results revealed that McKenzie's range equations demonstrated the strongest correlation, whereas the equations by Richards and Moore (2002) exhibited a weaker correlation.

2.6.2 Projectile Launch Velocity

As stated by Raina, et al. (2014), Lundborg (1974) incorporated in the model the estimation of the initial launch velocity based on the conservation of momentum combined with the scaling law of spherical charges. This resulted in the relationship between the charge diameter and velocity as captured in Equation 11.

Launch velocity (V_o):

$$V_o = \frac{10 \times d \times 2600}{Xf \times P_r} \qquad \textit{Equation 11}$$

Where: V_o is the initial launch velocity (m.s^{-1}).
d is the hole diameter (in).
P_r is rock density (g/cc).
Xf is the size of the fragment (m).

Roth (1979) range equation (Equation 4) relies on having an initial velocity. Roth (1979) used the Gurney equation (Jones, et al., 1980) in order to estimate the velocity (Equation 12).

Launch velocity (V_o):

$$V_o = \sqrt{2E} \times f\left[\frac{m}{V_m}\right] \qquad \textit{Equation 12}$$

Where: V_o is the initial launch velocity (m.s^{-1}).
$\sqrt{2E}$ is the Gurney constant, which is related to the type of explosive.
m is linear charge mass (kg/m).
V_m is the mass of material per unit of length (kg/m).

Nguyen, et al. (2020) also utilise Equation 12 and supplies an equation for the function $\left[\frac{m}{V_m}\right]$ as shown in Equation 13.

Velocity function ($\left[\frac{m}{V_m}\right]$):

$$\left[\frac{m}{V_m}\right] = \frac{m}{P_r \times \left(B^2 \times \tan\left(\frac{\alpha}{2}\right)\right)} \qquad \textit{Equation 13}$$

Where: m is linear charge mass (m/kg).
B is the burden to the free face (m).
α is the breakout angle (°).
P_r is rock density (kg/m^3).

Zhang, et al. (2021) conducted similar work on burden velocities. The use of a form of the Gurney equation to estimate velocity is also supported and considered by Szendrei and Tose (2023).

Chiapetta (1983) estimation of the launch velocity (face burst) is given in Equation 14.

Launch velocity (V_o):

$$V_o = a \times \left(\frac{B}{E^{\frac{1}{3}}} \right)^{-b}$$ *Equation 14*

Where: V_o is the initial launch velocity (m.s^{-1}).
B is the front burden (m).
E is explosive energy per unit of explosive (kcal.m^{-1}).
a and *b* are constants obtain from site specific design curves. Good initial approximation is a=12.5 and b=1.17.

Richards and Moore (2002), supply an estimation of the initial velocity based on the scaled burden as captured in Equation 15.

Launch velocity (V_o):

$$V_o = k \times \left(\frac{\sqrt{m}}{B} \right)^{1.3}$$ *Equation 15*

Where: V_o is the initial launch velocity (m.s^{-1}).
k is a constant.
B is the front burden (m).
m is the charged mass per metre (kg/m).

The model proposed by Richards and Moore (2002) is simplistic and easy to implement, however it relies on a site constant. If it is used in a framework, this constant will need to be calibrated and verified for all the geotechnical domains on a operation.

In Equation 16, the predictive model for initial flyrock velocity is based on the assumption that the rock's velocity is generated by an impulse (Gibson & George, 2001).

Launch velocity (V_o):

$$V_o = \frac{3 \times P_e \times VOD^2 \times \Delta t}{32 \times de \times P_r}$$ *Equation 16*

Where: V_o is the initial launch velocity (m.s^{-1}).
P_e is the density of the explosive (g/cc).
VOD is the velocity of detonation (m.s^{-1}).
de is the equivalent diameter of the fragment (mm).
Δt is the length of time of the impulse (ms).
P_r is rock density (kg/m^3).

In the paper, Gibson and George (2001) proposed that *Δt* is determined from the analysis of captured flyrock data.

McKenzie (2009, 2022) again build on the work done by Lundborg (1974) for the launch velocity of flyrock. McKenzie (2009, 2022) adjusted the units, so it is in the same metric form. Furthermore, McKenzie (2009, 2022) also correlated Lundborg (1974) velocity coefficients with the SDOB metric to take confinement of the explosive charge into account. This is captured in Equation 17 and Equation 18.

Velocity Coefficient (K_v):

$$K_v = 0.0728 \times SDOB^{-3.251}$$ *Equation 17*

Launch velocity (V_o):

$$V_o = K_v \times \left(\frac{d}{Xf}\right) \times \left(\frac{2.6}{P_r}\right)$$ *Equation 18*

Where: *Kv* is the velocity coefficient.
V_o is the initial launch velocity (m.s^{-1}).
P_r is the density of the rock (kg/m^3).
d is the hole diameter (mm).
Xf is the fragment size (mm).

Blair (2022) stated that McKenzie's equation for velocity does not have a dimension of time. Blair (2022) proposed an alternative as shown in Equation 19.

Launch velocity (V_o):

$$V_o = K \times SDOB^{-3} \times \left(\frac{d \times VOD}{Xf \times P_r}\right) \qquad \textit{Equation 19}$$

Where: V_o is the initial launch velocity (m.s^{-1}).
P_e is the density of the explosive (g/cc).
VOD is the velocity of detonation m.s^{-1})
d is the hole diameter (mm).
Xf is the fragment size (mm).
P_r is rock density (kg/m^3).
K is a dimensionless constant.

However, the constant K still needs to be determined for site conditions, and this can be done according to Blair (2022) through flyrock measurements.

2.6.3 Fragment Size Prediction

Understanding the potential size of the flyrock fragment being ejected from a blast is essential if the forces acting on the fragment, other than gravity, are required to calculate the flyrock trajectory estimations. Lundburg (1974), related the size of the fragment produced to the hole diameter as illustrated in Equation 20. Note that the fragment size was a requirement for the velocity estimate (Equation 11) used by Lundborg (1974).

Fragment size (Xf):

$$Xf = 0.1 \times d^{\frac{2}{3}} \qquad \textit{Equation 20}$$

Where: *Xf* is the flyrock fragment size (mm).
d is the hole diameter (in).

In the model by Gibson and George (2001) the assumption was made that the size of the fragment is known.

Chernigovskii (1985) presumed that the average size of the fragment is equal to the edge of a cube of equal volume to the volume of the parallelepiped that

circumscribe the fragment. Chernigovskii (1985) also stated that the true volume of the fragment is about 2.2 times smaller than the mentioned parallelepiped. This resulted in Equation 21 and Equation 22.

Fragment size (Xf):

$$Xf = 1.3 \times \sqrt[3]{Vf} \qquad \textit{Equation 21}$$

Fragment mass (M):

$$M = \frac{Xf^3}{2.2} \qquad \textit{Equation 22}$$

Where: *Xf* is the flyrock fragment size (mm).
M is the mass of the fragment (kg).
Vf is the true volume of the fragment (m^3).

McKenzie (2009) continued utilising Lundborg (1974) work and the use of the SDOB to establish a fragment size prediction expression (Equation 23).

Fragment size (Xf):

$$Xf = 2.82 \times SDOB^{-2.167} \times \left(\frac{2600}{P_r}\right) \times (d)^{0.667} \times Sf^{0.333} \qquad \textit{Equation 23}$$

Where: *Xf* is the flyrock fragment size (mm).
d is the drill hole diameter (mm).
P_r is the rock density (kg/m^3).
Sf is the shape factor (1.2 is used mostly).

Again in a more recent publication by McKenzie (2022), the equation was updated, using the latest field data (coefficient updated and shape factor removed), as shown in Equation 24.

Fragment size (Xf):

$$Xf = 3 \times SDOB^{-2.167} \times \left(\frac{2600}{P_r}\right) \times (d)^{0.667}$$ *Equation 24:*

2.6.4 Forces Impacting Fragment in Flight

Raina (2023) illustrated in Figure 17, the components that made up the complexity of flyrock. Raina (2023) refers to it as the 'domains' and in the previous section aspects of the 'mine domain' were discussed. In this section the focus will be on the 'air domain'.

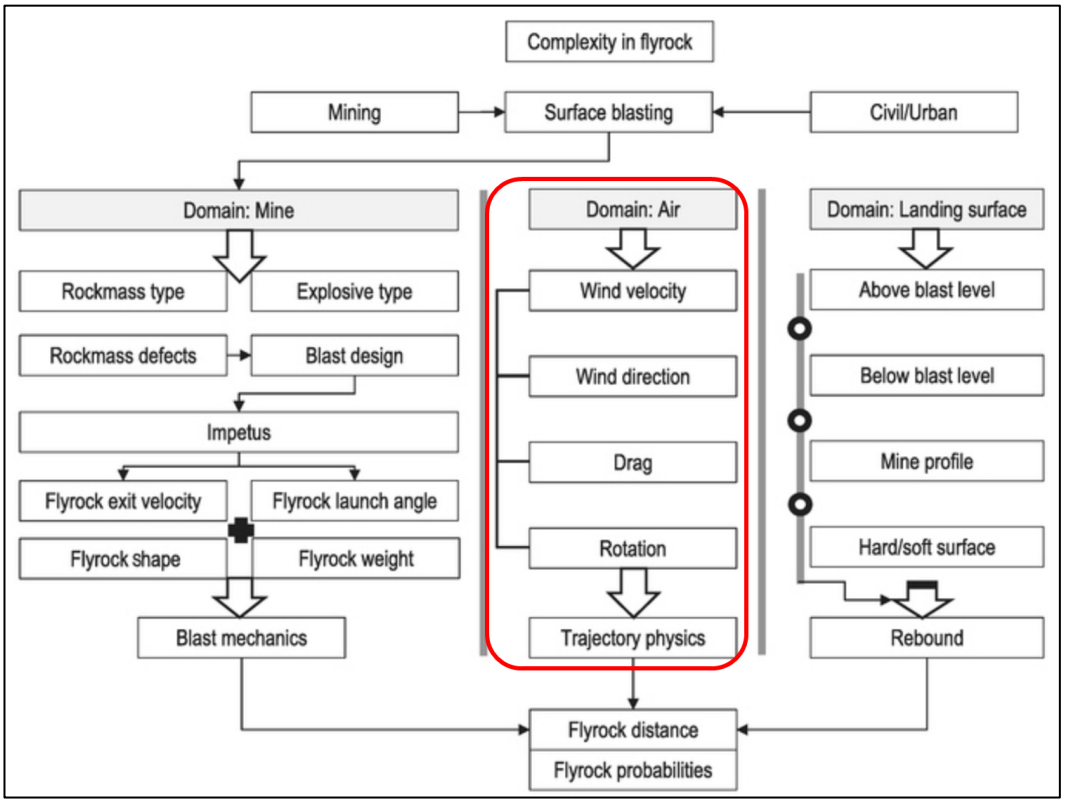

Figure 17: The complexity of flyrock and its prediction (Raina, 2023)

Apart from gravity, various forces act on the fragment while it is in flight through the air. As adapted from Figure 17, three main forces are relevant, namely lift force, drag force and the Magnus effect caused by the rotational force acting on the fragment. No attempts in literature were made to incorporate the Magnus effect into flyrock modelling (Raina, 2023).

One of the more applicable forces acting of the fragment is air drag. Chernigovskii (1985) and Stojadinović, et al. (2013) highlighted the relationship between the effect of air drag and the velocity of the fragment.

Air drag is the resistance force experienced by the fragment while it is moving through the air and is influence by the viscosity of the medium, pressure created, etc. and is expressed in the Reynold's criterion (Chernigovskii, 1985).

The drag force is represented in Equation 25 (Stojadinović, et al., 2011).

Drag force (D_f):

$$D_f = \frac{P_{air} \times S \times C_d \times {V_o}^2}{2} \qquad \textit{Equation 25}$$

Where: D_f is the drag force (N).
S is the cross sectional area of the fragment (m^2).
C_d is the drag coefficient.
V_o is the initial launch velocity ($m.s^{-1}$).
P_{air} is the air density (kg/m^3).

Stojadinović , et al. (2013), determined the drag coefficient from force equilibrium at terminal velocity (Equation 26).

Drag coefficient (C_d):

$$C_d = \frac{2 \times M \times g}{P_{air} \times S \times {V_T}^2} \qquad \textit{Equation 26}$$

Where: C_d is the drag coefficient.
S is the cross sectional area of the fragment (m^2).
M is the mass of the fragment (kg).
V_T is the terminal velocity ($m.s^{-1}$).
g is the gravitational acceleration ($m.s^{-2}$).
P_{air} is the air density (kg/m^3).

Chernigovskii (1985) states that the drag coefficient for flyrock fragments varies between 1.2 to 1.8 with a mean value of 1.5. Chernigovskii (1985) concludes that the quadratic law of resistance can be applied to flyrock and calculates a drag factor (b_d) based on the drag coefficient, fragment size, rock density and air density. If the mean value, 1.5, for drag coefficient is used and the air density of 1.29 kg/m³ (at 0°C and sea level pressure), the drag factor is calculated using Equation 27 (Chernigovskii, 1985).

Drag factor (b_d):

$$b_d = \frac{1.3}{Xf \times P_r} \qquad \textit{Equation 27}$$

Where: b_d is the drag factor.
Xf is the fragment size (mm).
P_r is the rock density (kg/m^3).

The incorporation of the lift force component in the flyrock prediction is limited as it was seen as having a minor influence (Stojadinović, et al., 2011). Blair (2022) however on the other hand, stated that in some cases the lift force can sometimes exceed the drag force.

2.6.5 Trajectory Representation

Chernigovskii (1985) formulated the representation of the motion of a fragment using an orthogonal co-ordinate system as illustrated in Figure 18. From these differential equations were formulated to represent the motion of the fragment with respect to the z and y axis (Equation 28).

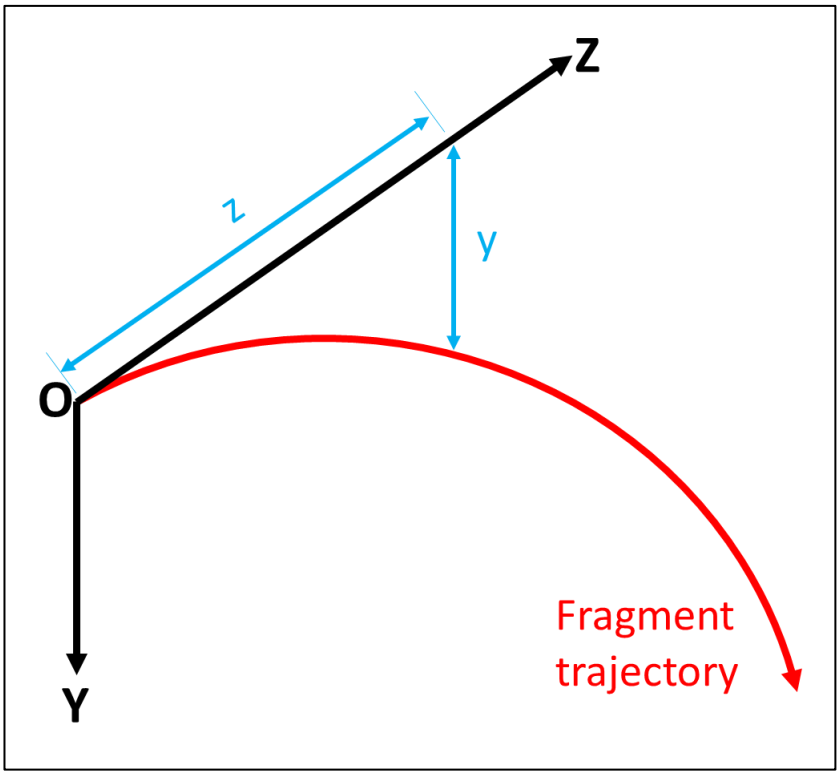

Figure 18: Oblique-angled system of co-ordinates (Chernigovskii, 1985)

Trajectory equation:

$$\begin{pmatrix} z = \frac{1}{b_d} \times \ln(1 + b_d \times V_o \times t) \\ y = \frac{1}{b_d} \times \ln\left(\frac{e^{2 \times t \times \sqrt{b_d \times g}} + 1}{2 \times e^{t \times \sqrt{b_d \times g}}}\right) \end{pmatrix}$$

Equation 28

Where: *z* is the distance in the direction of projection (m)

y is the distance of fall of the fragment vertically (m)

b_d is the drag factor.

V_o is the initial launch velocity ($m.s^{-1}$).

g is the gravitational acceleration ($m.s^{-2}$).

t is the time component (sec).

Using Equation 28 in a numerical method, the full trajectory can be estimated and plotted. Stojadinović, et al. (2011) also presented a numerical solution based on differential equations with the base expressions represented in Equation 29.

Trajectory equation:

$$\begin{pmatrix} M\ddot{x} = -\left(\frac{P_{air} \times S \times C_d \times {V_o}^2}{2}\right) \times \cos\theta \\ M\ddot{y} = -M \times g - \left(\frac{P_{air} \times S \times C_d \times {V_o}^2}{2}\right) \times \sin\theta \end{pmatrix}$$

Equation 29

Where: $M\ddot{x}$ is the horizontal component of the system acceleration (m.s^{-2})

$M\ddot{y}$ is the vertical component of the system acceleration (m.s^{-2})

S is the cross-sectional area of the fragment (m^2).

C_d is the drag coefficient.

V_o is the initial launch velocity (m.s^{-1}).

P_{air} is the air density (kg/m^3).

g is the gravitational acceleration (m.s^{-2}).

θ is the ejection angle with the horizonal axis (°).

The system, based on Equation 29, is then further expanded to derive a set of differential equations (Equation 30).

Trajectory equation:

$$\begin{pmatrix} \frac{dv}{dt} = -g \times \sin\theta - \left(\frac{P_{air} \times S \times C_d \times {V_o}^2}{2}\right) \\ \frac{d\theta}{dt} = -\frac{g \times \cos\theta}{v} \\ \frac{dx}{dt} = v \times \cos\theta \\ \frac{dy}{dt} = v \times \sin\theta \end{pmatrix}$$

Equation 30

This set of equations can be solved at discrete timesteps using a fourth-order Runge-Kutta algorithm (Stojadinović, et al., 2011). The graphical representation of the co-ordinate output at the discrete points represents the trajectory of the fragment. The two methods described so far utilises differential equations that is solved using numerical methods.

Chudinov (2005, 2010, 2011, 2014, 2016, 2019, 2021, 2022, 2024) presented approximate analytical equations to describe a projectiles motion with the drag force applied. The work is not directly related to flyrock but Little and Blair (2010) as well as Blair (2017) do refer to work of Chudinov (2005).

The process of establishing the analytical equations is complex, but the derived equations are basic enough so it can be utilised even with a calculator. Results obtained were compared to numerical methods and the variances reported was in most cases less than one percent (Chudinov, 2022).

The fragment is treated as a point mass, but the effect of the drag force is applied by the inclusion of a constant that Chudinov (2022) refers to as the proportionality factor derived in Equation 31. It is closely linked to Equation 26.

Proportionality factor (k):

$$k = \frac{p_{air} \times C_d \times S}{2 \times M \times g} \qquad \textit{Equation 31}$$

Where: k is the proportionality factor.
P_{air} is the air density (kg/m^3).
C_d is the drag coefficient.
S is the cross sectional area of the fragment (m^2).
M is the mass of the fragment (kg).
g is the gravitational acceleration (m.s^{-2}).

Equation 32 is the set of derived equations to calculate the trajectory parameters.

Trajectory equation:

Equation 32

$$
\left(\begin{array}{c}
H = \dfrac{{V_o}^2 \times \sin^2\theta}{g \times \left(2 + k \times {V_o}^2 \sin\theta\right)} \\
\\
T = 2 \times \sqrt{\dfrac{2 \times H}{g}} \\
\\
V_a = \dfrac{V_o \times \cos\theta}{\sqrt{1 + k \times {V_o}^2 \times \left(\sin\theta + \cos^2\theta \times \ln\left(\dfrac{\theta}{2} + \dfrac{\pi}{4}\right)\right)}} \\
\\
L = Lmax = V_a \times T \\
\\
t_a = \dfrac{T - k \times H \times V_a}{2} \\
\\
x_a = \sqrt{L \times H \times \cot\theta} \\
\\
\theta_i = \tan^{-1}\left(\dfrac{L \times H}{(L - x_a)^2}\right) \\
\\
v_i = V(\theta) \\
\\
y(x) = \dfrac{H \times (L - x)}{{x_a}^2 + (L - 2 \times x_a) \times x}
\end{array}\right)
$$

Where:

H is the trajectory apex height (m).

T is the time of flight (sec).

V_a is the velocity at apex ($m.s^{-1}$).

L is the horizontal range (m).

t_a is the time to apex (sec).

x_a is the horizontal range to the apex (m).

Θ_i is the impact angle (°).

V_i is the impact velocity ($m.s^{-1}$).

y(x) is vertical position given a horizontal distance *x* (m).

The parameters are also indicated in Figure 19.

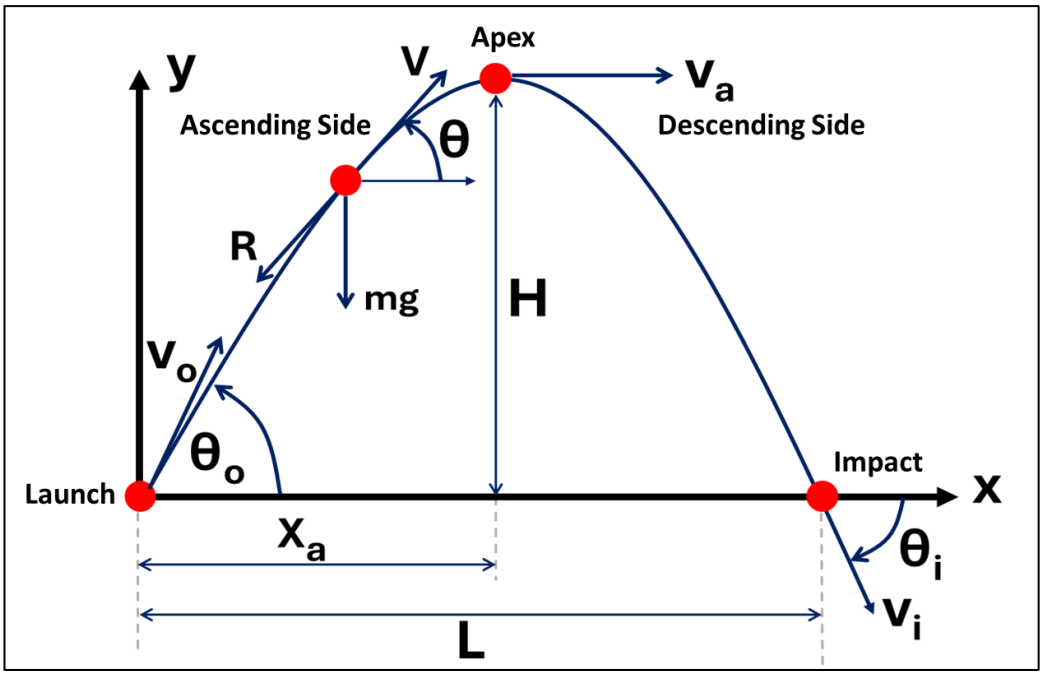

Figure 19: Chudinov's trajectory components (Chudinov, 2022)

Chudinov also derived equations for the vertical asymptote, optimal launch angle and projectile trajectories envelope Chudinov (2005, 2010, 2016).

2.6.6 Flyrock Footprint

Understanding the spread of projectiles from a blast can assist in evaluating the risk and associated probabilities it poses to the personnel clearance criteria. In the early work by Lundborg (1979), 'footprint' curves depicting the maximum flyrock range associated with different fragment sizes for different hole diameters were established (Figure 20).

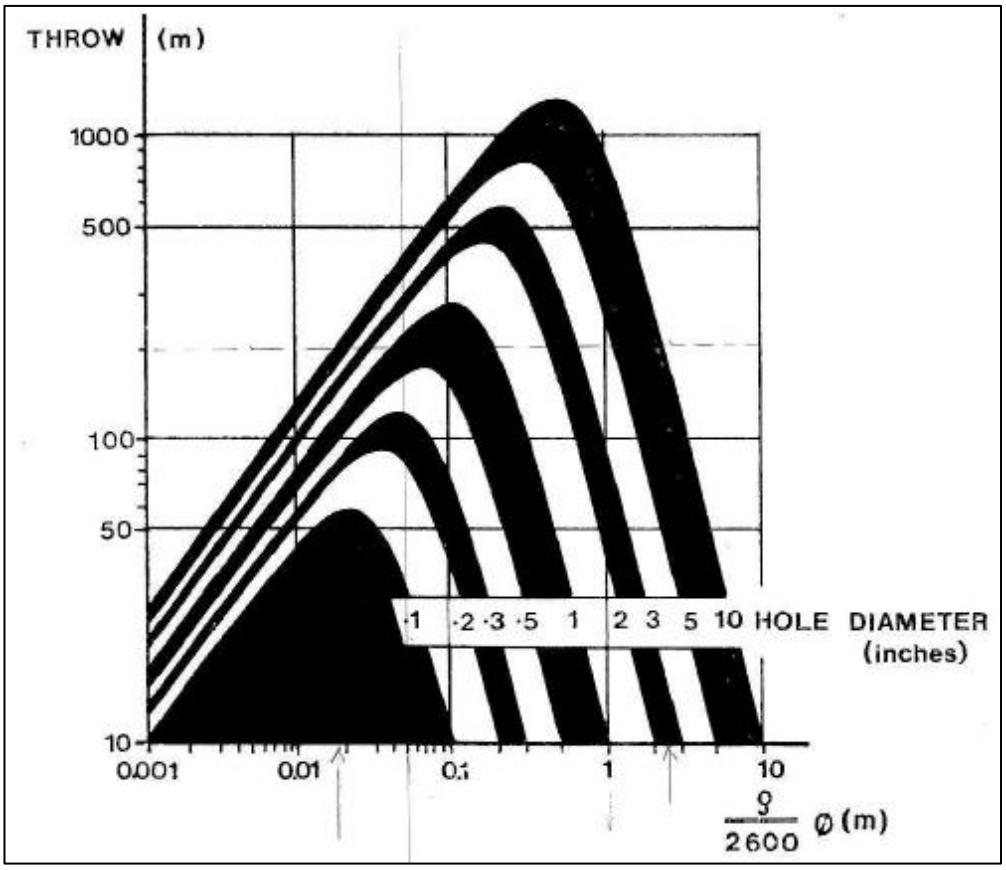

Figure 20: Maximum throw vs boulder size and borehole diameter (Lundborg, 1979)

McKenzie (2009) built upon Lundborg's (1979) work by integrating the SDOB to estimate flyrock fragment size and maximum range, thereby defining the flyrock footprint. McKenzie (2009) also combined it to show how it is linked to setting the required clearance distance taking the factor of safety into consideration (Figure 21).

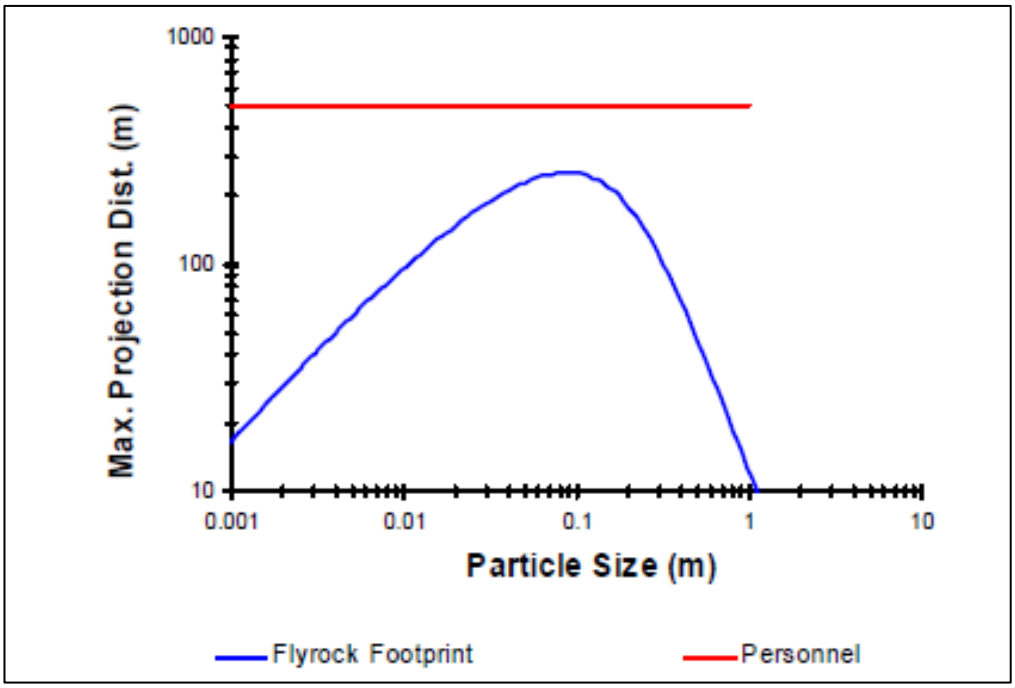

Figure 21: Flyrock footprint related to personnel clearance criteria (McKenzie, 2009)

By normalising the flyrock footprint the maximum projected distances associated with a range of fragment sizes, for any SDOB, is represented on a single output (McKenzie, 2022). If actual flyrock data is collected, it can be used to validate the risk using the normalised flyrock footprint. This was recently utilised by Foster (2024) to determine the required exclusion zones around misfired holes in blasted muckpiles, as illustrated in Figure 22.

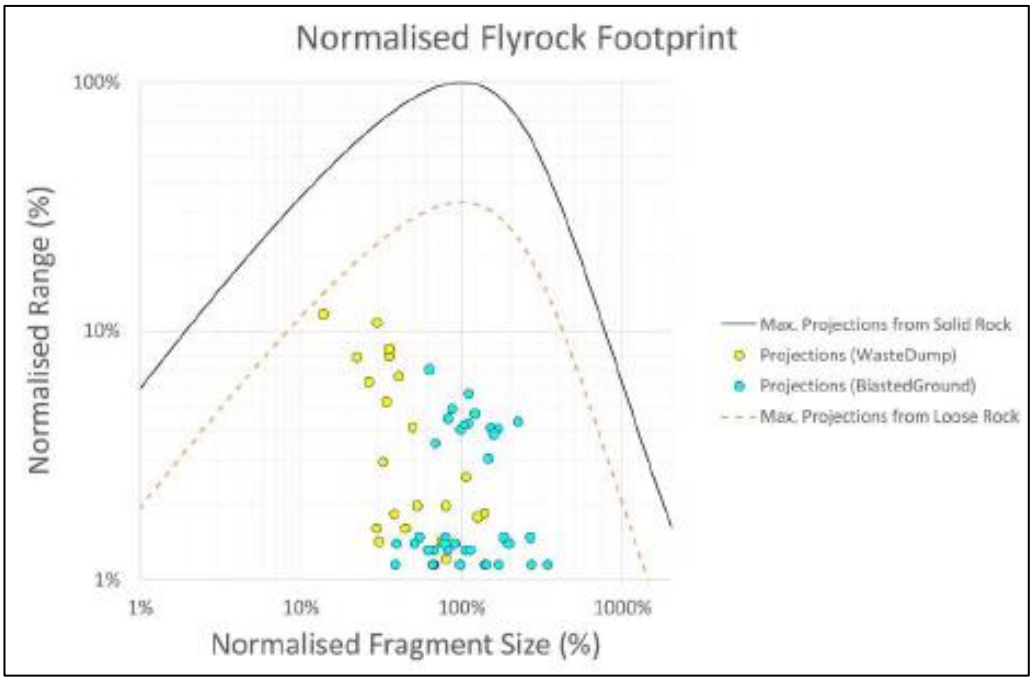

Figure 22: Comparison of maximum flyrock distances from blasted muckpile (Foster, 2024)

Figure 22 shows the designed normalised flyrock footprints for both solid rock and loose rock. The yellow and blue dots represent actual measured fragments. This indicates that the actual fragments produced were within the design footprint (Foster, 2024).

2.7 Flyrock Modelling: Discussion of Reviewed Models Used in the Project

In current commercial packages mainly two flyrock models are utilised - McKenzie (2009) and Richards and Moore (2002). Maptek's BlastLogic flyrock module (used in this project) integrates both these two widely referenced models.

The McKenzie (2009) model builds upon foundational work by Lundborg (1974) and Chernigovskii (1985), incorporating drag forces, fragment geometry, and the scaled depth of burial (SDOB) to estimate launch velocity and flyrock range. The model employs empirical correlations and numerical methods to simulate realistic trajectories, accounting for air resistance and confinement effects.

The Richards and Moore (2002) model extends the kinematic approach of Workman and Calder (1994), estimating launch velocity based on scaled burden and a site-specific constant. It simplifies trajectory modelling by considering only gravitational forces, making it computationally efficient but less accurate under complex conditions.

Chudinov (2022) offers simplified analytical equations with <1% variance from numerical methods to suitably estimate flyrock trajectories and its components when used in conjunction with input equations from Chernigovskii (1985) and McKenzie (2022).

2.8 Flyrock Monitoring and Measuring Techniques

The ability to monitor and measure actual flyorck occurances is a critical component of a flyrock framework. Van der Walt and Spiteri (2020) reviewed the shortcomings of measuring methods to validate the prediction models, stating that a more precise, reliable, and unbiased measurement method is necessary to accurately quantify the actual distance traveled by flyrock.

McKenzie, et al. (2015) states that one of the potential preventive measures of flyrock occurrences is continuous improvement in the blasting process. This depends on video capturing, storage of footage, and analysis and classification of the recorded blasts. Capturing data from flyrock events, even if it does not result in an accident, can substantially improve the accuracy and reliability of current predictive models (Zhou, et al., 2024).

The standards and use of instrumentation to measure and evaluate blast outcomes for ground vibration and air overpressure is well established. However, none exists for flyrock (Raina, 2023). In most cases historically, high-speed cameras were used to approximate the launch angles and initial velocities, which were then used to describe the projectile's trajectory and estimate the potential range (Van Der Walt & Spiteri, 2020; Mishra, et al., 2023).

High-speed cameras are valuable tools for analysing flyrock in surface mining, but come with several limitations:

- Although high-speed cameras can capture rapid events, the frame rate and resolution may still be insufficient to accurately track smaller fragments or very fast-moving flyrock (Mishra, et al., 2023).
- The limited field of view of high-speed cameras can restrict the ability to capture the entire trajectory of flyrock, especially if the flyrock travels a significant distance (Van Der Walt & Spiteri, 2020).
- Dust, fume, and lighting conditions during blasting can obscure the camera's view, making it difficult to obtain clear footage (Adermann, et al., 2015); and
- High-speed cameras are expensive and require regular maintenance to ensure functionality is sustained in harsh mining environments.

Another popular approach to monitor flyrock is by visual observation of flyrock occurrence using blast videos or with the naked eye (Van Der Walt & Spiteri, 2020). This is usually done from an observation point during blasting. One method of visual observation to determine the likelihood for flyrock occurrence from video footage is the violence factor. The violence factor is a way to evaluate the blast performance, from a blast video, by comparing the height of vertical material movement (sometimes in the form of blow-outs) of a blast to the associated bench height (Konya & Konya, 2020). Table 8 shows the violence factor ranges with associated breakage mechanisms.

Table 8: Violence factor selection criteria (Konya & Konya, 2020)

Vertical Displacement	Violence Factor	Breakage Mechanism	Expected Performance	Environmental Performance
No Displacement	0	Flexural failure with axisymmetric bending	Best Performance	Consistent and lowest PPV & AP
< 0,5 x Bench Height	1	Flexural failure with axisymmetric bending	Good Performance	Low PPV & AP
> 0,5 & < 1 x Bench Height	2	flexural failure with cantilever bending	Increase in boulders; toe left at grade; minor backbreak around 1 x the burden	Moderate PPV & AP
> 1 & < 2 x Bench Height	3	Cratering	Further increase in boulders; large toe left at grade and breakage below borehole; backbreak btween 1 and 3 x burden	High PPV & AP
> 2 x Bench Height	4	Cratering	Terrible fragmentation with mostly boulders and fines; severe breakage below grade under holes and severe toe between holes; backbreak over 3 x burden	Extreme PPV & AP

A violence factor of three and higher is linked to cratering which is a major mechanism for flyrock. Table 9 is an adaptation, by Anglo American Plc, of Table 8. The changes introduced were to increase the measurements to full bench

increments rather that half bench increments and referred to the new assessment as the Vertical Displacement Factor (VDF) (Tordoir, 2023). This was done mainly for simplification of the estimation from blast videos.

Table 9: Adjusted table for VDF

Konya's original Violence Factor					Anglo's Adaptation	
Vertical Displacement	Violence Factor (Konya)	Breakage Mechanism	Expected Performance	Environmental Performance	Vertical Displacement Factor (VDF)	Potential SDOB Range
No Displacement	0	Flexural failure with axisymmetric bending	Best Performance	Consistent and lowest PPV & Air Overpressure	No Displacement	1,43-1,82
< 0,5 x Bench Height	1	Flexural failure with axisymmetric bending	Good Performance	Low PPV & Air Overpressure	< 1 x Bench Height	1,11-1,42
> 0,5 & < 1 x Bench Height	2	flexural failure with cantilever bending	Increase in boulders; toe left at grade; minor backbreak around 1 x the burden	Moderate PPV & Air Overpressure	> 1 & < 2 x Bench Height	0,91-1,10
> 1 & < 2 x Bench Height	3	Cratering	Further increase in boulders; large toe left at grade and breakage below borehole; backbreak btween 1 and 3 x burden	High PPV & Air Overpressure	> 3 & < 4 x Bench Height	0,61-0,90
> 2 x Bench Height	4	Cratering	Terrible fragmentation with mostly boulders and fines; severe breakage below grade under holes and severe toe between holes; backbreak over 3 x burden	Extreme PPV & Air Overpressure	> 4 x Bench Height	0 -0,6

Part of this study is to verify the correlation between the SDOB and VDF and to see if the VDF is a good indicator for potential flyrock from cratering as stated in Table 9.

Integrated and automated processes for reviewing blasting outcomes from video footage have been developed, especially for detection of flyrock from hole collar ejections (McKenzie, et al., 2015). This patented approach uses computer vision methods to automatic track the trajectory of fragments from launch positions to apexes and estimates launch velocity (Papillon, et al., 2018). A screenshot of the application is displayed in Figure 23.

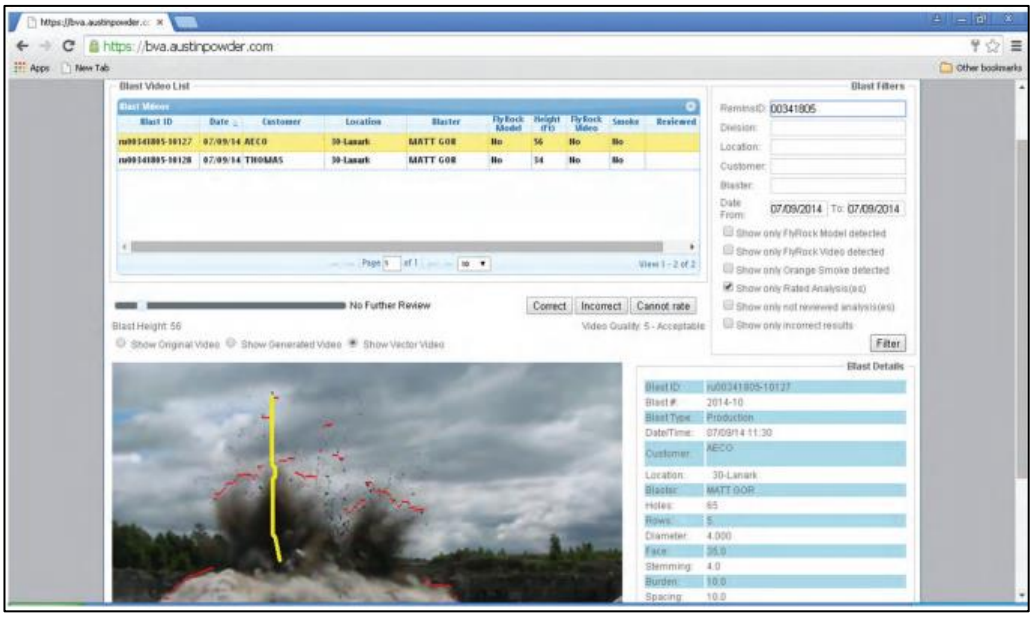

Figure 23: A report generated by the blast video analysis (BVA) system (McKenzie, et al., 2015)

The objective of this system is not to determine flyrock traveling distances from the video footage but use the system to automatically rate the blasts in terms of how violent the collar ejections were (early warning indicators of a flyrock risk). This is in line with the violent factor observations.

Van Der Walt (2019) investigated various other techniques, including photogrammetry, Radio Detection and Ranging (RADAR), Light Detection and Ranging (LiDAR), Visual Detection and Ranging (ViDAR) and various optical detection systems. Based on the results, Van Der Walt (2019) developed a conceptual framework for the quantification of the motion of flyrock. The proposed concept covered three main phases, namely:

- Data acquisition.
- Image processing and data analysis; and
- Data interpretation.

The detailed work has set the foundation for further advancement with the aim to allow sites to generate a flyrock database, and allow researchers to conduct quantitative research studies on flyrock occurances.

Using some of the traditional visual methods to analyse blast videos for flyrock can be time consuming (Papillon, et al., 2018; Van Der Walt, 2019). Technological advancement and improvements including artificial intelligence have presented opportunities to improve flyrock monitoring and measuring techniques. For example, drone technology, used appropriately can be deployed to monitor blasts from positions that were previously impossible to reach (Bhatawdekar, et al., 2018; Bamford, 2021).

Furthermore, video analysis and monitoring services can be automated to reduce the time spend on analysis significantly (Papillon, et al., 2018). Orica Digital Solutions developed BlastVision® (Muñoz, et al., 2024). BlastVision® is a blast performance analytics tool, that utilises high-speed drone footage of blasts and converts it into analytical data for decision-making. The system uses a three step workflow depicted in the Figure 24.

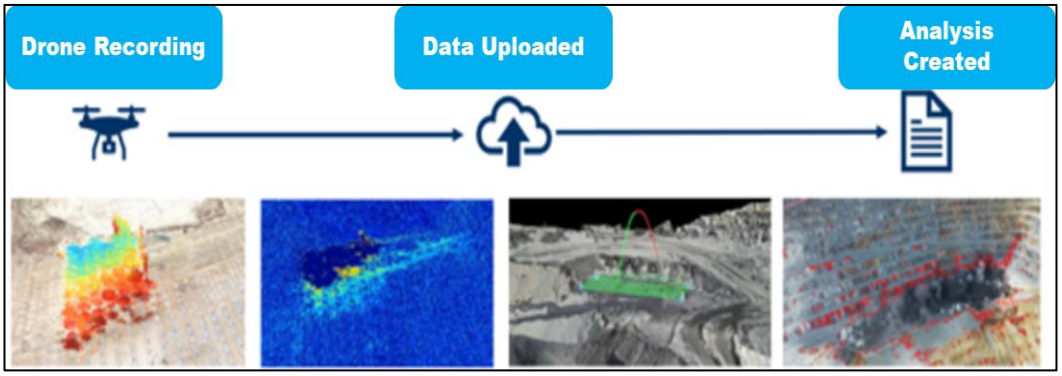

Figure 24: Workflow progress of BlastVision® and types of visualisations (GroundProbe - Orica Digital Solutions, 2024)

These process steps are:

I. Drone recording: High quality (4K+) that was captured from the correct position relative to blast area, with the initiation of the blast towards the drone.
II. Data uploading: Captured video footage, point cloud of pit and blast pattern polygon is uploaded for analysis; and
III. Analysis creation: The application employs proprietary algorithms to transform video footage into structured data, which is then analysed at the

pixel level to detect surface changes. Visualisation techniques such as luminance change detection and contour analysis are also utilised.

The findings from the analysis are then evaluated by an engineer and a report is generated and return for actioning.

2.9 Chapter Summary

This chapter focused on discussing previous work on the topic of flyrock. The sources and mechanisms of flyrock was explained. The chapter also focused on the past and present modelling methods. The prediction models used in commercial drill and blast software were broken down into the categories for comparison and review. The categories covered launch velocities, fragment size estimations, forces acting on projectiles, range predictions, and representation of the trajectory.

It is evident from the review of commercial drill and blast software that two predictive models are most commonly utilised: McKenzie (2009) and Richards and Moore (2002). Both models are based on kinematic equations, with the key distinction being that the McKenzie (2009) model accounts for air resistance. Riana's (2023) comparative analysis revealed that the McKenzie model showed a stronger correlation with actual flyrock measurements compared to the Richards and Moore (2002) model. The concept of the flyrock footprint as a visual representation of the range and size of flyrock was also elaborated on in this chapter.

Monitoring techniques from video analysis were reviewed. The concept of the violence factor as a visual key performance indicator from blast videos was also introduced. The possible automation of video analysis through a monitoring services or system such as Orica Digital Solutions' BlastVision® were also explored.

The objectives of this study are to validate current prediction models being utilised in the prescribed software, establishing a method and guideline to monitor and measure flyrock as well as to create a flyrock risk reporting dashboard. The topics

covered in the literature review supply the necessary background for the analysis to follow.

3 RESEARCH METHODS

3.1 Introduction

This chapter introduces the methodological framework used to develop a strategy for improving awareness of flyrock risks during the drilling and blasting process at Anglo American Plc's surface mining operations. It will present an account of the methods to be followed in achieving the aim and objectives of this study.

3.2 Research Approach

There are generally three types of research methods to follow when collecting and analysing data. These are the qualitative, quantitative and mixed methods approach (Taherdoost, 2022). The quantitative approach was selected for this study to facilitate in predicting outcomes and measuring relationships between variables by using numerical data collection and statistical analysis. Various literature on flyrock modelling and monitoring methods were reviewed to establish a basis for evaluating the components of the framework.

3.3 Data Collection

Figure 25 was designed to illustrate the methodological process flow followed for obtaining data for analysis.

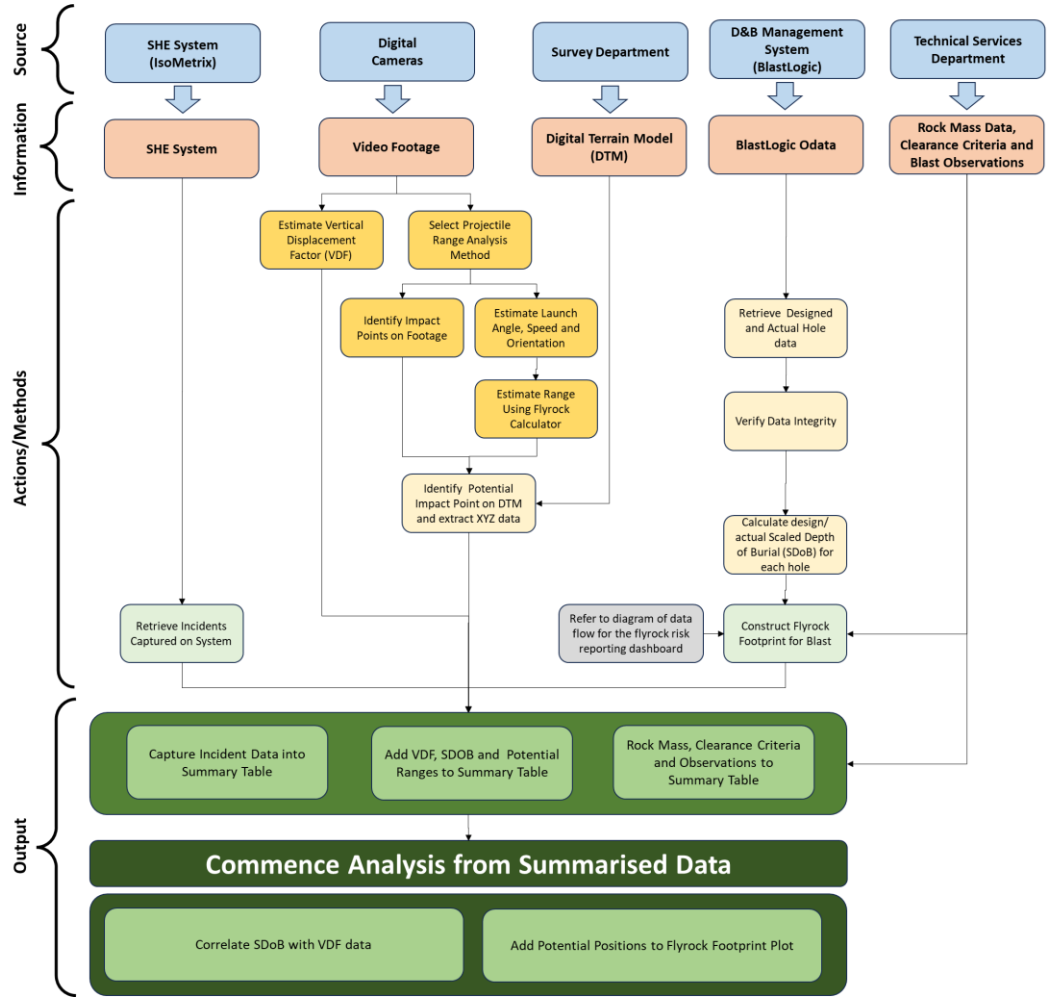

Figure 25: Methodology used in study for analysis

As shown in Figure 25, data for the quantitative analysis was extracted from various Anglo American Plc surface operations for the period of May 2023 to November 2024. The following information was retrieved from five main sources:

I. Reported flyrock incidents were extracted from Anglo American Plc's SHE system, IsoMetrix (IsoMetrix, 2025).

II. Video footage was obtained from different camera sources (drones, pit cameras, GoPro cameras, and high-speed cameras (Figure 26).

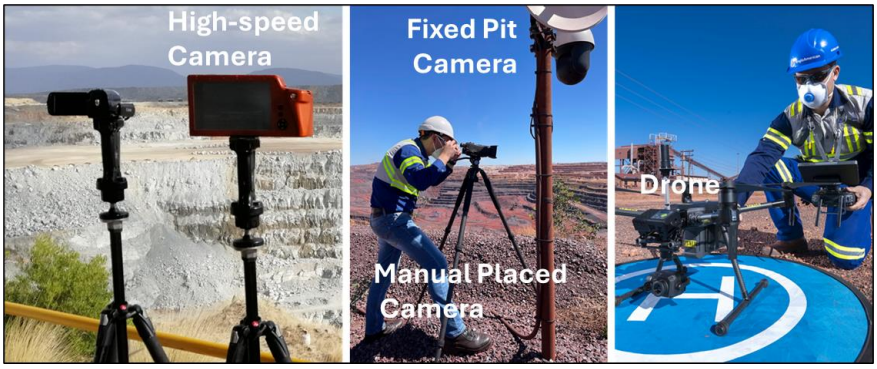

Figure 26: Various types of cameras used to capture footage of blasts

III. Latest applicable surveyed digital terrain models were supplied from the survey departments.

IV. Blast design and actual charge parameters were extracted from the drill and blast management system, BlastLogic (Maptek, 2024); and

V. The technical services departments (geology, rock engineering and drill and blast technical) supplied the rock mass, clearance criteria and other blast observation data (Table 10).

Table 10: Data gathered for analysis

General Data	Rock Mass Data	Observation Data
Mine/Site	Main Rock Density	Blast Type
Commodity	Uniaxial Compressive Strength (UCS)	Hole Diameter (Design parameters)
Pattern ID		Collar Conditions
Date of Blast		Loose Rocks on Bench
Time of Blast		Free Face Status
Video Source		Face Burst Observed
Incident Reference Number		Vertical Displacement Factor
		Water in Holes Status
		Stemming Material Type
		Actual Measured Projectile Range
		Actual Size Measured
		Site Fmax for Blast
		Blast Exclusion Zone

The data from Table 10 was used to do the verification on the prediction models utilised in the software application, correlate findings with observations and limits. Condition data such as free face status, water status, collar conditions and loose rocks on bench were captured but was not used in the analysis for this study. The decision to exclude specific data from the current analysis was guided by the need to maintain a focused scope aligned with the study's primary objectives. While the data collected holds potential for enhancing future iterations of the framework (particularly in refining flyrock prediction models), it was deemed beyond the analytical boundaries of this phase.

Video playback and analysis were done utilising various video modelling and annotation applications such as Kinovea (Kinovea, 2023), Tracker (Brown, et al., 2025), Vernier Video Analysis (Vernier, 2025), and ProAnalyst 2023 (Xcitex Inc., 2025). Measurements using supplied digital terrain models were done with Deswik.CAD (Deswik, 2025).

An accompanying flyrock calculator (Appendix C) was developed as part of the requirements stipulated in Figure 24. The calculator assisted in estimating the impact location if launch angle and velocity were the only observed inputs from the videos.

3.4 Data Validation Process

In the BlastLogic process, discussed in the literature (Figure 9), point two caters for validation of hole data. Similarly, point three also allows for verification using quality assurance. These points were critical in ensuring data integrity not only for this study, but the drill and blast process in general. However, it is worth mentioning that these points required human intervention, and errors were observed in the data. As part of the flyrock risk reporting dashboard, additional means of error checking were incorporated to highlight outliers for investigation or fixing.

3.5 Data Analysis Approach

The approach adopted for extraction, preparation and analysis of data from the sources discussed is illustrated in Figure 25. However, a few of the key steps adopted for the data analysis approach are discussed in more detail in this section.

3.5.1 Review Blast Video

Blast video was retrieved from the system and reviewed. The blast video review process included, but not limited to the following steps:

- Upload video in video playback and analysis application.
- Start by identifying impact points on the video.
- Match impact points to location on digital terrain model (DTM).
- Establish a reference object for scaling – ideally bench close to blast; and
- Estimate VDF as indicated in Figure 27.



Figure 27: Review blast video

The vertical displacement (blow-outs), from the top of the blast bench, was measured as increments of the original pre-blast bench height as indicated in Figure 27. This measurement was captured as the VDF number for the blast.

3.5.2 Identify Projectile Impact Point

The projectile range analysis method was selected. In the case of Figure 28 this was by identifying impact location.

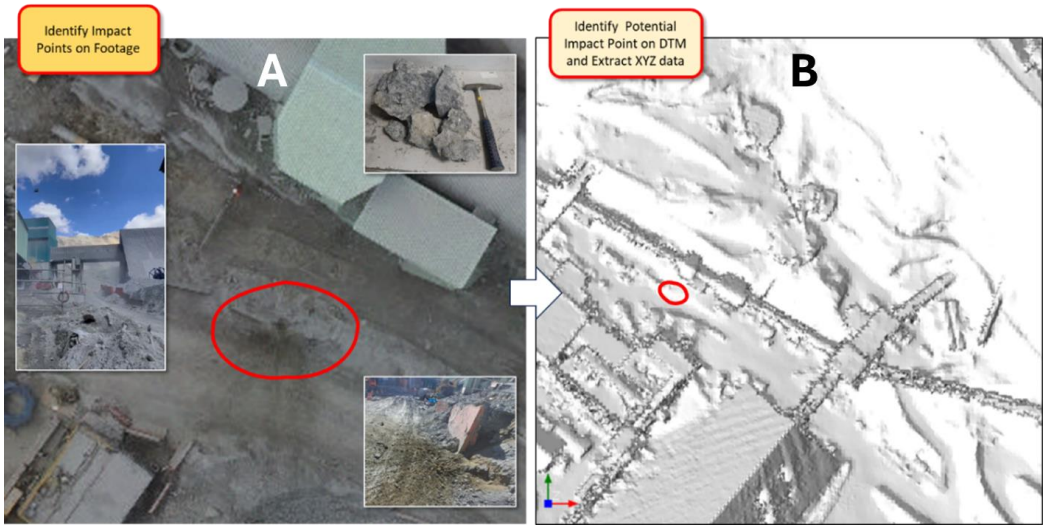

Figure 28: Identify projectile impact point

In Figure 28A, the impact point was observed in the video footage and the impact point co-ordinates were extracted from the DTM (Figure 28B), using the design software.

3.5.3 Verify Data from BlastLogic

As discussed, part of the flyrock risk reporting dashboard, visual tools were developed in this study to assist in verifying the compliance to plan of the data extracted from BlastLogic. Figure 29 to Figure 31 are snapshots from the visualisations.

The dashboard in Figure 29 compared the design hole locations (grey dots) with the actual drilled hole location (blue dots). The dashboard also indicated which holes were abandoned (holes not drilled or holes drilled but not charged) and how many holes were stemmed.

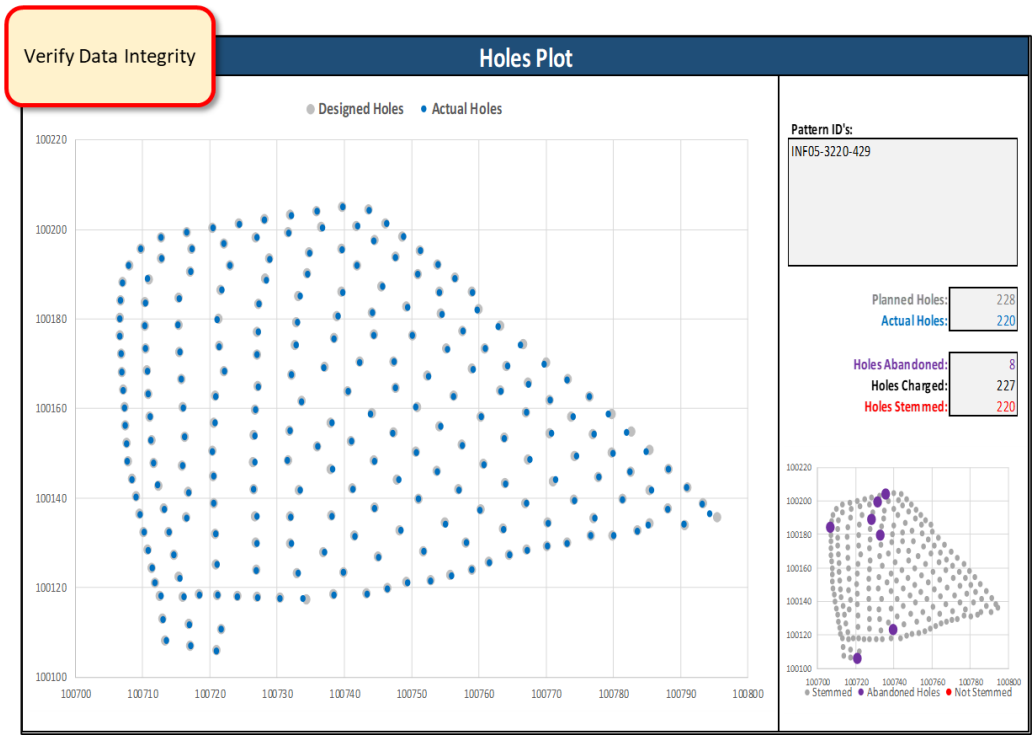

Figure 29: Holes plot of a drill pattern

The dashboard in Figure 30 indicated which holes were out of tolerance if the actual explosive charged mass was compared to the design charged mass per hole. Out of tolerance in this case was more than 10 percent variance.

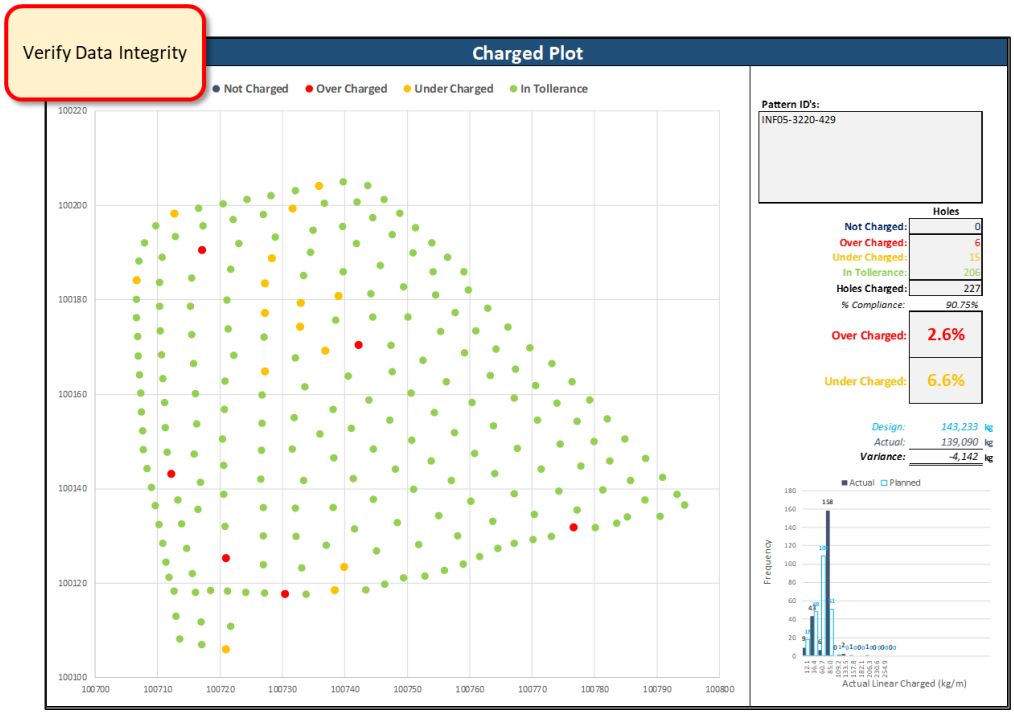

Figure 30: Charged plot of a drill pattern

Finally, the dashboard in Figure 31 highlighted which holes were out of tolerance if the actual stemming length was compared to the design stemming length per hole. Out of tolerance in this case was more than 0.5 m variance.

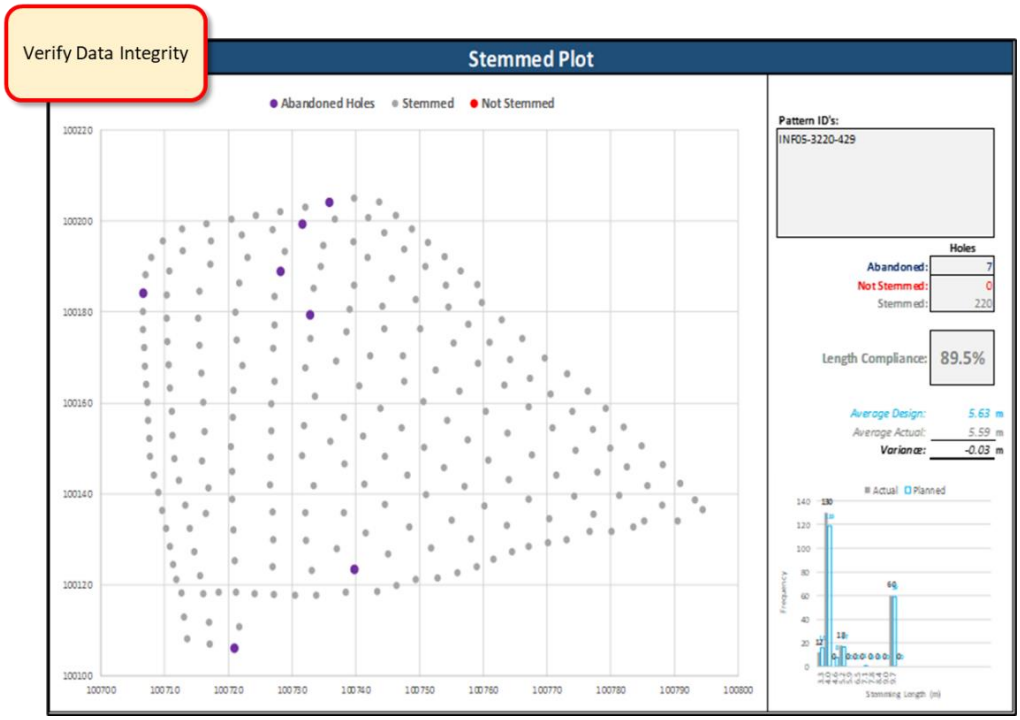

Figure 31: Stemming plot of a pattern

3.5.4 Establish Flyrock Footprint Plot

This step utilised the developed flyrock risk reporting dashboard. Figure 32 was compiled to highlight the flow of data in establishing the flyrock risk reporting dashboard that was used in the data analysis.

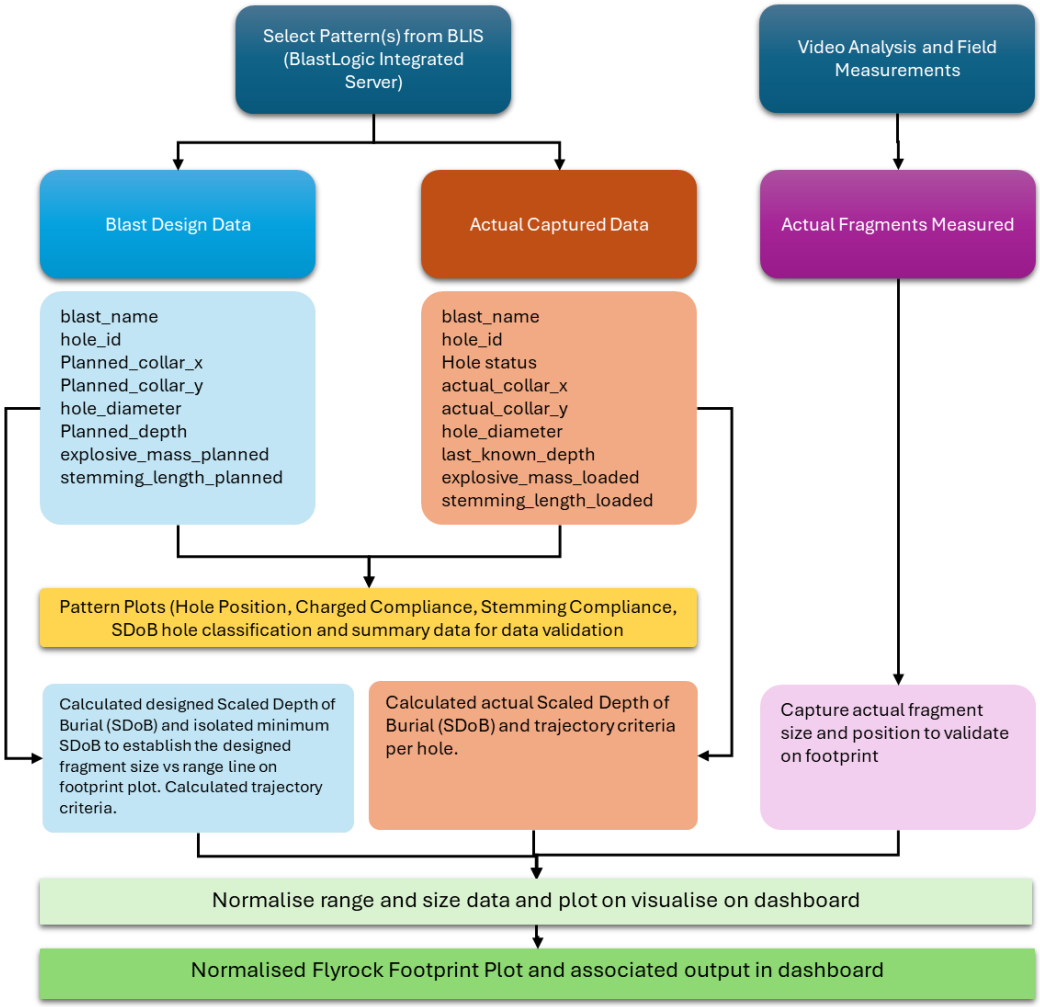

Figure 32: Data flow for the flyrock risk reporting dashboard

The design and actual data were retrieved from BlastLogic Integrated Server (BLIS). The planned data was then used to calculate the SDOB per planned hole. Utilising Equation 24 the potential fragment size, based on the SDOB, was estimated for each hole and subsequently the estimated mass of the fragment, based on Equation 22. A shape factor of 1.2 was used to align with the number that is utilised by the flyrock module in BlastLogic. This allowed the estimation of the proportionality factor based on Equation 31. Estimation of the launch velocity was based on Equation 18, where a rock density of 2 650 kg/m^3 was used. Finally, the trajectory and range were estimated from Equation 32. The hole with the largest range was selected and used to normalise and plot the flyrock design footprint (McKenzie, 2022).

Similarly, the actual captured data was used to get the same criteria as stipulated for the planned data. However, each hole's estimated actual range and fragment size were then normalised and plotted on the same graph as individual red data points. If the actual execution of the design was within tolerance, these red data points on the graph should be just within the footprint as indicated in Figure 33.

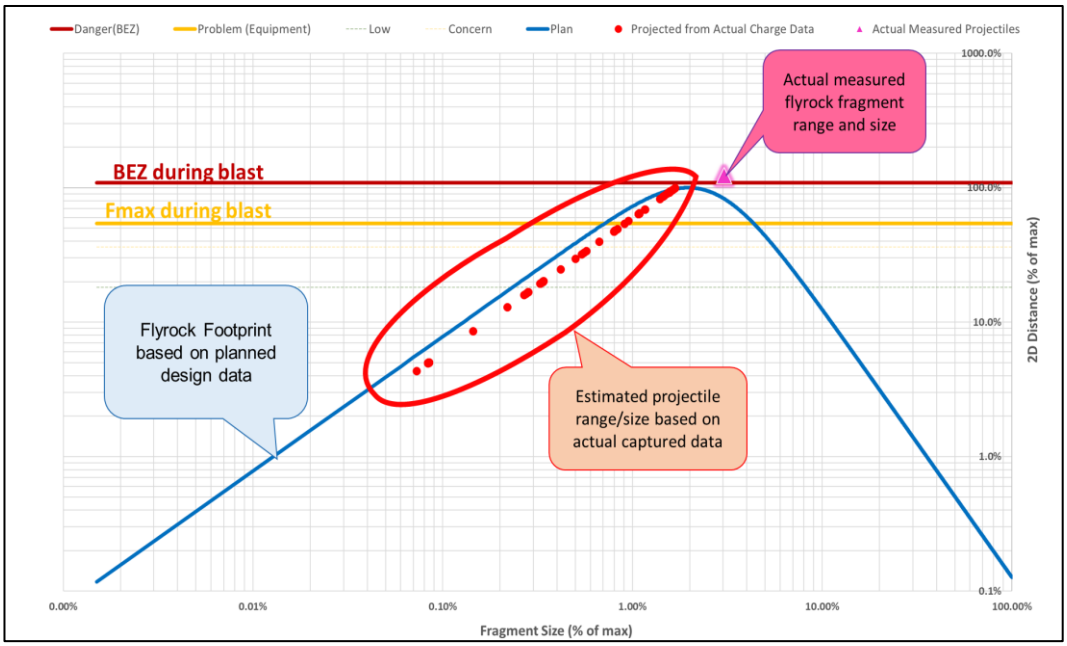

Figure 33: Flyrock footprint graph

Also captured on the footprint graph (Figure 33) were two lines, one for the applicable equipment radius (Fmax) and the other for the blast exclusion zone (people radius – BEZ). Both are based on the approved blast clearance plan that was applicable for the blast. An additional plot that was generated in the process is the SDOB plot which is depicted in Figure 34.

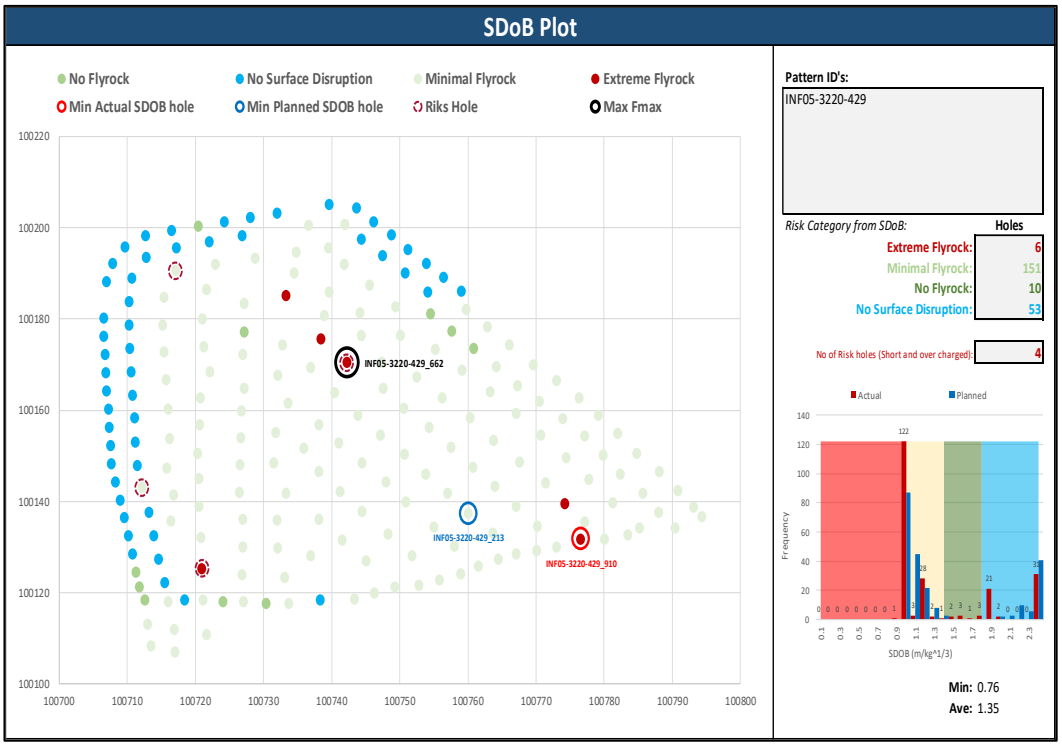

Figure 34: SDOB plot

This plot in Figure 34 was helpful in identifying possible problematic holes. The actual hole colouring was based on the classification of the SDOB as indicated in Figure 15.

Also highlighted on the SDOB plot were the following problematic criteria:

- The hole with the maximum range for both planned and actual data.
- The hole with the minimum calculated SDOB for both planned and actual data; and
- Risk holes, which are holes classified as short and overcharged holes relative to the set tolerances.

An example of the full output of the dashboard is supplied in Appendix D, with a breakdown of the various components on the dashboard.

3.5.5 Setup for BlastVision® Trials

Extracting potential projectile ranges manually from video footage, as per section 3.5.2, can be a time-consuming activity. As part of the study, Orica Digital Solutions' BlastVision®, described in the literature review, was evaluated as a potential video analysis and monitoring services.

As part of the analysis, it was agreed to evaluate two blasts, and the following data were requested by the GroundProbe team in order to assist with the analysis using their proprietary software:

- High quality (60-120 frames per second) and resolution (4K) drone footage of the blast at an angle of roughly 45° between the blasting area and the drone (Figure 35).
- A proper point cloud of the pre-blast area; and
- A polygon representing the outline of the blast pattern.

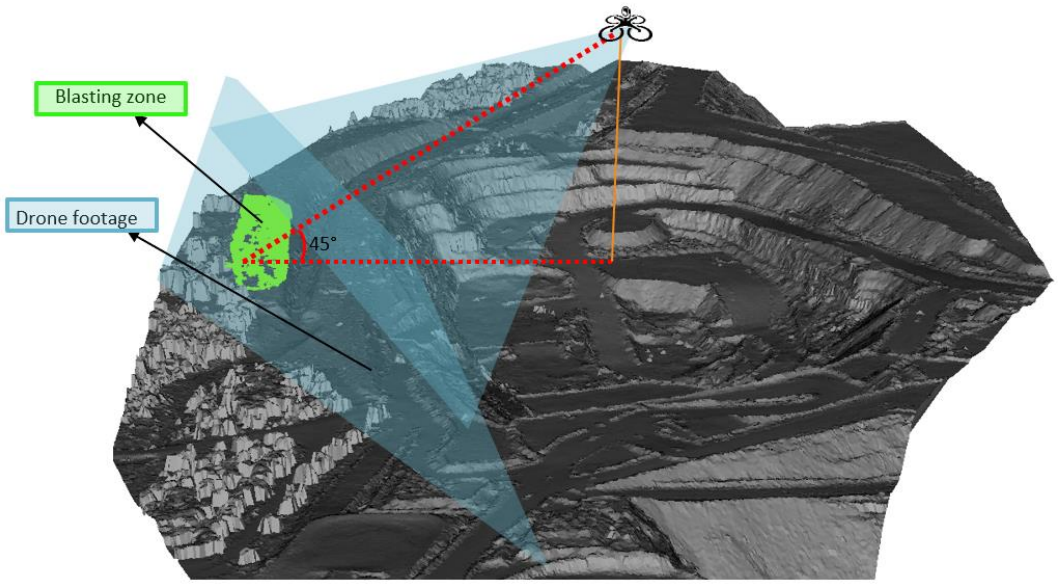

Figure 35: Drone configuration requirement (GroundProbe - Orica Digital Solutions, 2024)

This information was obtained. The same blasts were also manually evaluated, as discussed earlier in the chapter, to do a proper comparison with the findings of the GroundProbe team.

3.6 Chapter Summary

In this chapter the methodology applied for the research design was discussed. A quantitative research approach was used, and data was collected from various sources, including reported flyrock incidents, video footage, digital terrain models, and blast design parameters.

The methods and steps to follow in the analysis of the captured data were set out and the data flow used to establish the flyrock risk reporting dashboard was highlighted. Finally, requirements in order to test potential video analysis and monitoring services were listed.

4 RESULTS AND ANALYSIS

4.1 Introduction

The data obtained from the collection process is presented and discussed in this chapter. The data gathered is validated, summarised and analysed to confirm if there is a link between observable indicators such as the VDF and the potential for flyrock exceedances. Furthermore, the current predictive model used in modelling, as well as the developed flyrock risk reporting dashboard, were analysed to confirm if it is indicating potential flyrock risk. The capturing of blast videos and measuring actual flyrock occurrences are also discussed with the aim to identify improvements in these components.

4.2 Improved Flyrock Footprint Calculation

The establishment of the flyrock risk reporting dashboard was a critical part of the analysis of the data, but also a key output for the developed framework. Verifying if the developed flyrock risk reporting dashboard can accurately duplicate the flyrock ranges produced by the prediction model used in the software application (BlastLogic) was important. For the verification the trajectory and range estimates calculated based on the approach discussed in section 3.5.4 were compared to the range estimates using Equation 9 (which is utilised by BlastLogic). Using one of the observations (incident E from Table 4), a comparison graph of the projected ranges for each hole in the blasted pattern was compiled and shown in Figure 36.

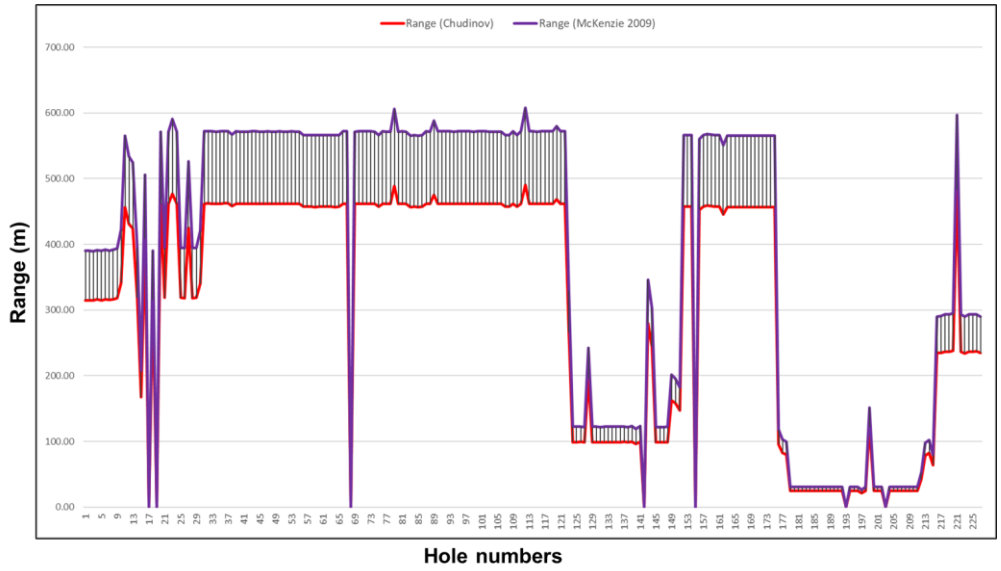

Figure 36: Range comparison graph with error

The purple line in Figure 36 is the estimated ranges based on Equation 9, while the red line represents the estimated ranges as calculated using Equation 32. It clearly indicated a constant variance (19 percent). Data used for the graph depicted in Figure 36 can be found in Appendix A.

It was observed that the approach used in section 3.5.4 excluded the shape factor of the fragment. As a result, the proportionality factor (Equation 31) was amended to include the fragment shape factor in the denominator as shown in Equation 33:

Adjusted proportionality factor (k):

$$k = \frac{p_{air} \times C_d \times S}{2 \times M \times g \times Sf} \qquad \textit{Equation 33}$$

Where: k is the proportionality factor.
P_{air} is the air density (kg/m^3).
C_d is the drag coefficient.
S is the cross-sectional area of the fragment (m^2).
M is the mass of the fragment (kg).
g is the gravitational acceleration (m.s^{-2}).
Sf is the shape factor.

The impact of the adjustment is indicated in the updated comparison graph (Figure 37). Data for the graph in Figure 37 is in Appendix B.

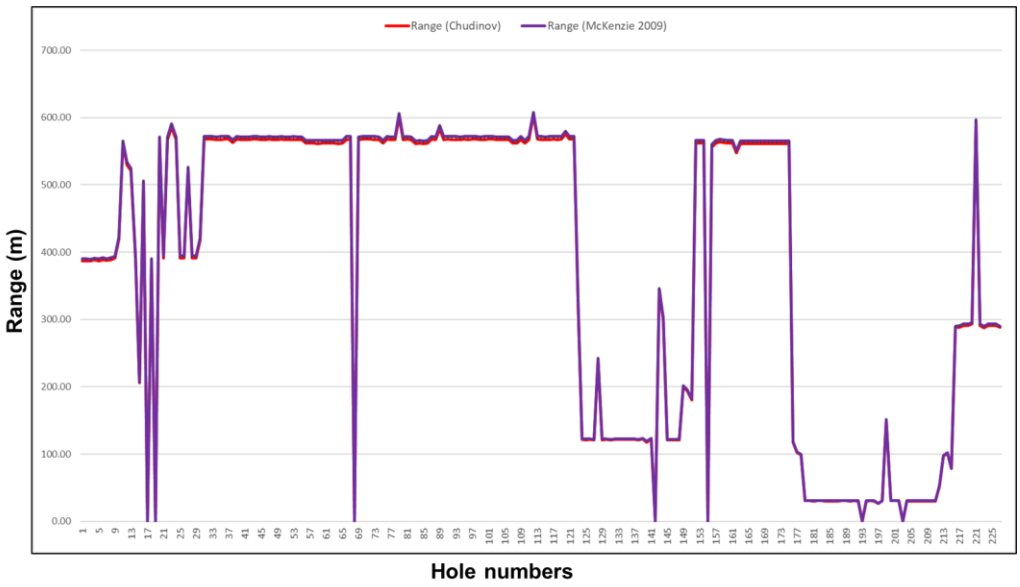

Figure 37: Adjusted range comparison graph

By amending the proportionality factor to include the shape factor, it resulted in reducing the variance to less than one percent between the purple line and the red line as shown in Figure 37.

The accompanying flyrock calculator (Appendix C) that was developed as part of the requirements indicated in Figure 25, also used the equations stipulated in section 3.5.4. The same amendment in the proportionality factor was applied. Figure 38 indicated the variance in the estimated trajectory in the flyrock calculator before the adjustment. In Figure 38 the analytical-based trajectory was also compared to two numerical methods, a fourth-order Runge-Kutta (RK4) method used by Stojadinović, et al. (2011) and the method proposed by Chernigovskii (1985), discussed in the literature review. Figure 39 shows the variance in the analytical-based trajectory after the amendment of the proportionality factor to include the fragment shape factor.

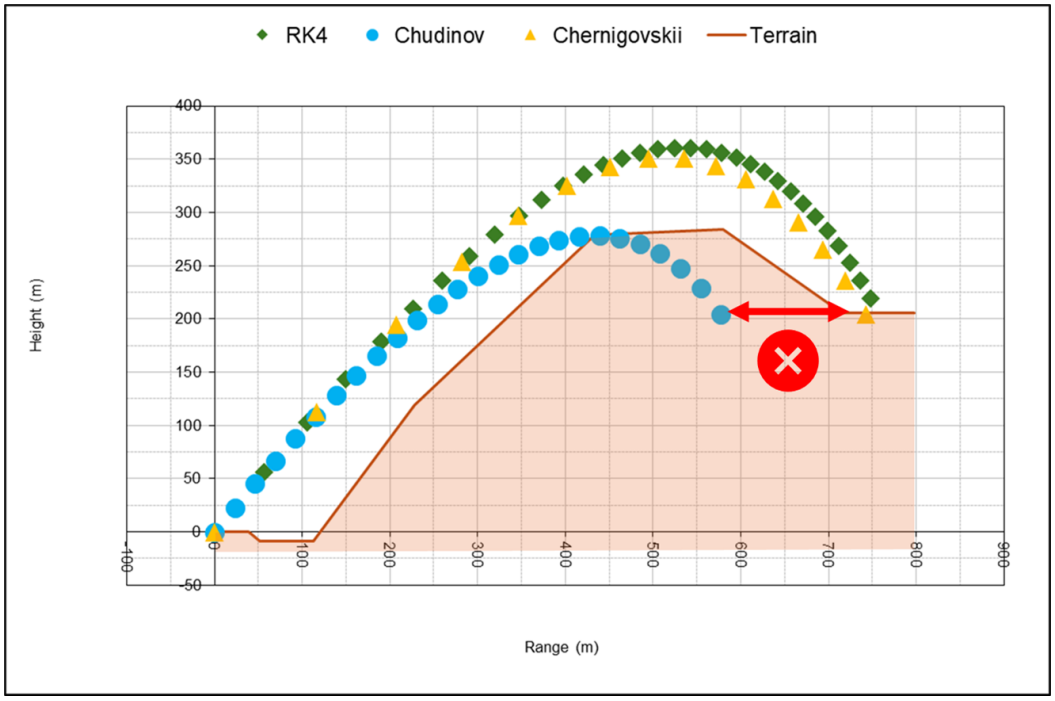

Figure 38: Trajectory comparison before change in Equation 33

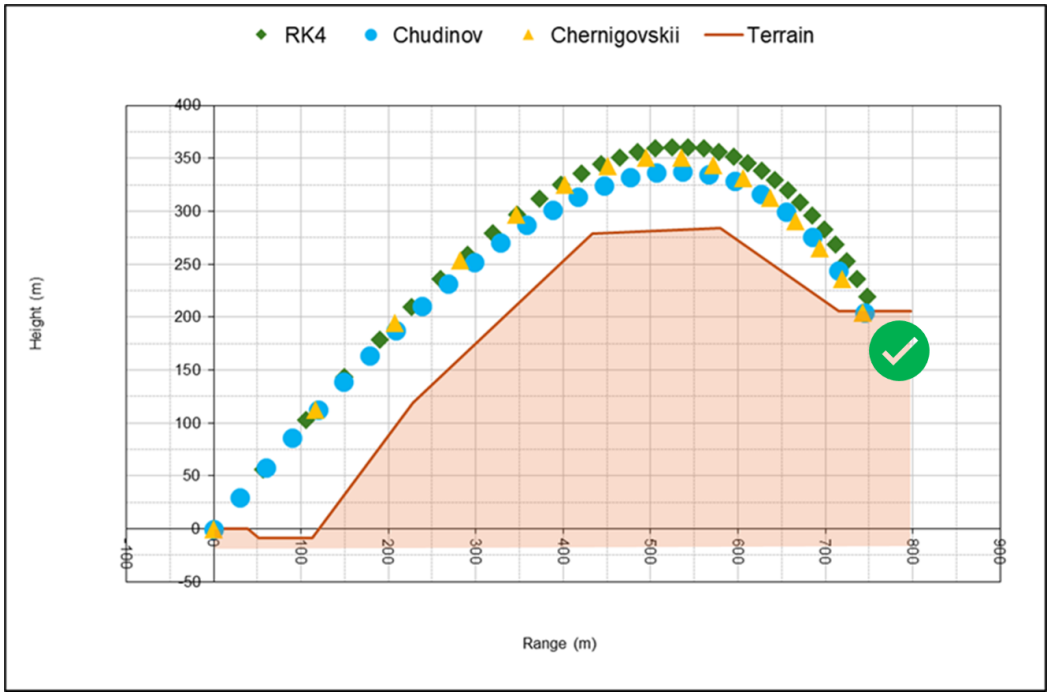

Figure 39: Trajectory comparison after change in Equation 33

The variances in the trajectory range compared to the numerical methods, after the amendment of the proportionality factor equation to include the shape factor, are summarised in Table 11.

Table 11: Percentage variances in trajectory comparison

	Method comparison	Range variance
Range estimation using modified Chudinov trajectory equations	4th order Runge-Kutta method (RK4)	0.93%
	Chernigovskii's method	0.28%

The range variances compared against the numerical methods, confirmed that the inclusion of the approach used was suitable to be implemented in the flyrock risk reporting dashboard as part of the developed framework. It also made the approach a valid method to check the results from BlastLogic' s flyrock module (McKenzie option).

4.3 Data from Video Analysis and Observations

For the analysis period, a sample of 23 blasts were reviewed from five sites.

The following data was captured and summarised:

- **General data** - Mine site, commodity, video source.
- **Rock mass data** - In-situ rock density (t/m³), Uniaxial compressive strength (MPa); and
- **Observation data** - Blast type, hole diameter (mm), collar conditions, bench conditions, free face status, face burst, VDF, water in hole status, stemming material quality, minimum SDOB, predicted range (m), actual range (m), actual range projected on same elevation (m), elevation difference between source and impact point (m), actual size of fragment (m), site's Fmax (m), site's Blast Exclusion Zone (m), Fmax exceedance, BEZ exceedance, exceedance reported.

The captured data is displayed in Table 12, while Figure 40 shows the spread of the observations per site. As observed, 43% of the video capturing was done using drones. Drone footage in general is better suited to identify source and

impact locations in the same footage. The quality of drone footage is also better than the manual placed cameras.

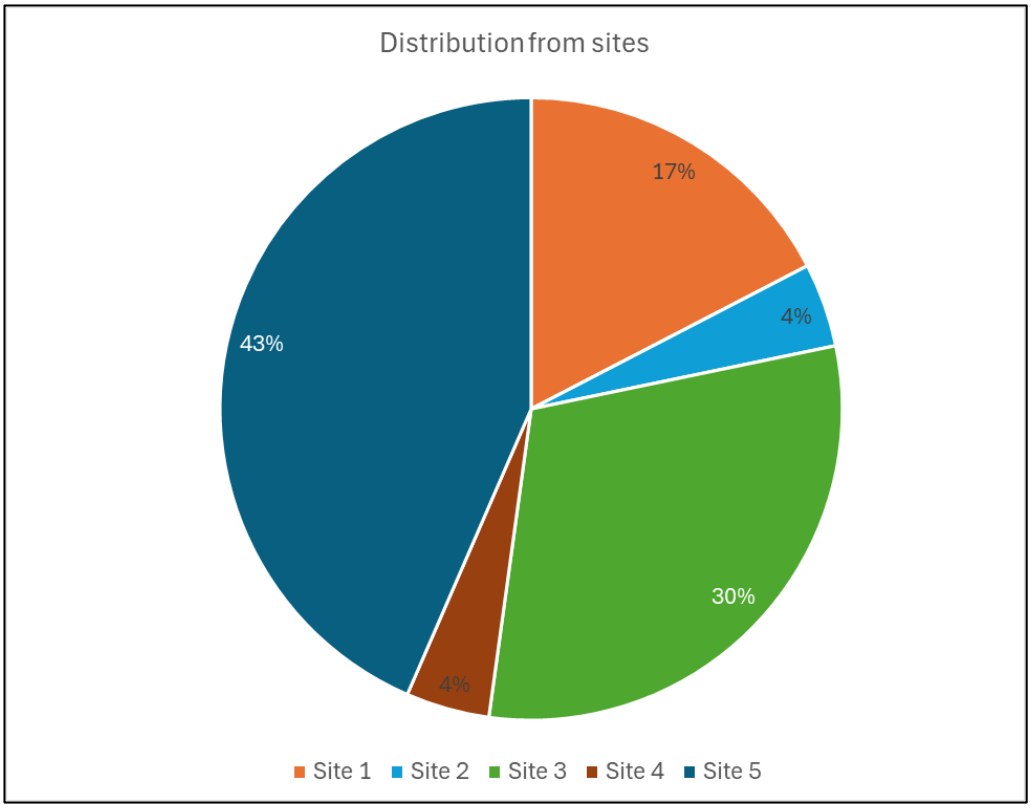

Figure 40: Observation distribution per site

The bulk of the observations were from site 3 and site 5. This was driven by data availability and ease of access to these sites during the data gathering period. The rock mass data associated with each blast observation is also displayed in Table 12. The denser material blasted was from the ore blocks located on the iron ore site, while the higher UCS rocks were from the waste blocks in the platinum site (Figure 41). Rock density plays a role in the estimation of ranges as highlighted in the literature review.

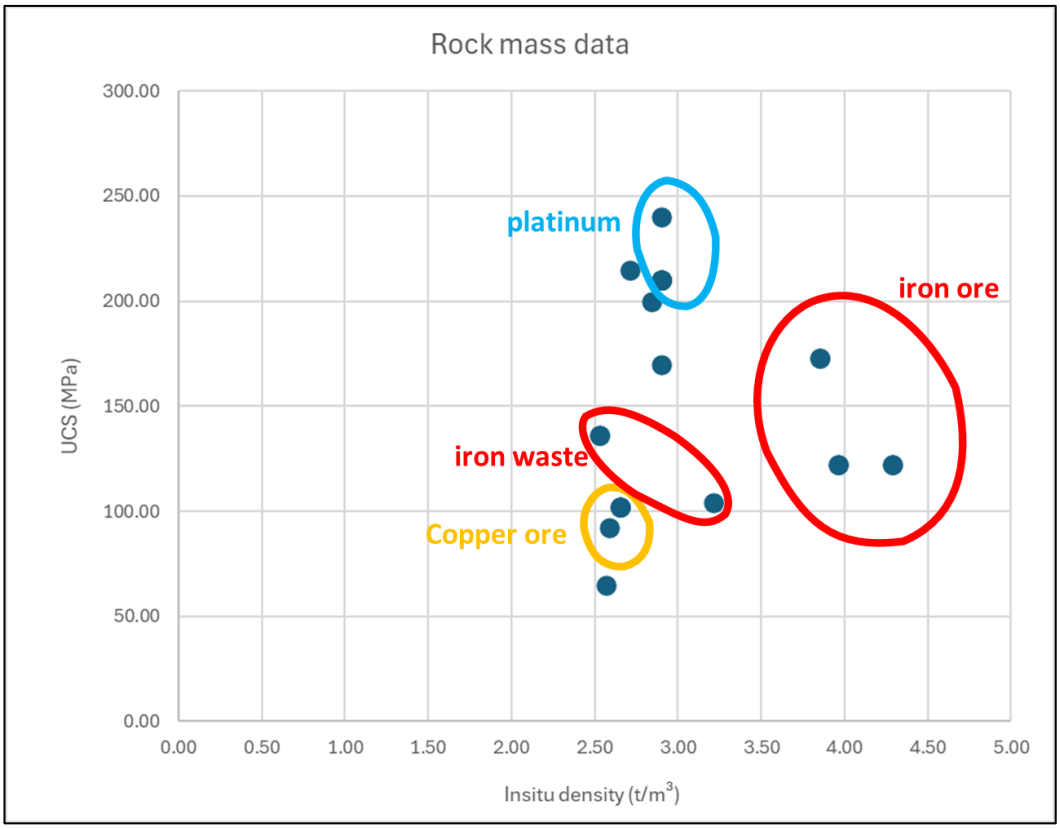

Figure 41: Density vs UCS plot

The captured data for the 23 entries is summarised in Table 12. Only in six of the events were the actual fragments, that traveled the furthest, retrieved and a physical size measurement obtained.

It is important that the actual ranges were taken as the horizontal distance between the launch point and the impact point. The prediction used for this analysis assumes that the horizontal range is on the same elevation, however 18 of the impact events were on different elevations. Of the 18 events mentioned, only in 12 the actual horizontal range were amended to the same elevation using the trajectory criteria.

Furthermore, it was also observed from Table 12 that in 90% of the blasts observed, the site used the default blast exclusion zones on the clearance plans communicated, even if the modelling indicated a larger potential range. This was subsequently addressed with the sites and exclusion zones are now validated through the developed flyrock framework.

Table 12: Captured data

Mine Site	Blast ID	Blast type	Hole diameter	Collar conditions	Main Rock Density (t/m³)	UCS (MPa)	Loose rocks on bench	Free face status	Face burst	VDF	Holes full of water	Stemming material quality	Minimum SDOB	Actual measured range	Actual range on same elevation	Elevation difference	Predicted range	Actual size of fragment	Site Fmax for Blast	Fmax Exceedance	Blast Exclusion Zone (BEZ)	BEZ Exceedance	Exceedance reported
Site 1	Blast 1	Production	270	Fractured	2.65	102	Yes	Partial	No	3.5	Yes	Right Size Aggregate	0.76	745	850	204	828	0.3	330	Yes	660	Yes	Yes
	Blast 2	Trim	270	Ideal	2.59	92	No	Full	No	3.5	Yes	Right Size Aggregate	0.57	502	524	157	1,553	0.15	250	Yes	500	Yes	Yes
	Blast 3	Hybrid	270	Ideal	2.65	102	No	Partial	No	3	No	Right Size Aggregate	0.9	210	330	70	577		250	No	500	No	
	Blast 4	Production	270	Ideal	2.65	102	No	Full	No	3.5	Yes	Right Size Aggregate	0.86	248			637		250	No	500	No	
Site 2	Blast 5	Box Cut	115	Fractured	2.84	200	Yes	None	No	4	No	Drill Chippings	0.67	522	522	-82	619	0.14	250	Yes	500	Yes	Yes
Site 3	Blast 6	Hybrid	250	Ideal	2.9	240	No	Full	Yes	3.5	No	Right Size Aggregate	0.93	386	386	0	510		300	Yes	800	No	No
	Blast 7	Box Cut	250	Ideal	2.9	210	No	None	No	4	No	Right Size Aggregate	0.63	716	861	139	1,188		300	Yes	800	No	No
	Blast 8	Box Cut	250	Ideal	2.9	210	No	None	No	4	No	Right Size Aggregate	0.63	622	707	138	1,188		300	Yes	800	No	No
	Blast 9	Box Cut	250	Ideal	2.9	210	No	None	No	4	No	Right Size Aggregate	0.63	564	663	137	1,188		300	Yes	800	No	No
	Blast 10	Production	250	Fractured	2.9	210	Yes	Partial	No	3	Yes	Right Size Aggregate	0.74	350	618	110	838	0.26	300	Yes	1,000	No	Yes
	Blast 11	Production	171	Fractured	2.9	170	Yes	Partial	No	4	Yes	Right Size Aggregate	0.45	1,127	1,195	173	1,912	0.3	300	Yes	800	Yes	No
	Blast 12	Secondary - Toes	115	Ideal	2.9	210								380					300	Yes	800	No	No
Site 4	Blast 13	Production	270	Ideal	3.21	104	Yes	Partial	No	3	No	Drill Chippings	0.85	360			653	0.22	500	No	1,000	No	
Site 5	Blast 14	Production	270	Ideal	2.53	136	No	Full	Yes	3.5	No	Right Size Aggregate	0.7	315			995		300	Yes	1,000	No	Yes
	Blast 15	Production	270	Ideal	2.53	136	No	Full	No	4	No	Right Size Aggregate	0.7	450			995		300	Yes	1,000	No	No
	Blast 16	Trim	270	Ideal	4.29	122	No	Full	Yes	3	No	Right Size Aggregate	1	210			459		300	No	1,000	No	
	Blast 17	Trim	270	Ideal	4.29	122	No	Full	No	2.5	No	Right Size Aggregate	1	152	433	38	459		300	No	1,000	No	
	Blast 18	Production	270	Ideal	3.96	122	No	None	No	2.5	No	Right Size Aggregate	1.01	260	330	51	449		300	No	1,000	No	
	Blast 19	Production	270	Ideal	3.96	122	No	None	No	3.5	No	Right Size Aggregate	0.74	500			882		300	Yes	1,000	No	Yes
	Blast 20	Production	270	Ideal	2.71	215	No	Partial	No	3.2	No	Right Size Aggregate	0.76	798			832		300	Yes	1,000	No	No

	Blast 21	Production	270	Ideal	3.85	173	No	Full	Yes	4	No	Right Size Aggregate	0.7	496			995		300	Yes	1,000	No	No
	Blast 22	Production	270	Ideal	2.57	65	No	Partial	No	3.5	No	Right Size Aggregate	0.85	515			653		300	Yes	1,000	No	No
	Blast 23	Production	270	Ideal	3.85	173	No	Full	No	4	No	Right Size Aggregate	0.7	813			995		300	Yes	1,000	No	No

4.4 Observed Flyrock Mechanisms and Ranges

As stated in the literature review, there are mainly three flyrock mechanisms, namely cratering, faced burst and rifling. Although in the developed flyrock framework the modelling component caters for all three mechanisms, the study focused on flyrock emanating due to cratering. This was done because historically at Anglo American Plc operations flyrock events predominantly came from cratering. In the analysis of the data gathered, this was confirmed as indicated in Figure 42.

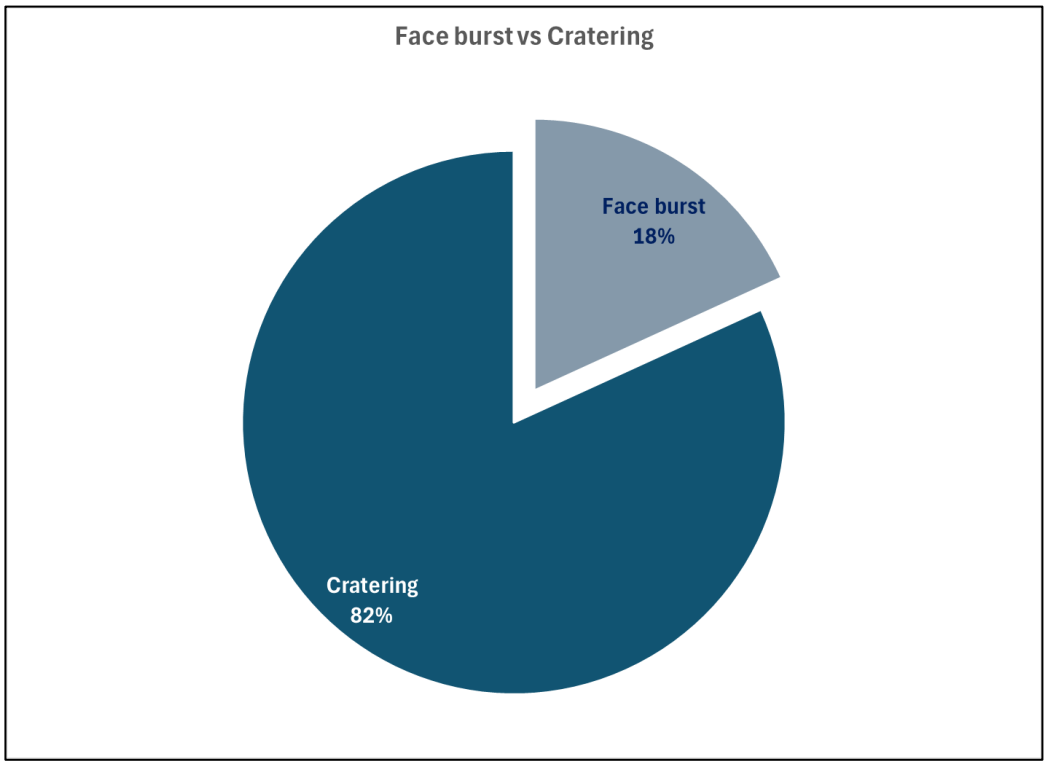

Figure 42: Cratering vs Face burst

Figure 42 shows that more than 80 percent of the projectiles analysed were from cratering. This also correlates to the work done by Muller and Oosthuizen (2015).

One of the objectives of the study was to verify if the current predictive model in BlastLogic used by the various sites was sufficient to highlight the risk of potential flyrock occurrence. Figure 43 is an extract out of Table 12 comparing the actual flyrock impact observations to the prediction from the model.

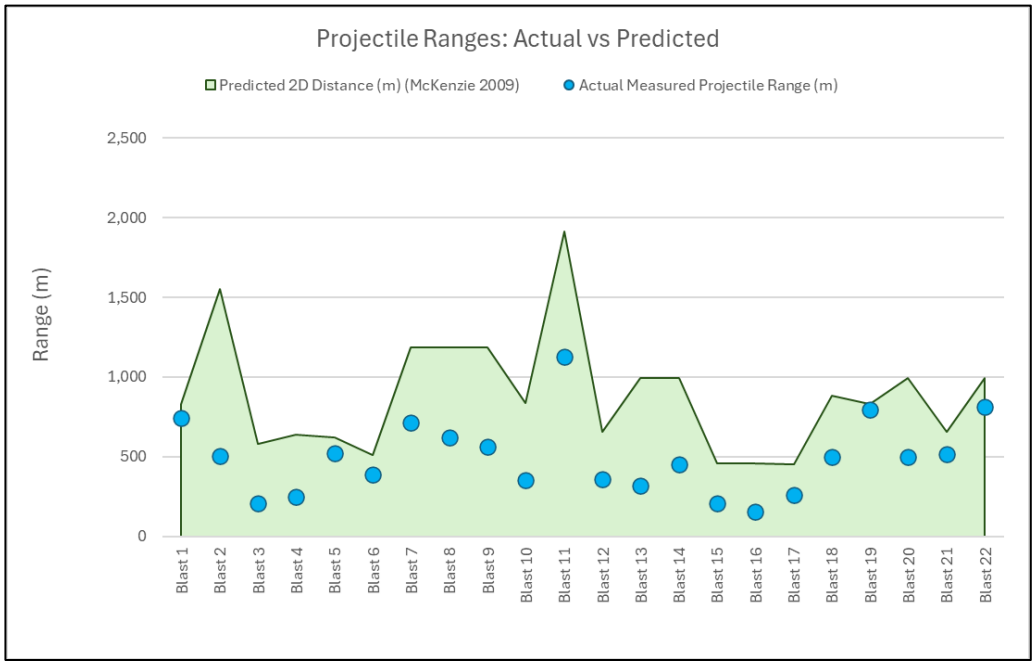

Figure 43: Actual vs Predicted (BlastLogic) Ranges

From Figure 43 it is clear the McKenzie (2009) predictive model used in BlastLogic, overestimated the range. This aligns with the statements in the literature. The significance of this finding is that the trend is in line with the model's indication of high risk. Designing blast exclusions zone based on predictive modelling ensures that sites cater for the worst-case scenario.

4.5 Vertical Displacement Factor

The VDF referenced from Tordoir (2023), which is an adaptation of the violence factor by Konya and Konya (2020), is a good visual indication for the likelihood that a blast might have produced flyrock from cratering. As previously shown in Table 9, the capturing of the VDF observations with the blasts in the study was to determine if there was some correlation between the SDOB categories and the VDF. The graph depicted in Figure 44 (data extracted from Table 12) was compiled to review the correlation between the VDF numbers and the SDOB numbers of the captured data.

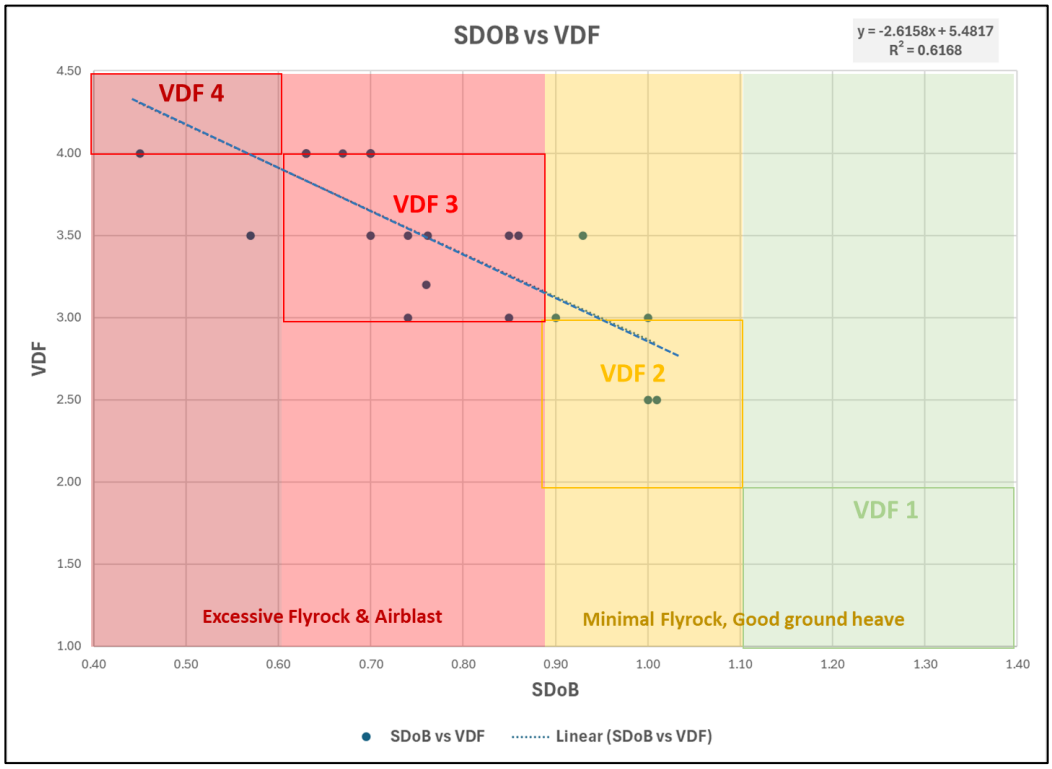

Figure 44: SDOB vs VDF

As can be observed in Figure 44, the correlation coefficient (R^2) was 0.6168 for VDF number and SDOB numbers. The following ranges depict the fit for correlation coefficient:

- 0 - 0.2 indicates a very poor fit.
- 0.21 - 0.4 represents a poor fit.
- 0.41 - 0.6 shows a moderate fit.
- 0.61 - 0.8 demonstrates a good fit; and
- 0.81 - 1.0 which is an excellent fit.

From Figure 44, the squared correlation coefficient obtained, demonstrates a moderate to good fit. This means that if a VDF above 2.5 (SDOB>0.9) is estimated from a blast video, it is a good trigger to analyse the video in more detail for impact points. This is because there is a higher probability for the potential of flyrock emanating from the blast. Furthermore, as indicated in Figure 44, the increase in VDF was also indicating an increase in the actual flyrock range measured.

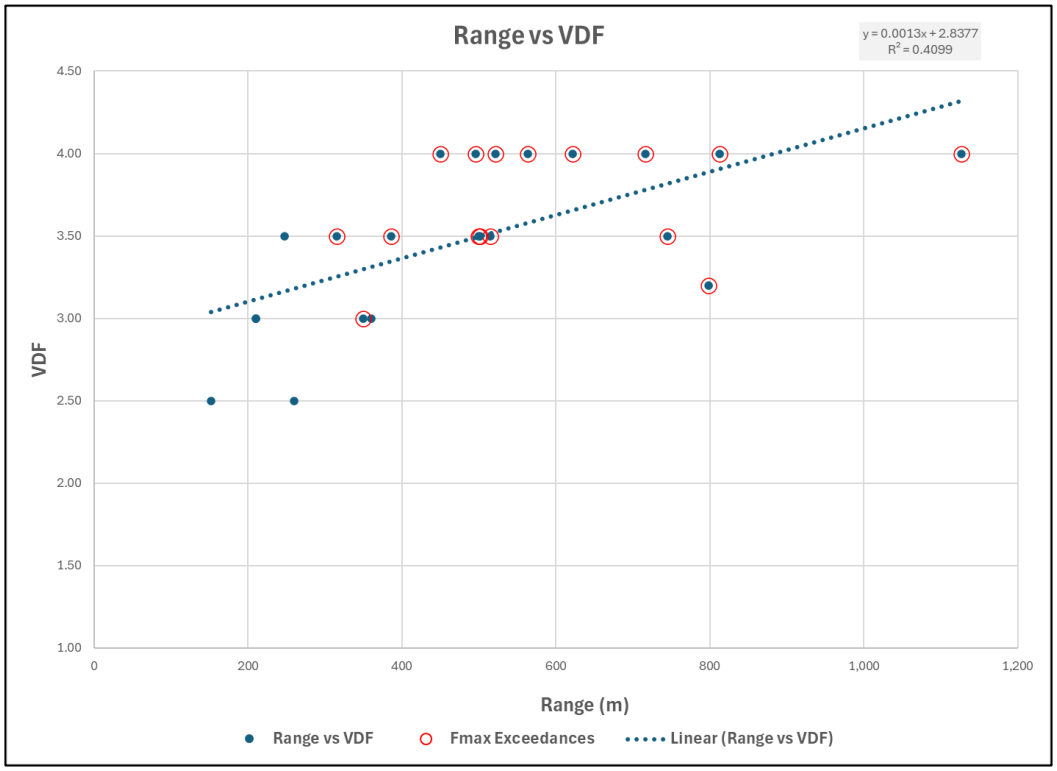

Figure 45: VDF vs range

The red circled points in Figure 44 were ranges measured where the set Fmax were also exceeded for the associated blast. The data indicated that a VDF of three and higher resulted in an exceedance.

As stated by Tordoir (2023) the VDF's were also correlated to shovel dig rates. Higher VDF ratings observed, led to reduced diggability. This could be attributed to the loss of explosive confinement. This same reduced confinement is also leading to higher occurrences of flyrock.

4.6 Flyrock Exceedances

A critical part of the study was to analyse the actual ranges measured against the exclusion criteria set for the blasts as well as what the predictive model estimated. Initial results of the analysis were given in Figure 43 comparing the actual ranges observed against the prediction ranges. A more detailed breakdown is visually represented in Figure 46.

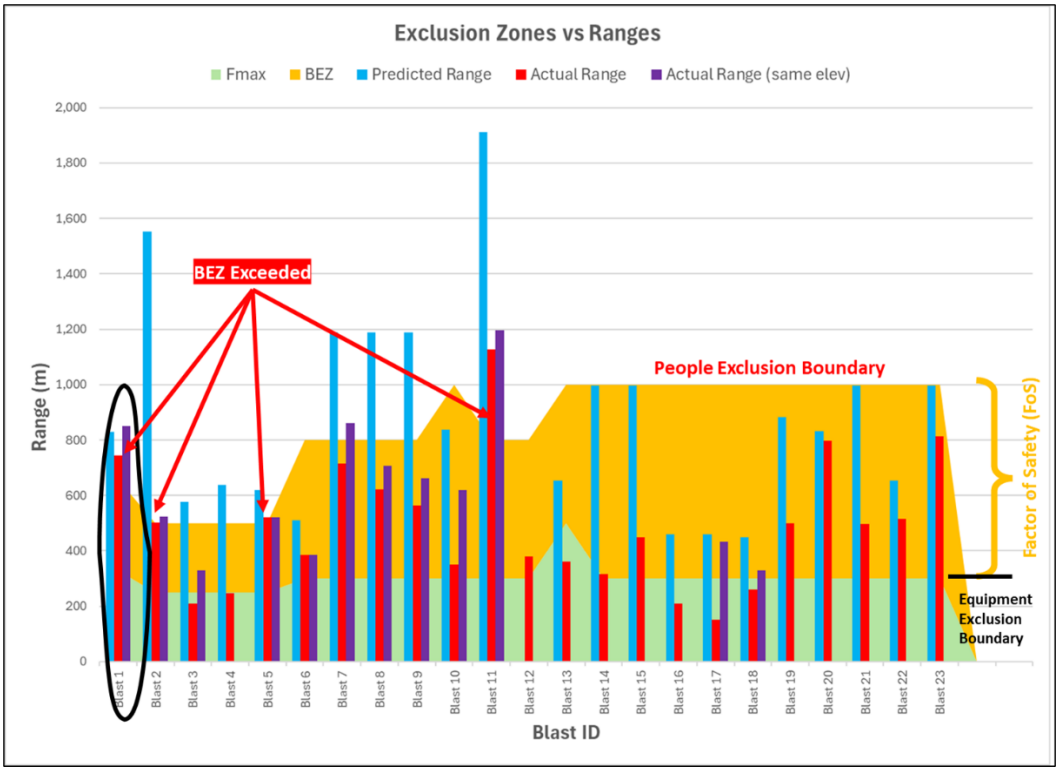

Figure 46: Predicted and actual ranges compared to the exclusion boundary

The horizontal axis in Figure 46 represents the blast number where the observation was taken. The light green area shows the Fmax per site set for the associated blast. The orange area is an indication of the factor of safety (FOS) applied to the Fmax to establish the BEZ. If any flyrock ranges goes beyond the orange zone it means that the BEZ was exceeded. It was clear from the data presented and indicated on Figure 46 that four actual measured ranges (red bars) exceeded the BEZ, while 13 exceeded the Fmax but not the BEZ. This means that the FOS of two was eroded away (reduced to 0.99).

The light blue bars indicate the predicted ranges from the model used in BlastLogic (McKenzie model option). It is important to note that the predictive model used (especially launch velocity estimates) was based on the model proposed by McKenzie (2009) in which it is stated that the model will give a maximum range. Szendrei and Tose (2022) also confirmed that it would probably overestimate the range. The purple bars represent where the actual ranges were projected onto the same elevations as the launch elevation. So, a true comparison was between the light blue bars and the purple bars. This was separately graphed in Figure 47.

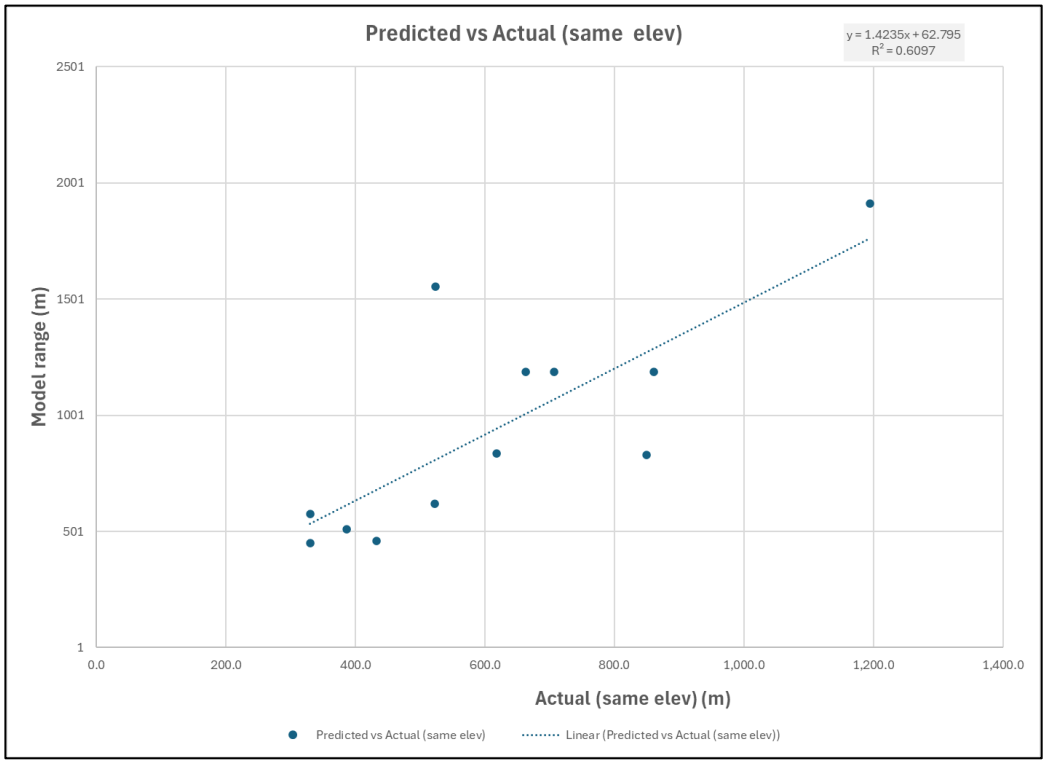

Figure 47: Predicted vs actual range

As previously stated, predicted values were higher in most cases than the actual ranges observed. It was important to link the findings to the flyrock risk reporting dashboard that forms part of the developed framework, to see if the equations used in the dashboard would have indicated the potential risk. Again, one of the incidents (E from site 1(Blast 1 circled in Figure 46)) was used in Figure 48. A similar analysis was run for all of the events observed.

Figure 48A indicate the flyrock footprint, while figure 48B shows a side view of the trajectory of the predicted flyrock.

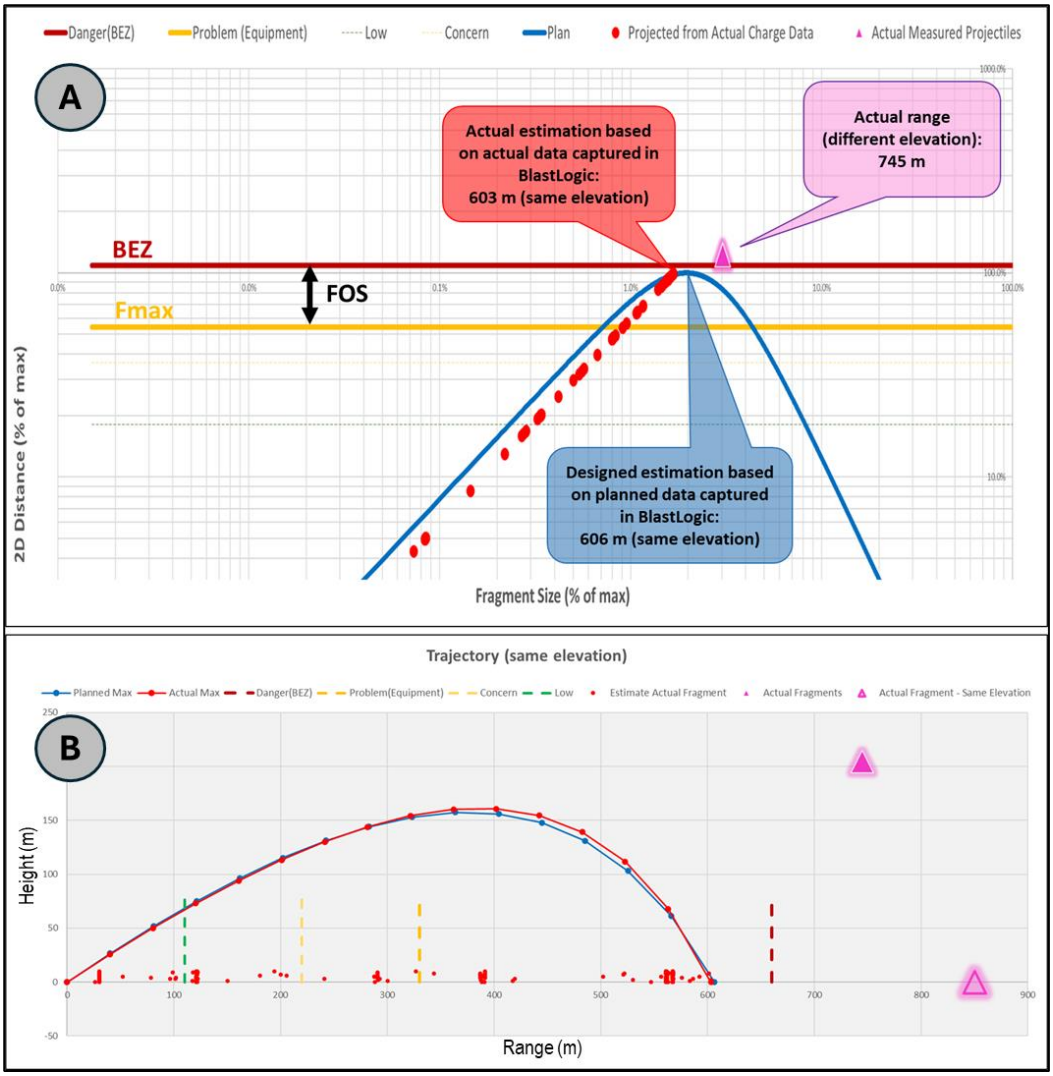

Figure 48: Flyrock risk reporting for incident E/Blast 1 - (A) Footprint, (B) Trajectory

As can be observed from Figure 48, the flyrock risk dashboard highlighted potential risk for exceeding Fmax, but in this case not the BEZ. However, the actual flyrock range reported in the incident was measured further than the BEZ as indicated as a purple triangle in Figure 48.

If the developed framework, that include the flyrock risk reporting dashboard, was in place and the flyrock risk report was run before the blast, the following observation and question could have been discussed and addressed:

I. The initial observation was that the blast was executed as per design, since the predicted ranges from the actual charged data per hole in BlastLogic (red points) were within the designed footprint based on the planned data in BlastLogic (blue line).

II. The question however remained, why was Fmax for the blast less than the designed footprint? If the probability was there to have a fragment travel to a predicted distance, then that prediction should be the minimum value of Fmax and following the group standard, the subsequent BEZ must be twice the Fmax to cater for a FOS of two. If that was the case and the process was followed, the actual flyrock event would have still exceeded Fmax, but not BEZ as indicated in Figure 49.

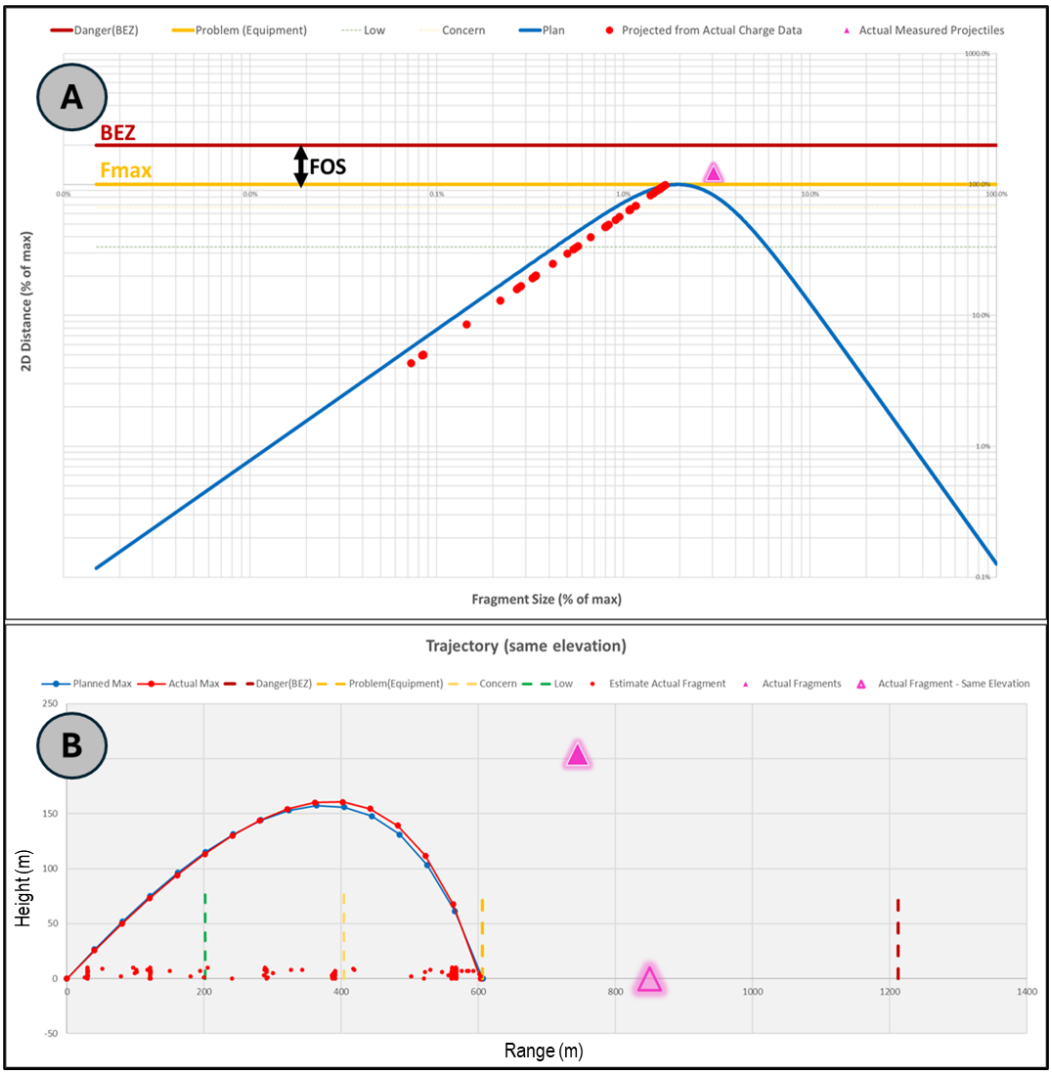

Figure 49: Adjusted Flyrock risk reporting for incident E/Blast 1 - (A) Footprint, (B) Trajectory

This analysis of incident E (Blast 1) shows the value of having a framework in place and a method of reporting the risk for potential flyrock in order to manage it before the initiation of the blast.

General observation made during this study, looking at the overall drill and blast flow at Anglo American Plc, is that the predictions for flyrock is mostly done early in the process with design data as indicated in Figure 50.

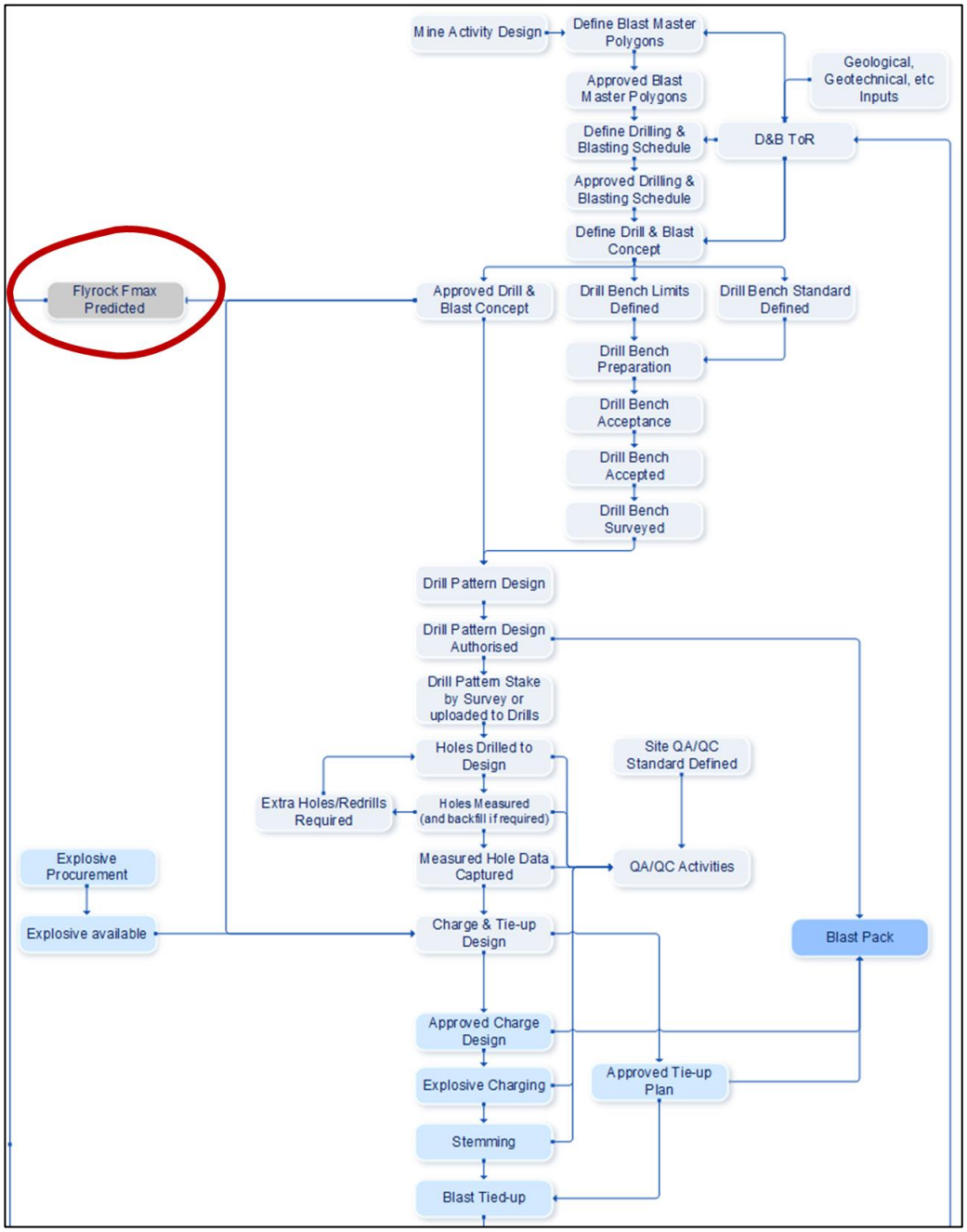

Figure 50: Section of Anglo American Plc drill and blast process flow

Any deviations from the designed hole depth and explosive charges can adversely affect the likelihood of flyrock. Short and overcharged holes (risk holes) will result in blow-outs that will lead to flyrock. A potential gap to close in the modelling of

flyrock is to run the prediction at various stages in the process. These include with ‘as-drilled’ (hole already drilled) and ‘as-charged’ (hole already charged with explosives) data.

4.7 BlastVision® Trials

As stated, the analysis of the blast videos can be time consuming. As part of improving the capturing of actual flyrock events, potential video analysis and monitoring services were evaluated. Two trial blasts were evaluated in conjunction with GroundProbe using Orica Digital Solutions’ BlastVision® at one of the operations.

4.7.1 Trial 1

Figure 51 is a tiled image showing the blasted area in four different views.

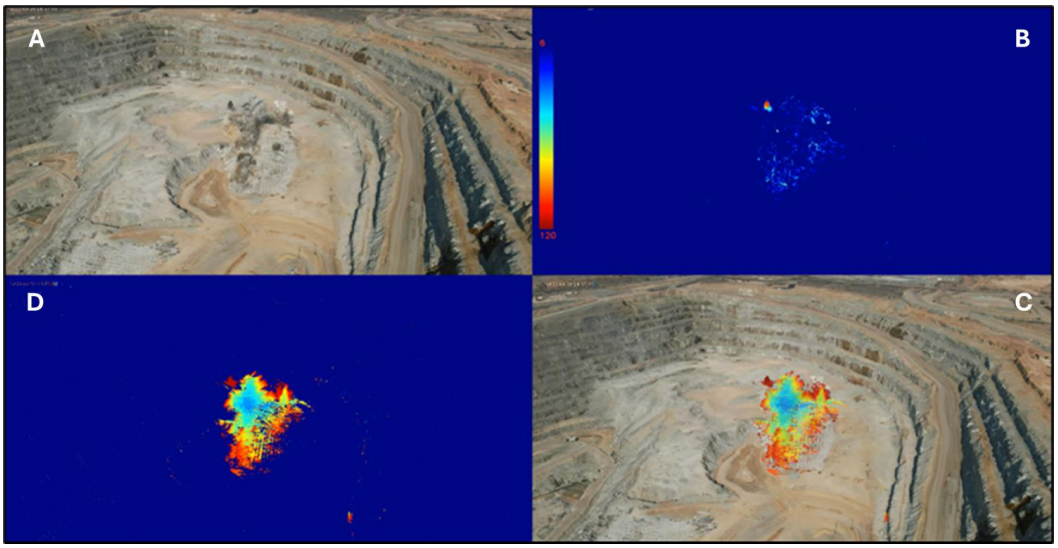

Figure 51: BlastVision® analysis of trial 1 (GroundProbe, 2023)

As per the GroundProbe (2023) report, Figure 51A was the raw footage while Figure 51B shows the normalised image. Figure 51D shows the amplified change reflector and Figure 51C indicated the blend of change in time with the video footage to show the accumulation of surface changes.

By using the point cloud area, the flyrock trajectories were analysed in a 3D view as indicated in the snapshot in Figure 52.

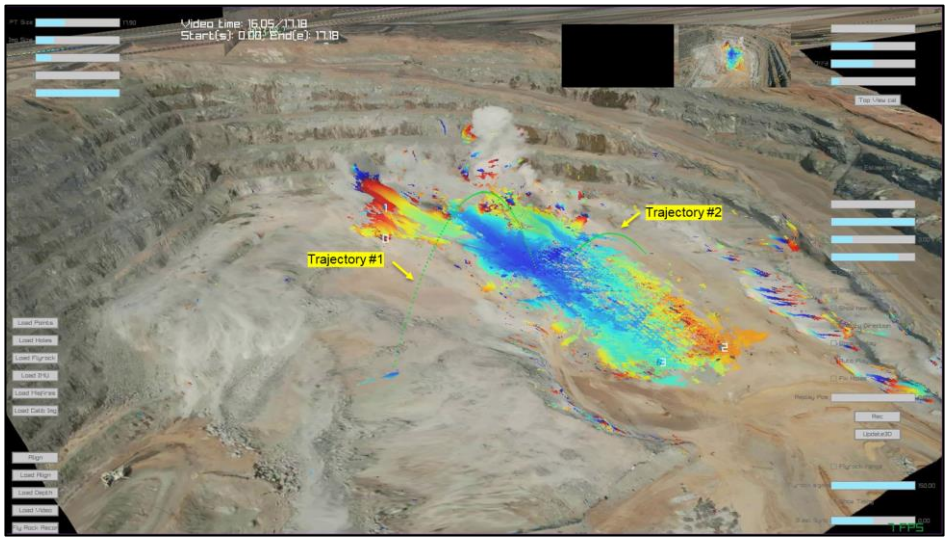

Figure 52: BlastVision® snapshot of flyrock trajectories (trial 1) (GroundProbe, 2023)

The detailed parameters of the flyrock(s) were measured by projecting the trajectories as displayed in Figure 53.

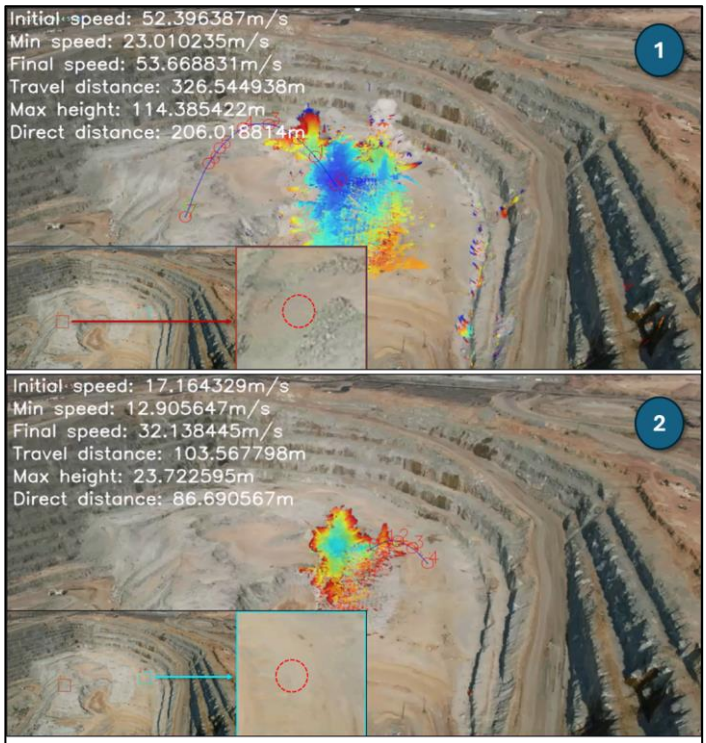

Trajectories Number	Travel Distance (m)	Direct Distance (m)	Initial Velocity (m/s)	Final Velocity (m/s)	Min. Velocity (m/s)	Max. Height (m)
1	326.54	206.02	52.39	53.67	23.01	114.39
2	103.57	86.69	17.16	32.14	12.91	23.72

Figure 53: BlastVision® details of flyrock trajectories (trial 1) (GroundProbe, 2023)

In Figure 53 the direct distance refers to the slope distance between the launch point and the impact point. The final velocity is indicated as higher than the initial velocity, which can only be true due to gravity if the impact point is lower in elevation than the launch point. This is true for trajectory 1 but for trajectory 2, the final velocity is suspicious. Manual analysis (by visually identifying impact locations and tracing it on DTM) of the video independently, as described in section 3.5, did not indicate any projectiles further than what the trial results indicated in Figure 53.

4.7.2 Trial 2

Figure 54 was a tiled image showing the blasted area in four different views.

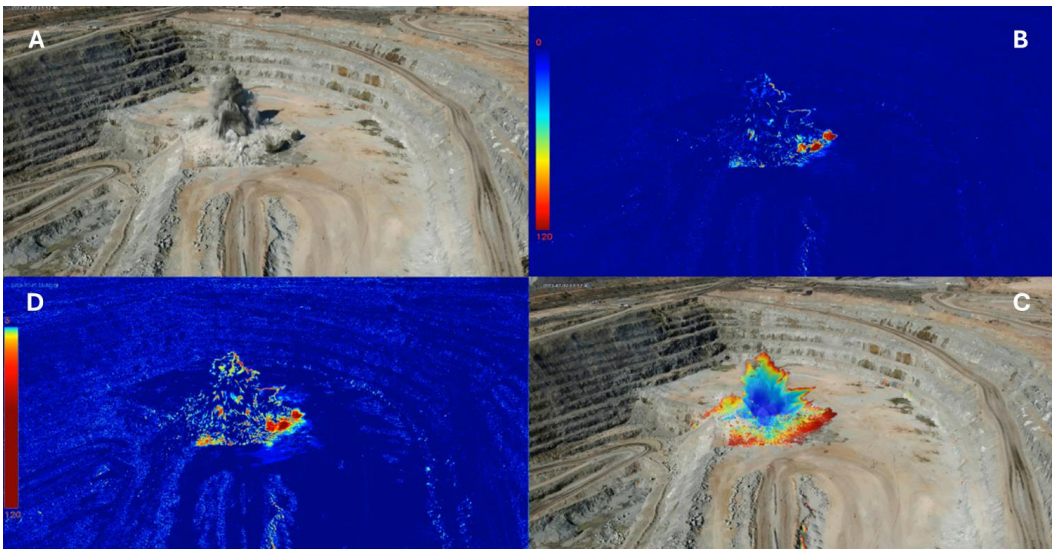

Figure 54: BlastVision® analysis of trial 2 (GroundProbe, 2023)

As per the GroundProbe (2023) report, Figure 54A was the raw footage while Figure 54B shows the normalised image. Figure 54D indicated the amplified change reflector and Figure 54C depicted the blend of change in time with the video footage to show the accumulation of surface changes.

The visualisation in Figure 54 aimed to detect the trajectories of the projectiles. Based on blend visualisation, some trajectories were observed and were validated using zoom analysis as indicated in Figure 55.

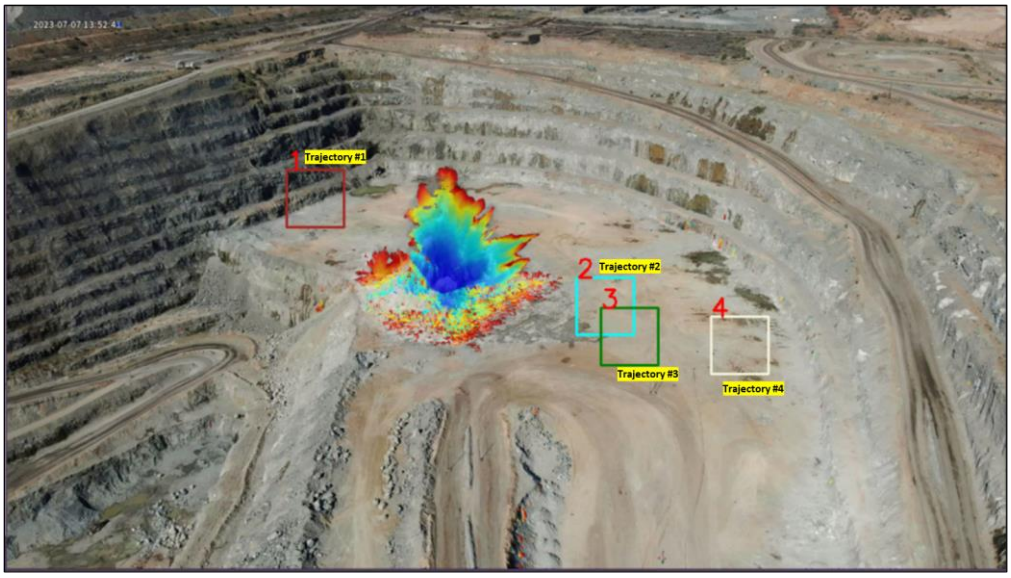

Figure 55: BlastVision® snapshot of flyrock impacts (trial 2) (GroundProbe, 2023)

The visualisation in Figure 55 shows the impacts with the furthest rock projectiles from the blast hole. Furthermore, the projection of flyrock trajectories with detailed parameters were given in Figure 56.

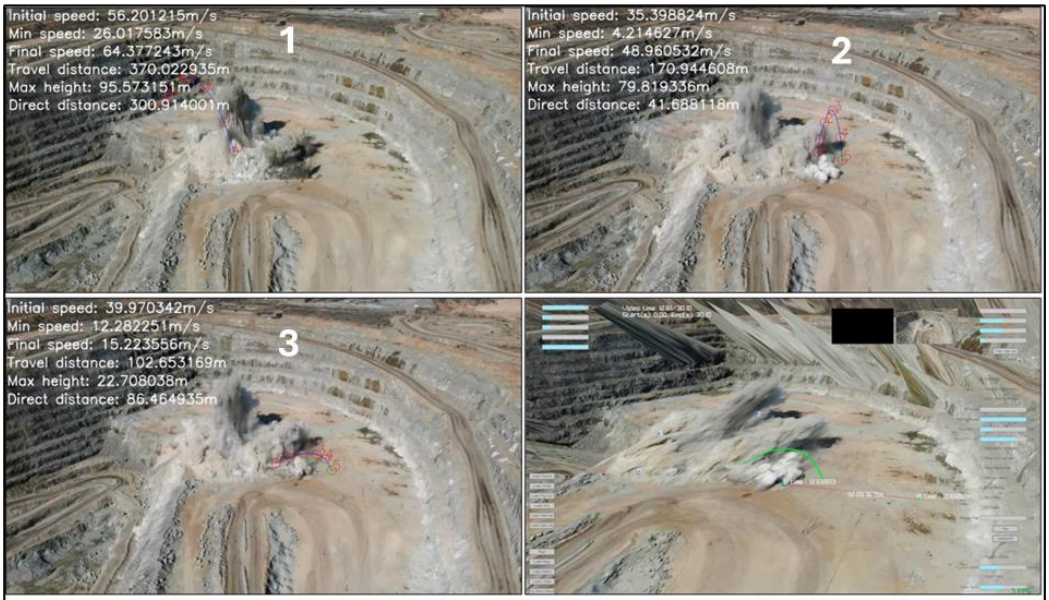

Trajectories Number	Travel Distance (m)	Direct Distance (m)	Initial Velocity (m/s)	Final Velocity (m/s)	Min. Velocity (m/s)	Max. Height (m)
1	370	300	56	64	26	95
2	170	41	35	48	4	79
3	86	86	39	15	12	22

Figure 56: BlastVision® details of flyrock trajectories (trial 2) (GroundProbe, 2023)

Additional feedback also received from the GroundProbe team was that the video quality supplied was optimal. Additionally, the trajectory of flyrock, whether directed away from or towards the drone was a limitation on estimating the flyrock parameters, thus at times, this trajectory may not be accurate. Some of the trajectories were not tracked properly. In these situations, the distance of the landing spot to the outer boundary of the blast pad was measured to capture the direct distance (GroundProbe, 2023).

For trial 2, the manual analysis (by visually identifying impact locations and tracing it on DTM) of the video independently, indicated projectiles in other areas and also at distances further than what the trial results showed in Figure 56. The results obtained from the independent manual analysis had significant differences as displayed in Figure 57.

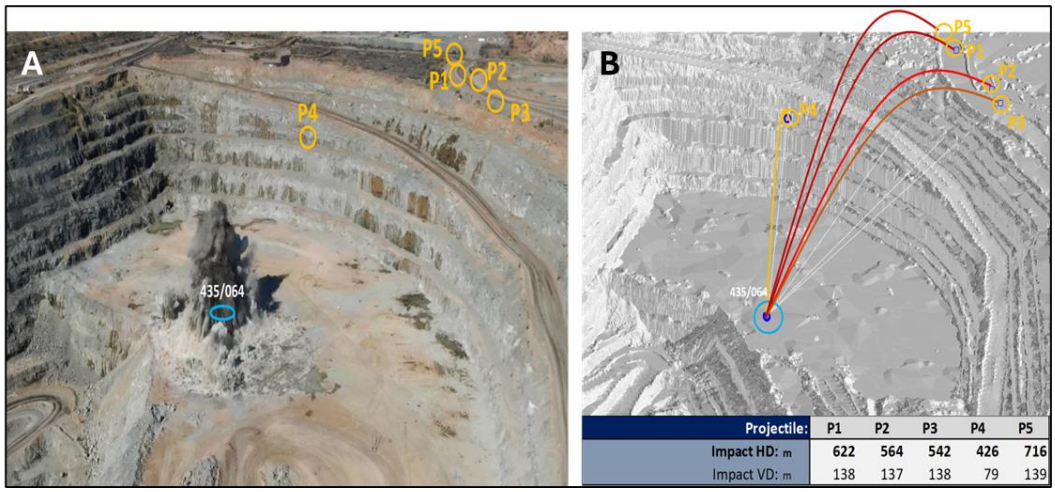

Figure 57: Independent manual analysis results

These discrepancies were discussed with the GroundProbe team that participated in the trial and on a second review, the software was able to pick up a projectile (P5 in Figure 57A) at 728m (slope distance) as shown in the output snapshot shared in Figure 58.



Figure 58: BlastVision® follow-up review (trial 2) (GroundProbe, 2023)

Figure 58 was a snapshot of the output screen from the BlastVision® application. In the snapshot the actual flyrock distance was measured and displayed.

This type of services is promising and with further advancement in computer vision and machine learning this will improve. However, at this stage the application still has inaccuracies and requires human verification as illustrated. BlastVision® is a viable option for sites limited by resource capacity to do video analysis, but this will require an additional budget to cater for the service.

4.8 Video Capturing Guideline

The position, quality and duration of blast videos significantly affect the analysis and ultimately the results obtained. A poorly positioned camera might miss key events like flyrock trajectories. Also angles that are too oblique or too close can distort distances and sizes, making measurements inaccurate. Low resolution footage can blur fine details like flyrock paths, and a low frame rate might miss fast-moving fragments. If the video ends too soon, flyrock impact positions might be missed.

A review of the current practices of capturing video footages on the operations revealed inconsistencies. These inconsistencies ranged from some sites not

capturing any footage at all and other sites capturing footage that cannot be used for flyrock analysis. No guideline or standard was in place to guide site teams to the importance of properly taken video footage to analyse flyrock or other blasting outcomes. For this reason, one of the objectives of the study was also to develop a guideline (to standardise across the group) for the placement of cameras, capturing, processing and storage of blast footage.

This guideline was compiled and tested on some of sites. The following sections of the chapter will cover key components of the developed guideline.

4.8.1 Purpose of the Video Footage

The use of video footage of each blast is a critical component of the Drill and Blast reconciliation process and is required by the group technical standard (Anglo American Plc, 2020). In South Africa it is also a requirement stipulated in the mandatory code of practice (South African Government, 2024). An important element when taking video footage(s) of a blast, is the need to identify firstly the purpose(s) for requiring the footage. The purposes are driven by what blast objectives the site wants to monitor the outcomes of. By Identifying the purposes will assist in planning what equipment will be required and where the equipment needs to be placed.

Examples of potential purposes (Figure 59):

- Vertical Displacement Factor.
- Flyrock tracking.
- Initiation sequence.
- Burden movement; and
- Fume tracking.

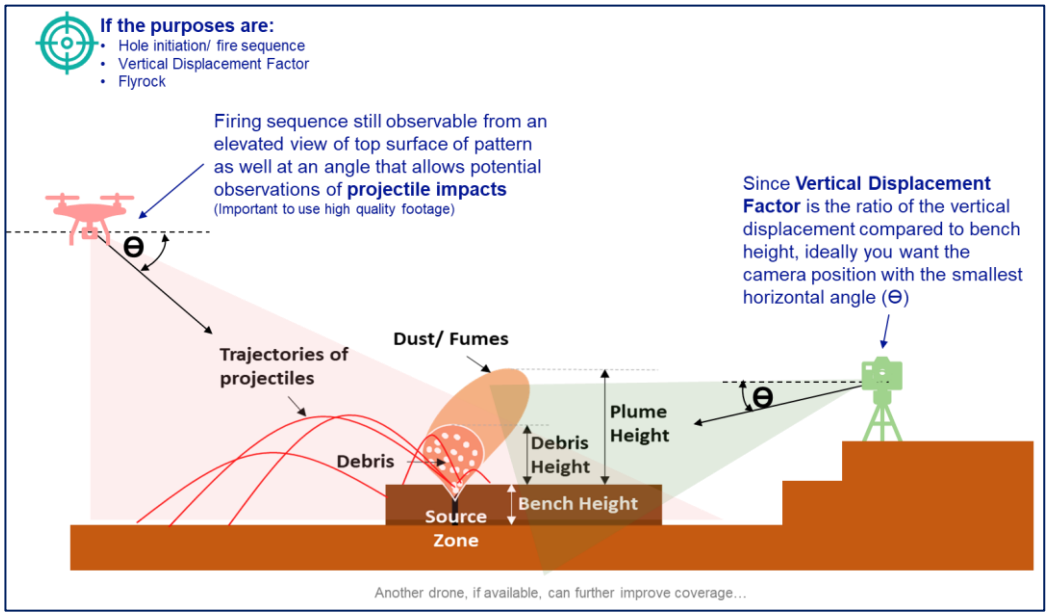

Figure 59: Example of camera placement based on purpose

Figure 59 is a diagram taken from the developed guideline, illustrating considerations for equipment selection based on the purpose(s) identified of the footage.

4.8.2 Planning the Capturing of the Video Footage

The planning element is referring to a detail strategic outline for capturing the blast videos based on the purposes identified. Planning ensures alignment and collaboration. Alignment and collaboration are critical since in some cases the equipment required is not always readily available and prior arrangements need to be made to secure equipment and resources to monitor the blast. It is important that the planning takes place well in advance of the planned blast. Ensure equipment is fully charged and in working conditions. One critical component of the planning element is to identify what camera equipment is required and if it is available. Examples are:

- Drones; and
- Ground based cameras such as highspeed cameras, mobile cameras.

Another component of the planning element is to use the location of the blast, the orientation (direction of movement), initiation points and the purposes of the

footage, to determine the optimised placement of the camera equipment. The following is taken into consideration:

- Clearance criteria for the blast.
- Planned time of blast.
- Predicted weather (overcast) conditions.
- Wind; and
- Sun position.

To help facilitate the process between departments, a Camera Placement Request is completed. An example is given in Figure 60.

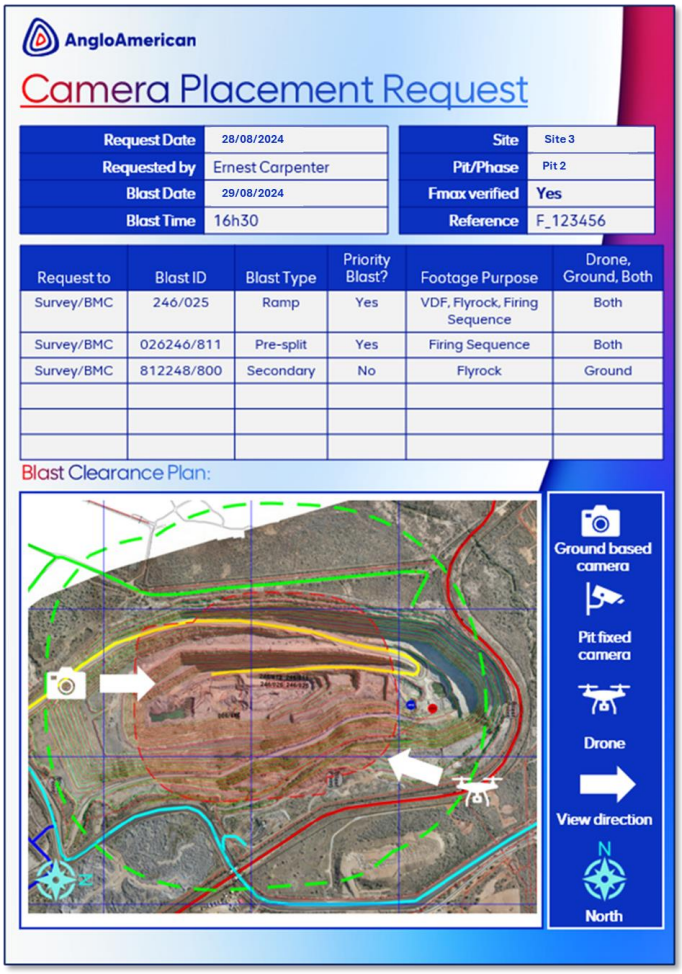

Figure 60: Example of a Camera Placement Request

The Camera Placement Request helps formalise communication. As indicated in the example in Figure 60, it can serve as the basis to plan logistics, etc.

4.8.3 Placement of the Cameras for Capturing the Video Footage

The placement element is also important as it determines the quality of the footage taken and ultimately the observations made from it. It is vital to ensure when placing cameras that mine safety rules are always adhered to. Use the plan created for the placement as the guide to physically place the cameras in advance of the blast clearance process commencing. If the position in the field requires a change, it is marked on the plan for record purposes. Placement must also take the camera equipment's battery life into consideration when placing remote cameras inside the BEZ. Also ensure positive communication with the operational team on progress of placement. When using drones, ensure communication with drone operator(s) to signal when to get into position.

4.8.4 Details Requirements During Capturing of the Video Footage

The capturing element refers to basic rules during the recording phase to ensure best possible footage available to do the analysis afterwards. Ensure video footage is captured at a high resolution to allow proper digital zoom during analysis.

Take note of the following considerations:

- Ensure camera is mounted securely to allow stability during blast.
- Ensure blast area and/or area to capture is in focus.
- Ensure that all cameras used, capture video at highest resolution.
- Record at least one minute before and after blast - do not pan or zoom during this period; and
- Capture all videos (except if using highspeed) at normal speed (can always in post processing change the playback).

4.8.5 Processing the Video Footage for Analysis

In the processing element the aim is to make sure the optimal footage captured is delivered for analysis in a timely manner. Use a proper naming convention and file management system for saving footage. Ensure that captured footage is processed at normal speed to allow velocity estimates. Do not compress footage (keep highest resolution).

A summary one pager of the main topics discussed in the guideline is displayed in Figure 61.

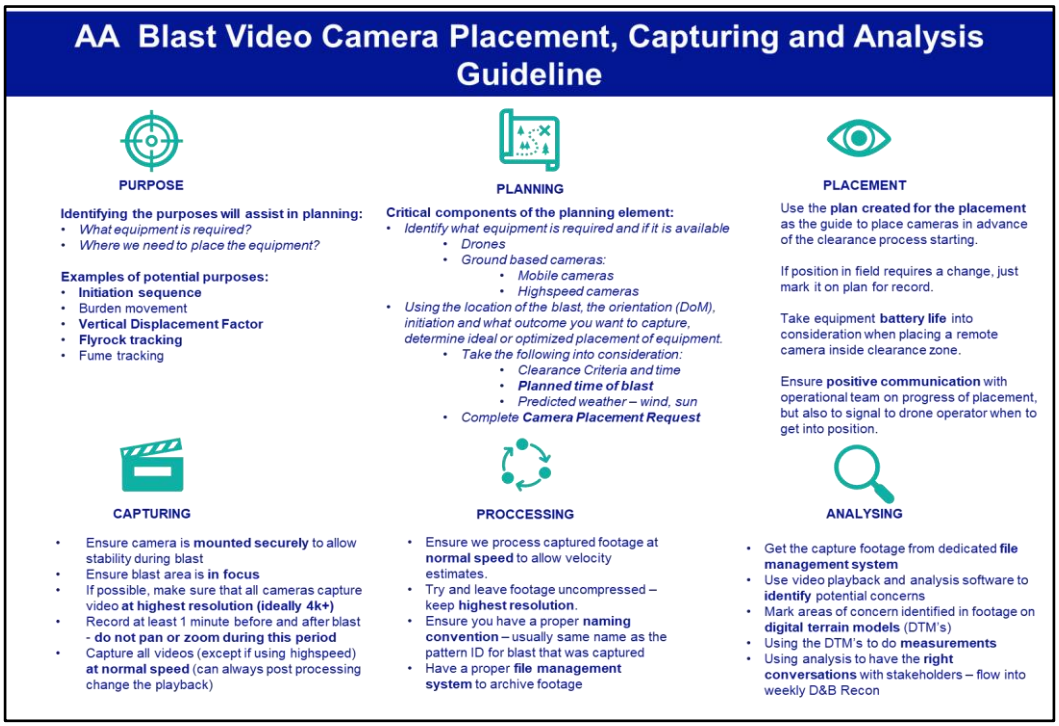

Figure 61: One pager of blast video camera placement, capturing and analysis guideline

The one pager depicted in Figure 61 was created as a poster as part of the roll-out of the guideline.

4.9 Chapter Summary

The lack of identifying flyrock concerns or being aware of the risks associated with flyrock on sites lead to the development of a framework to address it. This developed framework is a structured process that covers the prediction or modeling for flyrock and reporting concerns before the blast takes place. It also covers the monitoring of the actual blasts to measure actual flyrock. The framework allows for more data to be captured as it provides a process for sites to follow, and this will enable operations to do similar analysis as done in this chapter. The VDF is a quick and simple method to do an initial assessment using the blast video and in this analysis a link to the SDOB categories and flyrock exceedances were

highlighted. VDF links to other productivity indicators can help in managing overall process stability.

The data collected was also in this chapter summarised for analysis with the aim to see if there was any correlation between the data captured and the occurrence of flyrock. The observation data that was captured in this study with the footage for analysis can serve as a minimum standard of what data is captured with the video analysis as part of the developed framework. This will expand the datasets for future improvements in the modelling techniques as mentioned in the literature review.

Almost half of the footage reviewed in the study was from drones that were higher quality than the manual placed cameras. In general, the quality of all the blast videos varied depending on the equipment used. Furthermore, as shown, not all the information for all 23 blasts analysed was captured, but adequate information was captured to verify the need for the framework and to test the flyrock risk reporting dashboard's effectiveness.

The current flyrock modelling method used in BlastLogic (McKenzie model option), in most cases, overestimates the ranges, but the study did confirm that it was sufficient to identify that there was a risk for exceedance.

The testing of the developed flyrock risk reporting dashboard showed that it can be used to validate flyrock risk from the data supplied in BlastLogic. It can be used to ask the right questions at the right time to ensure all stakeholders are aware of the potential risk for a blast or blasts.

The testing of BlastVision® in conjunction with GroundProbe showed potential as a video analysis and monitoring services, but the workflow still requires human verification. The variance in footage quality observed highlighted concerns around inconsistency in capturing blast videos historically on sites, especially with the aim of monitoring and measuring actual flyrock occurrences. This confirmed the requirement of a guideline for sites when placing cameras, capturing and processing video footage. The details of the guideline developed were discussed.

5 CONCLUSIONS AND RECOMMENDATIONS

5.1 Introduction

In this final chapter of the research report, the preceding chapters are recapped, key findings and observations are highlighted. The limitations encountered and recommendations for future work are also presented.

5.2 Summary of Chapters

This research report presented five chapters that cover the following:

1. Introduction and background that prompted the research on the proposed framework for flyrock at Anglo American Plc operations.
2. A literature review on the associated topics to understand the key concepts and what was considered previously and what forms the basis on which the flyrock risk reporting is built on.
3. The research methodology used in this study, including collection, validation and analysis of the data obtained during the study.
4. Discussion on the data obtained. Highlighting concerns, limitations and key initial observations. The results of the analysis were also discussed and the findings presented; and
5. This chapter summarises the outcomes of the study and touching on possible future work.

5.3 Research Observations

The study revealed several key findings that will be summarised in this section.

5.3.1 Initial and Complimentary Studies

A preliminary analysis was done to evaluate the effectiveness of the VDF as an initial indicator for potential flyrock occurrence using observations of blast videos. A complementary analysis was also performed to verify if the predictive model used in the current drill and blast software for flyrock estimation is effective in highlighting the risk of flyrock exceedances.

The developed flyrock risk reporting dashboard was analysed to see if it would work as a tool for flyrock risk awareness. Evaluation of Orica Digital Solutions' BlastVision® service, as a potential video analysis and monitoring services, was also performed. These initial and complementary analysis provided valuable insights into the requirements for addressing the objectives of this research report.

5.3.2 Key Findings and Observations

The preliminary analysis around VDF data from the 23 blasts indicated good correlation between the VDF and SDOB and showed that if the VDF exceeds 2.5, the likelihood of flyrock increases. The effectiveness of the predictive model used in BlastLogic to highlight the risk of exceedances was confirmed. From the blasts observed as part of the study all actual flyrock ranges were within the predicted ranges. The model however does in most of the cases overestimate the flyrock range.

The flyrock risk reporting dashboard, developed as part of the study, indicated that it can be used as a proactive tool to show if a blast is at risk but moreover when multiple historic blasts are included, it can indicate if an operation's management of flyrock is in control. The two trials conducted using Orica Digital Solutions' BlastVision® had mixed but promising results, however there is still a lot more work required to automate the services to produce accurate results consistently.

5.4 Research Contributions

This study contributes to the existing body of knowledge on flyrock risk management in several ways. By combining the modelling, monitoring, measuring and reporting of flyrock in a structured process, it supplies the basis for and integrated approach to managing the risk of flyrock.

The expansion and validation of the VDF as an indicator for possible flyrock exceedances from cratering allows for it to be used as a potential trigger mechanism to decide if an in-depth video analysis for flyrock is required.

As part of the development of the flyrock risk reporting dashboard, the combination of previous empirical model criteria and analytical trajectory equations made the

processing quick. It even allows for detailed modelling using normal handheld calculators. The adjustment of the proportionality factor (Chudinov, et al., 2019), to include the shape factor (Equation 33), improved the trajectory estimations to ensure greater compatibility with contemporary, complex numerical approaches based on differential equations.

The occurrence of flyrock is not a consequence of initiating the blast, but in most of the observations, it is the consequence of a decision or action (controllable factors) taken earlier in the drill and blast process. This still aligns with Fletcher, (1983) observations that human factors play a significant role in surface blasting accidents. The five main reasons are listed as lack of planning, inadequate instructions, negligence, hasty decisions and overconfidence (Raina, 2023).

The evaluation of the risk of flyrock must not be limited just to the initial prediction during the drill and blast concept design phase but should take place at various stages in the drill and blast process (Figure 62).

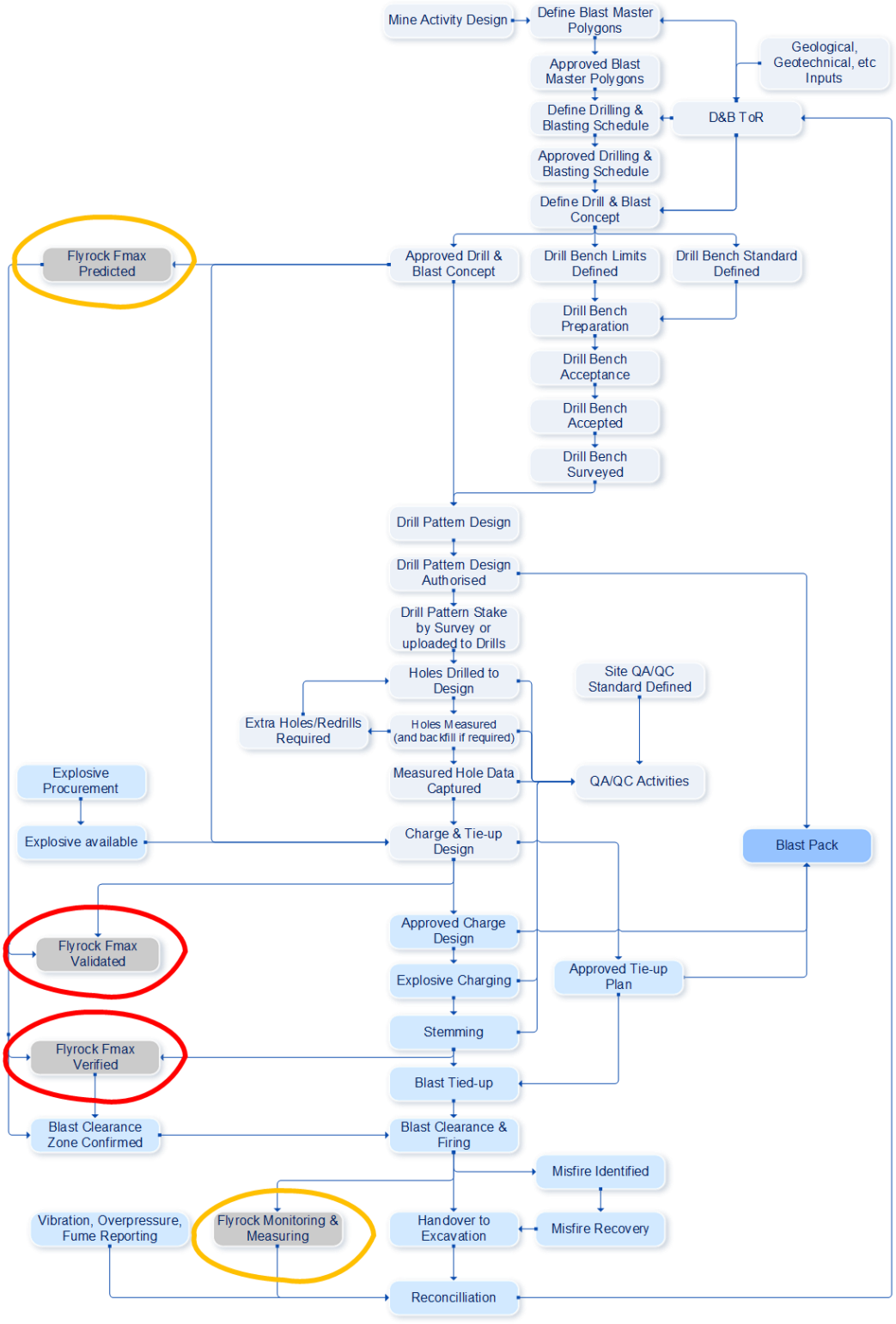

Figure 62: Amended Anglo American Plc drill and blast process flow

The amended drill and blast process (Figure 61), for Anglo American Plc operations, included the following changes:

- **Fmax prediction:** Designing an initial blast pattern layout to optimise blast results by predicting the potential for flyrock.
- **Fmax validation:** Checking flyrock potential before charging commences with ‘as drilled’ holes; and
- **Fmax verification:** Confirming flyrock potential prior to blast clearance with ‘as charged’ holes to allow final decision on blast clearance criteria.

5.5 Research Limitations

The study concentrated on the cratering flyrock mechanism. This was mainly done for two reasons. Firstly, the data of actual flyrock occurrences indicated that most originated due to catering. Secondly since the reporting dashboard is automated from data within BlastLogic, the actual minimum burden for front holes is currently not captured directly in the system, thus cannot be automatically extracted. However, the predictive flyrock model within BlastLogic do cater for face burst events as well as the flyrock calculator (Appendix C) developed for this study.

During the data capturing for the study, several secondary blasts (boulders, high spots and toes) were also observed that exceeded Fmax. An example is shown of ‘toes’ blasted in Figure 63.



Figure 63: Flyrock from secondary blasting

Flyrock from secondary blasting was not included in the study. Part of the reason for this is that no formal predictive model for secondary blasting is incorporated in the blast management software.

5.6 Recommendations for Future Research Work

Implementation of the flyrock framework across Anglo American Plc operations remains in its early phase. Further evaluation will be necessary to assess the full effectiveness of the complete framework after it has been operational for an extended duration.

As indicated in Figure 64, this study covered methods of predicting flyrock distances by analysing the projectile's trajectory. The methods used cater for estimations where the launch point and impact point elevations were the same, as well in case where they are different. However, one area that is considered but requires further work are the cases where a flyrock fragment rebounds after impact. This can have a significant impact (Raina, 2023). The impact is even larger if the impact point is especially below the launch point as is the case with some of Anglo American Plc's high altitude mines.

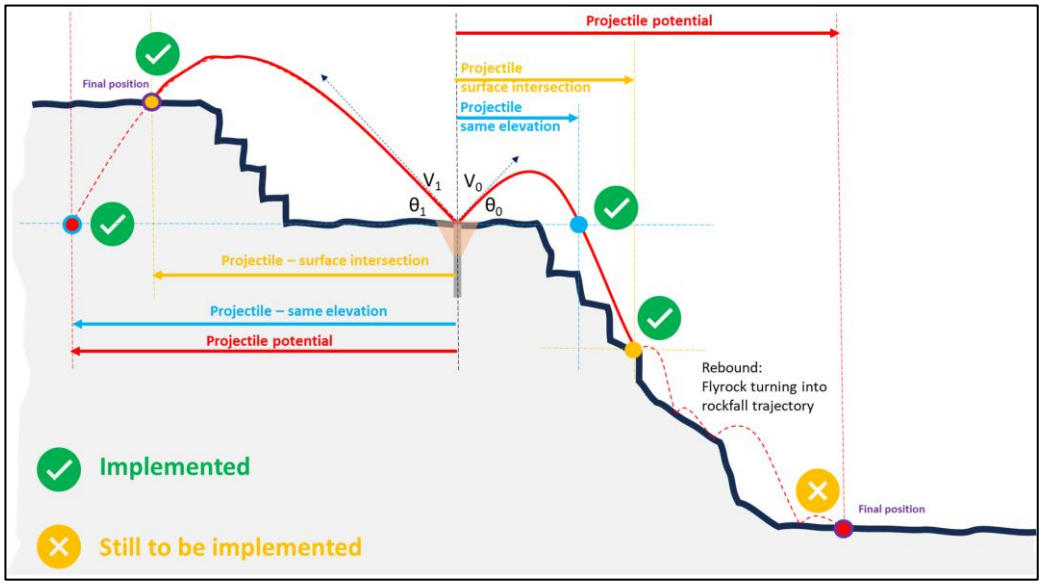

Figure 64: Trajectory analysis considerations

Initial expansion of the flyrock calculator (Appendix C) created in this study to validate some of the analysis, used elementary equations from Stevens (1998) to estimate the rebound distance. This however needs further work.

It is recommended that where the predictive model in BlastLogic indicate impact points on long extreme slopes, to run a separate statistical analysis (as in the example shown in Figure 65). using the site's rockfall simulation software to determine the possible endpoint distribution.

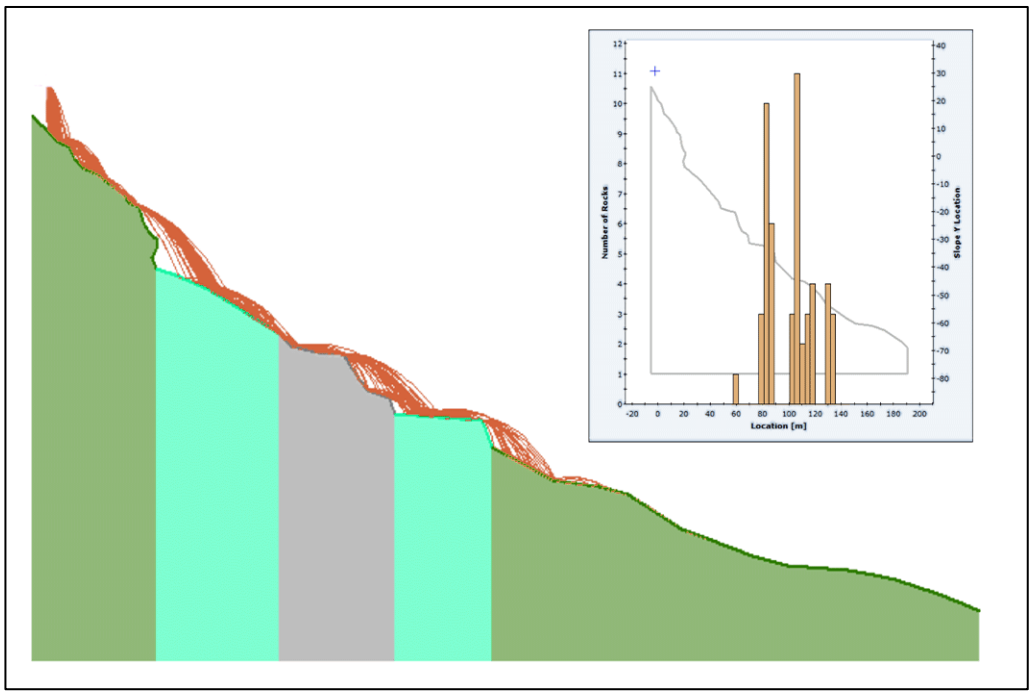

Figure 65: 2D Statistical Analysis in RocFall2 (Rocscience, 2024)

The flyrock risk reporting dashboard currently incorporates the risk from cratering. It is recommended to expand this to also include risk from face bursts. This needs further work as it involves changes in the source system. Additionally, recommendations for further work are to improve the prediction model's accuracy by evaluating the following effects on predicted ranges:

- Effect of air pressure on air drag calculations for high altitude sites.
- Effect of type of stemming material or lack of stemming.
- Influence of collar conditions; and
- Effect of loose material on the bench during blasting.

It is recommended to re-evaluate the parameter constants used in the equations, including the shape factor and other influential variables. Preliminary work in this area has shown that certain parameters are highly sensitive and can significantly affect the predicted ranges. This sensitivity is illustrated in Figure 66, which demonstrates the variation in Fmax resulting from incremental changes to selected parameters.

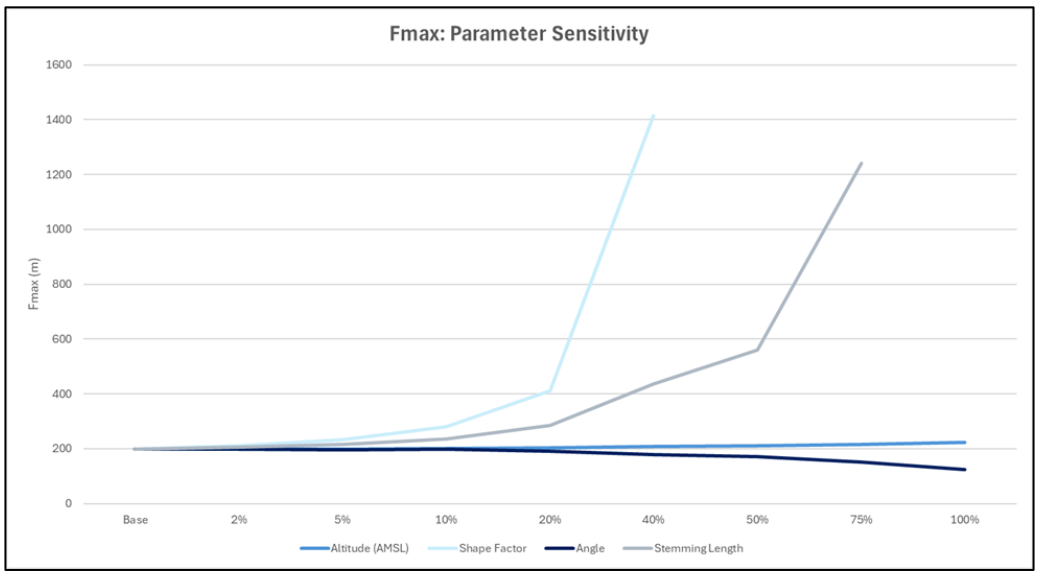

Figure 66: Parameter sensitivity impact on Fmax

As illustrated in Figure 66, incremental increases of the shape factor from 1.0 in 5% steps result in an exponential rise in Fmax once the increase surpasses 20% (1.2).

Prediction of flyrock occurrence from secondary blasting activities require more work as previously stated. In an ideal situation the focus should be to eliminate the occurrences of boulders, toes and high spots that require secondary blasting. However, it is still a reality and do occur and as such the risk for potential flyrock need to be considered.

Currently BlastLogic cannot handle the design and evaluation of boulders. No formal design package that is dedicated to drill and blast of boulders were found. Learnings from the study was utilised to establish a boulder drill and blast design and risk evaluation proposal (Figure 67).

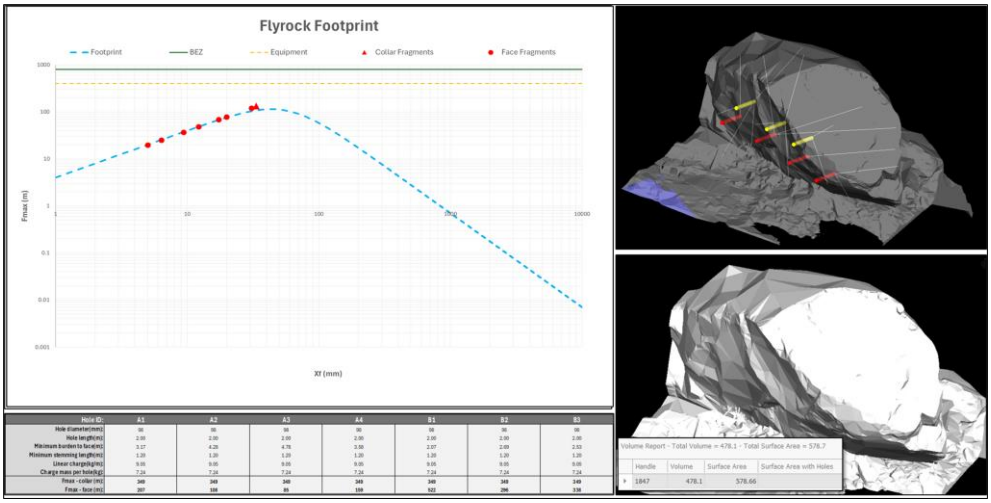

Figure 67: Initial boulder drill and blast design and risk evaluation proposal

Figure 67 shows the pattern design on a large boulder. Each hole was evaluated for flyrock risk in a similar manner using the flyrock footprint. This still requires more work to improve, formalise and integrate it into the framework.

Solutions such as BlastVision® from Orica Digital Solutions, shows promise to help automate or streamline the actual monitoring for flyrock from blast videos. This field will advance as technology improves and currently there is already some research dedicated in this field and linked fields such as in-flight dynamics for volcanic bomb trajectory tracking.

While Anglo American Plc provided a comprehensive and suitable basis for evaluating relevant theories and developing the framework, future research could be significantly enriched by incorporating data and insights from other mining companies globally. This broader inclusion would enhance the generalisability and robustness of the findings.

REFERENCE LIST

Adermann, D., Chalmers, D., Martin, C. & Wellink, S., 2015. High-speed video—An essential blasting tool, Sydney: Proceedings of the 11th International Symposium on Rock Fragmentation by Blasting, pp 471-476.

Adhikari, G. R., 1999. Studies on Flyrock at Limestone Quarries. Rock Mechanics and Rock Engineering , 32(1), pp. 291-301. https://doi.org/10.1007/s006030050049

Anglo American Plc, 2020. Explosives Handling Standard V3 AA_TS_405_001.Unpublished, London: Anglo American Plc.

Anglo American Plc, 2024. Where we operate. [Online] Available at: https://www.angloamerican.com/about-us/where-we-operate [Accessed 05 03 2024].

Armaghani, D. J. et al., 2016. Risk Assessment and Prediction of Flyrock Distance by Combined Multiple Regression Analysis and Monte Carlo Simulation of Quarry Blasting. Rock Mechanics and Rock Engineering, Volume 49, pp. 3631-3641. https://doi.org/10.1007/s00603-016-1015-z

Armaghani, D. et al., 2016. Evaluation and prediction of flyrock resulting from blasting operations using empirical and computational methods. Engineering with Computers, 32(1), pp. 109-121. https://doi.org/10.1007/s00366-015-0402-5

Austin Powder, 2024. Paradigm. [Online] Available at: https://paradigm.austinpowder.com/Features [Accessed 14 03 2025].

Babaeian, M. et al., 2023. Application of Soft Computing, Statistical and Multi-Criteria Decision-Making Methods to Develop a Predictive Equation for Prediction of Flyrock Distance in Open-Pit Mining. Mining, 3(1), pp. 304-333. https://doi.org/10.3390/

Bajpayee, T. S., Rehak, T. R., Mowrey, G. I. & Ingram, D. K., 2004. Blasting Injuries In Surface Mining With Emphasis On Flyrock And Blast Area Security, CDC Stacks. https://stacks.cdc.gov/view/cdc/8766/cdc_8766_DS1.pdf

Bamford, T. M., 2021. Application of Unmanned Aerial Systems to Blast Monitoring in Open Pit Mines. PhD thesis, University of Toronto. http://hdl.handle.net/1807/109323

Bhatawdekar, R. M., Choudhury, S. & Modmad, E. T., 2018. UAV Applications on Projects Monitoring in Mining and Civil Engineering. Journal of Mines, Metals and Fuels, 66(12), pp. 867-872.

Blair, D. P., 2017. Cut-off in surface delays due to flyrock; Proceedings of Stockholm Conference. Stockholm, European Federation of Explosives Engineers.

Blair, D. P., 2022. Probabilistic analysis of flyrock from blasting in surface mines and quarries. International Journal of Rock Mechanics and Mining Sciences, 159(105204), p. 9. http://dx.doi.org/10.1016/j.ijrmms.2022.105204

Blast Training International, 2015. Manage Drill & Blast Operations - Module S4. Wynnum: Blast Management International.

BoganaVijaykumar, S., 2024. Strategies for curating high-quality datasets to train effective ML models. International Research Journal of Engineering and Technology, 11(05), pp. 2111-2121.

Brown, D., Christian, . W. & Hanson, R. M., 2025. Tracker - Video Analysis and Modeling Tool. [Online] Available at: https://opensourcephysics.github.io/tracker-website/ [Accessed 14 03 2025].

Carpenter, E., 2022. Blasting Exclusion Zone Technology Concepts: History at Anglo. Unpublished, Johannesburg: Anglo American.

Chernigovskii, A. A., 1985. Application of directional blasting in mining and civil engineering, New Delhi: Amerind Publishing Co Pyt Ltd. https://www.osti.gov/biblio/5611570

Chiapetta, R. F., Bauer, A., Dialey, P. J. & Burchnell, S. L., 1983. The use of high-speed motion picture photography in blast evaluation and design, Proceedings of 9th conference on explosives and blasting techniques. Dallas, USA, International Society of Explosives Engineers.

Chiappetta, R. F., Treleaven, T., Nixon, E. & Smith, J. D., 1998. History and expansion of the Panama Canal. International Journal for Blasting and Fragmentation, 2(3), pp. 313-340. http://doi.org/10.1080/13855149809408780

Chudinov, P., 2005. The envelope of projectile trajectories in midair, Moscow, Russia: Department of Theoretical Mechanics, Faculty of Applied Mathematics and Physics.

Chudinov, P., 2014. Approximate analytical description of the projectile motion with a quadratic drag force. Athens J. Nat. Formal Sci, Volume 1, pp. 97-106.

Chudinov, P., 2022. Projectile motion in midair using simple analytical approximations. The Physics Teacher, 60(9), pp. 774-778. https://doi.org/10.1119/5.0053162

Chudinov, P., 2024. Projectile motion in a medium with quadratic drag at wind influence, Perm, Russia: Department of Engineering, Perm State Agro-Technological University. https://doi.org/10.21203/rs.3.rs-3825674/v1

Chudinov, P., Eltyshev, V. & Barykin, Y., 2016. Simple Analytical Algorithm for constructing the envelope of the projectile trajectories in midair. Journal for Advances in Physics, 11(5), pp. 3312-3321.

Chudinov, P., Eltyshev, V. & Barykin, Y., 2019. Highly precise analytic solutions for classic problem of projectile motion in the air. Journal of Physics: Conference Series, 1287(1), pp. 12-32.

Chudinov, P., Eltyshev, V. & Barykin, Y., 2021. Analytical construction of the projectile motion trajectory in midair. Momento, Issue 62, pp. 79-96. https://doi.org/10.15446/mo.n62.90752

Chudinov, P. S., 2005. An Optimal Angle of Launching a Point Mass in a Medium with Quadratic Drag Force, Moscow: Department of Theoretical Mechanics.

Chudinov, P. S., 2010. Approximate formula for the vertical asymptote of projectile motion in midair. International Journal of Mathematical Education in Science and Technology, 41(1), pp. 92-98. https://doi.org/10.1080/00207390903125215

Chudinov, P. S., 2011. Approximate analytical investigation of projectile motion in a medium with quadratic drag force. International Journal of Sports Science and Engineering, 5(1), pp. 27-42.

Davies, P. A., 1995. Risk-based approach to setting of flyrock 'danger zones' for blast sites. *Institute of Mining & Metallurgy,* Volume 104, pp. 96-100. http://doi.org/10.1016/0148-9062(95)99212-G

Deswik, 2025. Deswik.CAD - Design & Solids Modeling. [Online] Available at: https://www.deswik.com/product-detail/deswik-cad/ [Accessed 14 03 2025].

Dotto, M. S. & Pourrahimian, Y., 2024. The Influence of Explosive and Rock Mass Properties on Blast Damage in a Single-Hole Blasting. Mining, 4(1), pp. 168-188. https://doi.org/10.3390/mining4010011

Faramarzi, F., Mansouri, . H. & Farsangi, M. A. E., 2014. Development of rock engineering systems-based models for flyrock risk analysis and prediction of flyrock distance in surface blasting. Rock Mechanics and Rock Engineering, 47(4), pp. 1291-1306. https://doi.org/10.3390/mining4010011

Fletcher, L. R., 1983. Analysis of Recent Mine Blasting Accidents, Cleveland: International Society of Explosives Engineers.

Fletcher, L. R., & D'Andrea, D. V., 1986. Control of flyrock in Blasting, Proceedings of the 12th Annual Conference on Explosives and Blasting Techniques, Atlanta, Georgia, pp. 167 – 177.

Foster, S., 2024. Flyrock from Charges in Blasted Muckpile; Proceedings of 8th Drill & Blast Down Under Conference. Perth, WA, International Society of Explosives Engineers - Australia.

Ghasemi, E., Sari, M. & Ataei, M., 2012. Development of an empirical model for predicting the effects of controllable blasting parameters on flyrock distance in surface mines. *International Journal of Rock Mechanics and Mining Sciences,* 52(1), pp. 163-170. https://0-doi-org.innopac.wits.ac.za/10.1016/j.ijrmms.2012.03.011

Gibson, M. F. & George, J. D., 2001. Estimation of Flyrock Travel Distances: A Probabilistic Approach. The Australasian Institute of Mining and Metallurgy, 1, p. 4.

Graham, D. J. & Midgley, N. G., 2000. Graphical representation of particle shape using triangular diagrams: an Excel spreadsheet method. Earth Surface Processes and Landforms, 25(13), pp. 1473-1477. https://doi.org/10.1002/1096-9837(200012)25:13%3C1473::AID-ESP158%3E3.0.CO;2-C

GroundProbe - Orica Digital Solutions, 2024. An Innovative Approach to Blast Analytics Using Drone Technology for Enhanced Safety and Productivity. [Online]
Available at: https://www.groundprobe.com/an-innovative-approach-to-blast-analytics/
[Accessed 29 12 2024].

GroundProbe, 2023. BlastVision Trials for Anglo American South Africa, Unpublished, Orica Digital Solutions.

Hasanipanah, M. et al., 2018. A Risk-Based Technique to Analyze Flyrock Results Through Rock Engineering System. Geotech Geol Eng, Volume 36, pp. 2247-2260. https://doi.org/10.1007/s10706-018-0459-1

Hudaverdi, T. & Agan, Y., 2023. Application of Intelligent Models for Flyrock Prediction Considering Design Parameters and Bench Face Characteristics. Mining, Metallurgy & Exploration, 40(6), pp. 2331-2347. https://doi.org/10.1007/s42461-023-00879-y

International Organization for Standardization, 2023. Risk management — Guidelines (ISO 31000:2018). [Online]
Available at: https://www.iso.org/standard/65694.html#lifecycle
[Accessed 06 03 2025].

InterVal, 2024. August 10, 2020 Supplement to April 24, 2020 Flyrock and Other Impacts from Quarry Blasting Operations. [Online]
Available at: https://intval.com/articles/Flyrock-and-Other-Impacts-from-Quarry-Blasting-Operations.pdf
[Accessed 10 12 2024].

IsoMetrix, 2025. Globally Trusted Sustainability Reporting & Risk Management. [Online]
Available at: https://www.isometrix.com/#
[Accessed 14 03 2025].

Johnson, C. E., 2018. Effect of Wave Collision on Fragmentation, Throw, and Energy Efficiency of Mining and Comminution. In: K. Awuah-Offei, ed. Energy Efficiency in the Minerals Industry. Cham: Springer, pp. 55-70. https://doi.org/10.1007/978-3-319-54199-0_4

Jones, G. E., Kennedy, J. E. & Bertholf, L. D., 1980. Ballistics calculations of R. W. Gurney. American Journal of Physics, Volume 48, pp. 264-269. https://doi.org/10.1119/1.12135

Kecojevic, V. & Radomsky, M., 2005. Flyrock phenomena and area security in blasting-related accidents. Safety Science, 43(9), pp. 739-750. doi:10.1016/j.ssci.2005.07.006

Kinovea, 2023. A microscope for your videos. [Online]
Available at: https://www.kinovea.org/
[Accessed 14 03 2025].

Kitameraki, 2023. Digging Deeper: Machine Learning and AI Applications in Mining. [Online]
Available at: https://www.kitameraki.com/post/digging-deeper-machine-learning-and-ai-applications-in-mining
[Accessed 13 03 2025].

Konya, A. & Konya, C. J., 2020. Violence Factor – The New Tool for Blast Performance Analysis, Proceedings of the 46 annual conference on explosives and blasting technique. Denver, International Society of Explosives Engineers, p. 10.

Kovačević, N., Stojiljković, A. & Kovač, M., 2019. Application of the matrix approach in risk assessment. Operational Research in Engineering Sciences: Theory and Applications, 2(3), pp. 55-64.

Li, C. et al., 2023. Prediction of Flyrock Distance in Surface Mining Using a Novel Hybrid Model of Harris Hawks Optimization with Multi-strategies-based Support Vector Regression. Natural Resources Research, 32(6), pp. 2995-3023. https://doi.org/10.1007/s11053-023-10259-4

Little, T. N., 2007. Flyrock Risk. Wollongong, NSW Australia, Proceedings of EXPLO 2007 Blasting: Techniques and Proceedings of EXPLO 2007 Blasting: Techniques and Technology.

Little, T. N. & Blair, D. P., 2010. Mechanistic Monte Carlo models for analysis of flyrock risk. In: Sanchidrián, ed. Rock Fragmentation by Blasting. London: Taylor & Francis Group, pp. 641-647.

Lundborg, N., 1974. The hazard of flyrock in rock blasting, Stockholm, Sweden: Swedish Rock Blasting Committee.

Lundborg, N., 1979. The probability of flyrock damage, Stockholm, Sweden: SveDeFo.

Lwin, M. M. & Aung, Z. M., 2019. Prediction and Controlling of Flyrock due to Blasting for Kyaukpahto Gold Mine. *International Journal of Advances in Scientific Research and Engineering,* 5(10), pp. 338-346. https://doi.org/10.31695/IJASRE.2019.33574

Maptek, 2024. Maptek BlastLogic. [Online] Available at: https://www.maptek.com/products/blastlogic/ [Accessed 30 11 2024].

Masir, R. N., Ataei, M. & Motahedi , A., 2020. Risk assessment of Flyrock in Surface Mines using a FFTA-MCDM Combination. Journal of Mining and Environment, 12(1), pp. 191-203. https://doi.org/10.22044/jme.2020.9107.1799

McKenzie, C. K., 2009. Flyrock range and fragment size prediction, Proceedings of the 35th annual conference. Cleveland, International Society of Explosives Engineers.

McKenzie, C. K., 2022. Flyrock model validation and application. In: X. G. Wang, ed. Rock Fragmentation by Blasting. Beijing: Metallurgical Industry Press, pp. 21-36.

McKenzie, C. K., Kharitonenko, I., Papillon, B. E. & Popov, P., 2015. An Automated System for Flyrock and Fume Monitoring of Blasts, Proceedings of the 11th International Symposium on Rock Fragmentation by Blasting. Sydney, Australasian Institute of Mining and Metallurgy, pp. 417-424.

Mishra, A. K. & Mallick, D. K., 2012. Analysis of blasting related accidents with emphasis on flyrock and its mitigation in surface mines. In: S. A. Singh P K,

ed. Rock Fragmentation by Blasting. London: Taylor and Francis, pp. 555-561.

Mishra, R., Mishra, A. K. & Choudhary, B. S., 2023. High-Speed Motion Analysis-Based Machine Learning Models for Prediction and Simulation of Flyrock in Surface Mines. Applied Sciences, 13(9906), p. 33. https://doi.org/10.3390/app13179906

Muller, K. & Oosthuizen, T., 2015. Should the Blast Exclusion Zone Be Based on a Qualitative or Quantitative Analysis? A Practical Implementation Conundrum; In Proceedings of 11th International Symposium on Rock Fragmentation by Blasting. Sydney, The Australasian Institute of Mining and Metallurgy.

Muñoz, L., Gontijo, G., Machado, D. & Baracho, E., 2024. Blasting Near Communities: A review of new techniques and technologies to minimize the impact generated by blasting. International Society of Explosives Engineers, 1 1, p. 12.

Nguyen, A. T. et al., 2020. Simulation of Flyrock Distance as a Function of Blast Conditions: a Case Study in Vietnam. Journal of the Polish Mineral Engineering Society, 1(2), pp. 275-282. http://doi.org/10.29227/IM-2020-02-33

Noble Desktop, 2024. Understanding the Generalization Error in Machine Learning. [Online]
Available at: https://www.nobledesktop.com/learn/python/understanding-the-generalization-error-in-machine-learning
[Accessed 13 03 2025].

O-Pitblast, 2023. Flyrock model manual. [Online]
Available at: https://downloads.o-pitblast.com/files/manual/O-Pitblast%20-%20Flyrock%20Model%20Manual.pdf
[Accessed 14 03 2025].

Orica Digital Solutions, 2024. Exclusion Zone Tool. [Online]
Available at: https://support.blastiq.com/hc/en-us/articles/900007101403-Exclusion-Zone-Tool
[Accessed 14 03 2025].

Papillon, B. E. et al., 2018. Methods and sytem for blasting video analysis. United States, Patent No. US 9,995,843 B2.
https://patents.google.com/patent/US9995843B2/en

Raina, A. K., 2023. Flyrock in Surface Mining: Origin, Prediction, and Control. 1 ed. Oxon: CRC Press. https://doi.org/10.1201/9781003327653

Raina, A. K. & Bhatawdekar, R. M., 2022. Chapter 14 - Blast-induced flyrock: risk evaluation and management. In: Risk, Reliability and Sustainable Remediation in the Field of Civil and Environmental Engineering. Elsevier, pp. 209-247.
https://doi.org/10.1016/B978-0-323-85698-0.00016-2

Raina, A. K., Chakraborty, A. K., Choudhury, P. B. & Sinha, A., 2011. Flyrock danger zone demarcation in opencast mines: a risk based approach. Bulletin of Engineering Geology and the Environment, 70(1), pp. 163-172.
https://doi.org/10.1007/s10064-010-0298-7

Raina, A. K., Murthy, V. M. & Soni, A. K., 2015. Flyrock in surface mine blasting: Understanding the basics to develop a predictive regime. Current Science, 108(4), pp. 660-665.

Raina, A. K., Murthy, V. M. S. R. & Soni, A. K., 2014. Flyrock in bench blasting: a comprehensive review. Bulletin of Engineering Geology and the Environment, 73(1), pp. 1199-1209. https://doi.org/10.1007/s10064-014-0588-6

Rawnaq, E. et al., 2024. A Comparative Study of Two Tree-Based Models for Predicting Flyrock Velocity at Open Pit Bench Mining. Open Journal of Applied Sciences, 14(1), pp. 267-287.
https://doi.org/10.4236/ojapps.2024.142019

Richards, A. B. & Moore, A. J., 2002. Flyrock Control - by Chance or Design, Proceedings of the annual conference. Orleans, International Society of Explosives Engineers, pp. 335-348.

Rocscience, 2024. RocFall2 - 2D Rockfall Analysis Software. [Online] Available at: https://www.rocscience.com/software/rocfall [Accessed 28 12 2024].

Roth, J. A., 1979. A model for the determination of flyrock ranges as a function of shot conditions, Los Altos, CA: Department of Commerce, NTIS.

Scovira, S., 2012. Flyrock Elimination Program Part 1: Corporate Initiative, Proceedings of the 37th Conference on Explosives and Rock Blasting Technique, International Society of Explosives Engineers, p. 6.

Sevelka, T., 2022. Preventing the Potentially Deadly Consequences of Flyrock: Mandatory Minimum Setbacks and Separation Distances Required. Grassroots Journal of Natural Resources, 5(4), pp. 66-98. https://doi.org/10.33002/nr2581.6853.050405

Sevelka, T., 2024. Ontario Aggregate Industry and Ministry of Natural Resources Continue to Ignore or Trivialize the Notoriously Dangerous and Potentially Deadly Consequences of Flyrock from Blasting (Detonation of Explosives). Journal of Policy and Governance, 4(2), pp. 1-33. https://doi.org/10.33002/jpg040201

Sevelka, T., 2025. Flyrock: The "Hits" Just Keep On Coming!. Journal of Policy & Governance, 5(1), pp. 1-15. https://doi.org/10.33002/jpg050101

Shadabfar, M. et al., 2021. Estimation of Damage Induced by Single-Hole Rock Blasting: AReviewonAnalytical, Numerical, and Experimental Solutions. Energies, 14(29), p. 24. https://dx.doi.org/10.3390/en1 4010029

South African Government, 2024. Mine Health and Safety Act: Guideline for a Mandatory Code for Practice for Minimum Standards on Ground Vibrations, Noise, Air-Blast and Flyrock near Surface Structures and Communities to

be protected. [Online]
Available at: https://www.gov.za/documents/notices/mine-health-and-safety-act-guideline-mandatory-code-practice-minimum-standards
[Accessed 30 12 2024].

Stevens, W. D., 1998. RocFall, a tool for probabilistic analysis, design of remedial measures and prediction of rockfalls, Toronto: University of Toronto. http://hdl.handle.net/1807/16244

Stojadinović , S. et al., 2013. A new model for determining flyrock drag coefficient. International Journal of Rock Mechanics and Mining Sciences, 62(1), pp. 68-73. http://dx.doi.org/10.1016/j.ijrmms.2013.04.002

Stojadinović, S., Pantović, R. & Žikić, M., 2011. Prediction of flyrock trajectories for forensic applications using ballistic flight equations. International Journal of Rock Mechanics and Mining Sciences, 48(7), pp. 1086-1094. http://dx.doi.org/10.1016/j.ijrmms.2011.07.004

Szendrei, T. & Tose, S., 2022. Flyrock in surface mining - Limitations of current predicitve models and a better alternative through modelling the aerodynamics of flyrock trajectory. Journal of the Southern African Institute of Mining and Metallurgy, 122(12), pp. 725-732. http://dx.doi.org/10.17159/2411-9717/1873/2022

Szendrei, T. & Tose, S., 2023. Flyrock in surface mining Part II — Causes, sources, and mechanisms of rock projection. The Journal of the Southern African Institute of Mining and Metallurgy, 132(12), pp. 557-564. http://dx.doi.org/10.17159/2411-9717/2583/2023

Szendrei, T. & Tose, S., 2024. Flyrock in surface mining Part III: Shock wave, stress wave, blasthole expansion. Journal of the Southern African Institute of Mining and Metallurgy, 124(9), pp. 507-516. http://dx.doi.org/10.17159/24119717/3321/2024

Taherdoost, H., 2022. What are Different Research Approaches? Comprehensive Review of Qualitative, Quantitative, and Mixed Method

Research, Their Applications, Types, and Limitations. Journal of Management Science & Engineering Research, 5(1), pp. 53-63. https://doi.org/10.30564/jmser.v5i1.4538

Tobin, G., 2013. The Importance of Energy Containment to the Blast Outcome & Justification for use of Stemming Plugs in Over Burden Removal, Australia: Oresome Products.

Tordoir, A., 2023. A Strategic Approach to Delivering Drill and Blast Step Change Across Anglo American Operations, Proceedings of 26th World Mining Conference. Brisbane, CSIRO.

Tordoir, A. & Roberts, M., 2019. Benchmarking Drill and Blast Compliance to Design, A Case Study. International Society of Explosive Engineers.

Van Der Walt, J., 2019. Developing a concept that can be used to quantify the motion of flyrock, with the intention of eventually producing a measuring tool for future flyrock research, Dissertation (MEng), Pretoria: University of Pretoria. http://hdl.handle.net/2263/73702

Van Der Walt, J. & Spiteri, W., 2020. A critical analysis of recent research into the prediction of flyrock and related issues resulting from surface blasting activities. Journal of the Southern African Institute of Mining and Metallurgy, 120(12), pp. 701-714. https://doi.org/10.17159/2411-9717/1103/2020

Van Der Walt, J. & Spiteri, W., 2023. A conceptual technique to mathematically quantify the trajectory of flyrock. Journal of the Southern African Institute of Mining and Metallurgy, 123(4), pp. 165-174. https://doi.org/10.17159/2411-9717/2168/2023

Verakis, H., 2011. Flyrock: A Continuing Blast Safety Threat, Cleveland: International Society of Explosives Engineers.

Verakis, H. & Lobb, T., 2007. Flyrock Revisited: An Ever-present Danger in Mine Blasting, Cleveland: International Society of Explosives Engineers.

Vernier, 2025. Vernier Video Analysis. [Online]
Available at: https://www.vernier.com/product/video-analysis/
[Accessed 14 03 2025].

Workman, J. L. & Calder, P. N., 1994. Flyrock Prediction and Control in Surface Mine Blasting, Cleveland: International Society of Explosives Engineers.

Xcitex Inc., 2025. ProAnalyst 2023 - Powerful software for professional motion analysts. [Online]
Available at: https://xcitex.com/products/proanalyst/2023
[Accessed 14 03 2025].

Zhang, Z.-X., Chi, L.-Y. & Changping, Y., 2021. An emperical approach for predicting burden velocities in rock blasting. Journal of Rock Mechanics and Geotechnical Engineering, Volume 13, pp. 767-773. http://dx.doi.org/10.1016/j.jrmge.2021.04.004

Zhou, J., Zhang, Y. & Qiu, Y., 2024. State-of-the-art review of machine learning and optimization algorithms applications in environmental effects of blasting. Artificial Intelligence Review, 57(5), pp. 1-54. https://doi.org/10.1007/s10462-023-10636-8

APPENDIX A. Data for Graph 34 (Flyrock Footprint Calculation)

Table 13: Flyrock footprint calculation data

Hole ID	Hole Status	Hole diameter (m)	Hole depth (m)	Explosives (kg)	Stemming (m)	Xf (mm)	sa(m^2)	pr(kg/m³)	pa(kg/m³)	cd	g	m(kg)	k	Kv	Vo(m/s)	Launch Angle (θo)	H(m)	T(sec)	Va(m/s)	Range (m) (Chudinov)	Range (m) (McKenzie 2009)	Range (m) (McKenzie 2009)
101	Fired	0.270	15.2	770	5.00	107.2	0.006897348	2650	1.29	1.5	9.81	1.485	0.000458987	56.92	140.57	33.12	86.45	8.40	37.50	314.87	389.88	(75.01)
102	Fired	0.270	15.0	755	5.00	107.2	0.006898642	2650	1.29	1.5	9.81	1.485	0.000458944	56.93	140.57	33.12	86.45	8.40	37.50	314.90	389.91	(75.01)
103	Fired	0.270	14.3	702	5.00	107.2	0.006896513	2650	1.29	1.5	9.81	1.484	0.000459015	56.91	140.56	33.12	86.44	8.40	37.50	314.85	389.85	(75.00)
104	Fired	0.270	13.5	645	5.00	107.6	0.006949171	2650	1.29	1.5	9.81	1.501	0.000457273	57.24	140.83	33.12	86.77	8.41	37.57	316.05	391.34	(75.29)
105	Fired	0.270	14.0	680	5.00	107.3	0.006905977	2650	1.29	1.5	9.81	1.487	0.000458700	56.97	140.61	33.12	86.50	8.40	37.51	315.07	390.12	(75.05)
106	Fired	0.270	14.0	684	5.00	107.7	0.006964741	2650	1.29	1.5	9.81	1.506	0.000456761	57.34	140.91	33.12	86.87	8.42	37.59	316.40	391.78	(75.37)
107	Fired	0.270	15.5	795	5.00	107.4	0.006926946	2650	1.29	1.5	9.81	1.494	0.000458006	57.10	140.72	33.12	86.63	8.41	37.54	315.55	390.71	(75.17)

108	Fired	0.270	14.0	684	5.00	107.7	0.0069 64741	2650	1.29	1.5	9.81	1.506	0.0004 56761	57.34	140.91	33.12	86.87	8.42	37.59	316.40	391.7 8	(75.37)
109	Fired	0.270	13.0	613	5.00	108.4	0.0070 47636	2650	1.29	1.5	9.81	1.533	0.0004 54067	57.85	141.33	33.12	87.38	8.44	37.70	318.28	394.1 0	(75.82)
110	Fired	0.270	15.0	843	5.00	116.2	0.0080 96712	2650	1.29	1.5	9.81	1.888	0.0004 23631	64.16	146.32	33.12	93.66	8.74	39.04	341.15	422.4 2	(81.26)
111	Fired	0.270	15.0	831	4.00	155.5	0.0145 11486	2650	1.29	1.5	9.81	4.531	0.0003 16436	99.44	169.31	33.12	125.40	10.11	45.17	456.73	565.5 1	(108.7 8)
112	Fired	0.270	15.0	767	4.00	146.8	0.0129 35054	2650	1.29	1.5	9.81	3.813	0.0003 35164	91.18	164.51	33.12	118.39	9.83	43.89	431.21	533.9 1	(102.7 1)
113	Fired	0.270	13.0	613	4.00	144.4	0.0125 04166	2650	1.29	1.5	9.81	3.624	0.0003 4089	88.89	163.12	33.12	116.40	9.74	43.52	423.96	524.9 5	(100.9 8)
114	Fired	0.270	16.0	843	5.00	108.4	0.0070 55212	2650	1.29	1.5	9.81	1.536	0.0004 53823	57.87	141.36	33.12	87.43	8.44	37.71	318.45	394.3 1	(75.86)
115	Fired	0.270	15.7	220	4.00	57.0	0.0019 47661	2650	1.29	1.5	9.81	0.223	0.0008 63744	22.04	102.45	33.12	45.93	6.12	27.34	167.31	207.1 8	(39.87)
116	Fired	0.270	10.5	421	4.00	139.2	0.0116 27594	2650	1.29	1.5	9.81	3.250	0.0003 53506	84.18	160.18	33.12	112.24	9.57	42.73	408.83	506.2 1	(97.38)
117	Aband oned	0.270	0.5	0	-			2650	1.29	1.5	9.81											

118	Fired	0.270	12.0	529	5.00	107.3	0.0069 14017	2650	1.29	1.5	9.81	1.490	0.0004 58434	57.00	140.65	33.12	86.55	8.40	37.52	315.25	390.3 5	(75.10)
119	Aband oned	0.270	0.5	0	-			2650	1.29	1.5	9.81											
121	Fired	0.270	15.0	843	4.00	157.2	0.0148 26755	2650	1.29	1.5	9.81	4.679	0.0003 13054	101.01	170.22	33.12	126.75	10.17	45.41	461.67	571.6 2	(109.9 6)
122	Fired	0.270	15.5	805	5.00	108.5	0.0070 59243	2650	1.29	1.5	9.81	1.537	0.0004 53694	57.89	141.38	33.12	87.46	8.45	37.72	318.54	394.4 3	(75.88)
123	Fired	0.270	10.5	498	4.00	157.2	0.0148 20891	2650	1.29	1.5	9.81	4.676	0.0003 13115	100.98	170.20	33.12	126.73	10.17	45.40	461.58	571.5 1	(109.9 3)
124	Fired	0.270	15.0	882	4.00	162.4	0.0158 2781	2650	1.29	1.5	9.81	5.161	0.0003 02992	106.08	173.02	33.12	130.96	10.33	46.16	477.00	590.6 1	(113.6 1)
125	Fired	0.270	15.0	843	4.00	157.2	0.0148 26755	2650	1.29	1.5	9.81	4.679	0.0003 13054	101.01	170.22	33.12	126.75	10.17	45.41	461.67	571.6 2	(109.9 6)
126	Fired	0.270	14.0	690	5.00	108.5	0.0070 59243	2650	1.29	1.5	9.81	1.537	0.0004 53694	57.89	141.38	33.12	87.46	8.45	37.72	318.54	394.4 3	(75.88)
127	Fired	0.270	13.0	613	5.00	108.4	0.0070 53701	2650	1.29	1.5	9.81	1.535	0.0004 53872	57.86	141.36	33.12	87.42	8.44	37.71	318.42	394.2 7	(75.85)
128	Fired	0.270	16.0	820	4.00	144.7	0.0125 63146	2650	1.29	1.5	9.81	3.650	0.0003 40089	89.21	163.31	33.12	116.67	9.75	43.57	424.96	526.1 8	(101.2 2)

129	Fired	0.270	16.0	843	5.00	108.4	0.0070 55212	2650	1.29	1.5	9.81	1.536	0.0004 53823	57.87	141.36	33.12	87.43	8.44	37.71	318.45	394.3 1	(75.86)
130	Fired	0.270	16.2	859	5.00	108.5	0.0070 63202	2650	1.29	1.5	9.81	1.539	0.0004 53566	57.92	141.40	33.12	87.48	8.45	37.72	318.63	394.5 4	(75.90)
201	Fired	0.270	15.6	889	5.00	115.7	0.0080 36828	2650	1.29	1.5	9.81	1.867	0.0004 25206	63.81	146.05	33.12	93.32	8.72	38.96	339.89	420.8 5	(80.96)
202	Fired	0.270	15.8	905	4.00	157.3	0.0148 43123	2650	1.29	1.5	9.81	4.687	0.0003 12881	101.09	170.27	33.12	126.82	10.17	45.42	461.92	571.9 4	(110.0 2)
203	Fired	0.270	15.2	860	4.00	157.4	0.0148 68516	2650	1.29	1.5	9.81	4.699	0.0003 12614	101.22	170.34	33.12	126.93	10.17	45.44	462.32	572.4 3	(110.1 1)
204	Fired	0.270	14.9	836	4.00	157.3	0.0148 43775	2650	1.29	1.5	9.81	4.687	0.0003 12874	101.10	170.27	33.12	126.82	10.17	45.42	461.93	571.9 5	(110.0 2)
205	Fired	0.270	15.0	843	4.00	157.2	0.0148 26755	2650	1.29	1.5	9.81	4.679	0.0003 13054	101.01	170.22	33.12	126.75	10.17	45.41	461.67	571.6 2	(109.9 6)
206	Fired	0.270	16.6	966	4.00	157.2	0.0148 35225	2650	1.29	1.5	9.81	4.683	0.0003 12964	101.05	170.24	33.12	126.79	10.17	45.42	461.80	571.7 9	(109.9 9)
207	Fired	0.270	15.2	860	4.00	157.4	0.0148 68516	2650	1.29	1.5	9.81	4.699	0.0003 12614	101.22	170.34	33.12	126.93	10.17	45.44	462.32	572.4 3	(110.1 1)
208	Fired	0.270	15.8	906	4.00	157.4	0.0148 66823	2650	1.29	1.5	9.81	4.698	0.0003 12631	101.21	170.33	33.12	126.92	10.17	45.44	462.29	572.4 0	(110.1 1)

209	Fired	0.270	15.4	864	4.00	155.9	0.0145 90633	2650	1.29	1.5	9.81	4.568	0.0003 15576	99.80	169.54	33.12	125.74	10.13	45.23	457.98	567.0 5	(109.0 8)
210	Fired	0.270	15.5	882	4.00	157.3	0.0148 43329	2650	1.29	1.5	9.81	4.687	0.0003 12879	101.09	170.27	33.12	126.82	10.17	45.42	461.92	571.9 4	(110.0 2)
211	Fired	0.270	18.0	1073	4.00	157.2	0.0148 2857	2650	1.29	1.5	9.81	4.680	0.0003 13034	101.02	170.22	33.12	126.76	10.17	45.41	461.69	571.6 6	(109.9 6)
212	Fired	0.270	18.0	1073	4.00	157.2	0.0148 2857	2650	1.29	1.5	9.81	4.680	0.0003 13034	101.02	170.22	33.12	126.76	10.17	45.41	461.69	571.6 6	(109.9 6)
213	Fired	0.270	18.0	1073	4.00	157.2	0.0148 2857	2650	1.29	1.5	9.81	4.680	0.0003 13034	101.02	170.22	33.12	126.76	10.17	45.41	461.69	571.6 6	(109.9 6)
214	Fired	0.270	15.5	882	4.00	157.3	0.0148 43329	2650	1.29	1.5	9.81	4.687	0.0003 12879	101.09	170.27	33.12	126.82	10.17	45.42	461.92	571.9 4	(110.0 2)
215	Fired	0.270	15.8	905	4.00	157.3	0.0148 43123	2650	1.29	1.5	9.81	4.687	0.0003 12881	101.09	170.27	33.12	126.82	10.17	45.42	461.92	571.9 4	(110.0 2)
216	Fired	0.270	15.0	843	4.00	157.2	0.0148 26755	2650	1.29	1.5	9.81	4.679	0.0003 13054	101.01	170.22	33.12	126.75	10.17	45.41	461.67	571.6 2	(109.9 6)
217	Fired	0.270	13.8	751	4.00	157.2	0.0148 25718	2650	1.29	1.5	9.81	4.679	0.0003 13065	101.00	170.22	33.12	126.75	10.17	45.41	461.65	571.6 0	(109.9 5)
218	Fired	0.270	14.0	767	4.00	157.3	0.0148 44544	2650	1.29	1.5	9.81	4.688	0.0003 12866	101.10	170.27	33.12	126.83	10.17	45.42	461.94	571.9 7	(110.0 2)

219	Fired	0.270	16.5	958	4.00	157.2	0.0148 27771	2650	1.29	1.5	9.81	4.680	0.0003 13043	101.02	170.22	33.12	126.75	10.17	45.41	461.68	571.6 4	(109.9 6)
220	Fired	0.270	18.0	1073	4.00	157.2	0.0148 2857	2650	1.29	1.5	9.81	4.680	0.0003 13034	101.02	170.22	33.12	126.76	10.17	45.41	461.69	571.6 6	(109.9 6)
221	Fired	0.270	17.0	997	4.00	157.3	0.0148 42394	2650	1.29	1.5	9.81	4.687	0.0003 12889	101.09	170.26	33.12	126.82	10.17	45.42	461.91	571.9 2	(110.0 1)
222	Fired	0.270	18.0	1073	4.00	157.2	0.0148 2857	2650	1.29	1.5	9.81	4.680	0.0003 13034	101.02	170.22	33.12	126.76	10.17	45.41	461.69	571.6 6	(109.9 6)
223	Fired	0.270	18.0	1073	4.00	157.2	0.0148 2857	2650	1.29	1.5	9.81	4.680	0.0003 13034	101.02	170.22	33.12	126.76	10.17	45.41	461.69	571.6 6	(109.9 6)
224	Fired	0.270	17.5	1035	4.00	157.2	0.0148 35225	2650	1.29	1.5	9.81	4.683	0.0003 12964	101.05	170.24	33.12	126.79	10.17	45.42	461.80	571.7 9	(109.9 9)
225	Fired	0.270	18.0	1073	4.00	157.2	0.0148 2857	2650	1.29	1.5	9.81	4.680	0.0003 13034	101.02	170.22	33.12	126.76	10.17	45.41	461.69	571.6 6	(109.9 6)
226	Fired	0.270	16.5	958	4.00	157.2	0.0148 27771	2650	1.29	1.5	9.81	4.680	0.0003 13043	101.02	170.22	33.12	126.75	10.17	45.41	461.68	571.6 4	(109.9 6)
227	Fired	0.270	16.0	907	4.00	155.6	0.0145 33336	2650	1.29	1.5	9.81	4.541	0.0003 16198	99.51	169.37	33.12	125.49	10.12	45.18	457.08	565.9 4	(108.8 6)
228	Fired	0.270	17.0	983	4.00	155.7	0.0145 4224	2650	1.29	1.5	9.81	4.545	0.0003 16101	99.55	169.40	33.12	125.53	10.12	45.19	457.22	566.1 1	(108.9 0)

229	Fired	0.270	17.0	983	4.00	155.7	0.0145 4224	2650	1.29	1.5	9.81	4.545	0.0003 16101	99.55	169.40	33.12	125.53	10.12	45.19	457.22	566.1 1	(108.9 0)
230	Fired	0.270	15.5	869	4.00	155.6	0.0145 28304	2650	1.29	1.5	9.81	4.539	0.0003 16253	99.48	169.36	33.12	125.47	10.12	45.18	457.00	565.8 4	(108.8 4)
231	Fired	0.270	18.0	1058	4.00	155.6	0.0145 30029	2650	1.29	1.5	9.81	4.539	0.0003 16234	99.49	169.36	33.12	125.48	10.12	45.18	457.02	565.8 7	(108.8 5)
232	Fired	0.270	18.0	1058	4.00	155.6	0.0145 30029	2650	1.29	1.5	9.81	4.539	0.0003 16234	99.49	169.36	33.12	125.48	10.12	45.18	457.02	565.8 7	(108.8 5)
233	Fired	0.270	16.5	945	4.00	155.7	0.0145 37966	2650	1.29	1.5	9.81	4.543	0.0003 16148	99.53	169.38	33.12	125.51	10.12	45.19	457.15	566.0 3	(108.8 8)
234	Fired	0.270	17.0	983	4.00	155.7	0.0145 4224	2650	1.29	1.5	9.81	4.545	0.0003 16101	99.55	169.40	33.12	125.53	10.12	45.19	457.22	566.1 1	(108.9 0)
235	Fired	0.270	15.5	869	4.00	155.6	0.0145 28304	2650	1.29	1.5	9.81	4.539	0.0003 16253	99.48	169.36	33.12	125.47	10.12	45.18	457.00	565.8 4	(108.8 4)
236	Fired	0.270	17.0	983	4.00	155.7	0.0145 4224	2650	1.29	1.5	9.81	4.545	0.0003 16101	99.55	169.40	33.12	125.53	10.12	45.19	457.22	566.1 1	(108.9 0)
237	Fired	0.270	17.5	1035	4.00	157.2	0.0148 35225	2650	1.29	1.5	9.81	4.683	0.0003 12964	101.05	170.24	33.12	126.79	10.17	45.42	461.80	571.7 9	(109.9 9)
238	Fired	0.270	14.0	767	4.00	157.3	0.0148 44544	2650	1.29	1.5	9.81	4.688	0.0003 12866	101.10	170.27	33.12	126.83	10.17	45.42	461.94	571.9 7	(110.0 2)

239	Abandoned	0.270	0.5	0	4.00			2650	1.29	1.5	9.81										
240	Fired	0.270	12.0	613	4.00	157.2	0.014823579	2650	1.29	1.5	9.81	4.678	0.000313087	100.99	170.21	33.12	126.74	10.17	45.41	461.62	571.56	(109.94)
301	Fired	0.270	17.0	997	4.00	157.3	0.014842394	2650	1.29	1.5	9.81	4.687	0.000312889	101.09	170.26	33.12	126.82	10.17	45.42	461.91	571.92	(110.01)
302	Fired	0.270	16.4	951	4.00	157.3	0.01484274	2650	1.29	1.5	9.81	4.687	0.000312885	101.09	170.27	33.12	126.82	10.17	45.42	461.92	571.93	(110.02)
303	Fired	0.270	14.0	767	4.00	157.3	0.014844544	2650	1.29	1.5	9.81	4.688	0.000312866	101.10	170.27	33.12	126.83	10.17	45.42	461.94	571.97	(110.02)
304	Fired	0.270	14.5	805	4.00	157.2	0.014835225	2650	1.29	1.5	9.81	4.683	0.000312964	101.05	170.24	33.12	126.79	10.17	45.42	461.80	571.79	(109.99)
305	Fired	0.270	13.5	728	4.00	157.2	0.014825417	2650	1.29	1.5	9.81	4.679	0.000313068	101.00	170.22	33.12	126.74	10.17	45.41	461.65	571.60	(109.95)
306	Fired	0.270	12.0	605	4.00	155.7	0.014544912	2650	1.29	1.5	9.81	4.546	0.000316072	99.57	169.40	33.12	125.54	10.12	45.19	457.26	566.16	(108.91)
307	Fired	0.270	15.5	882	4.00	157.3	0.014843329	2650	1.29	1.5	9.81	4.687	0.000312879	101.09	170.27	33.12	126.82	10.17	45.42	461.92	571.94	(110.02)
308	Fired	0.270	16.2	935	4.00	157.2	0.014827588	2650	1.29	1.5	9.81	4.680	0.000313045	101.01	170.22	33.12	126.75	10.17	45.41	461.68	571.64	(109.96)

601	Fired	0.270	14.5	805	4.00	157.2	0.0148 23653	2650	1.29	1.5	9.81	4.678	0.0003 13086	101.04	170.21	33.12	126.74	10.17	45.41	461.62	571.5 6	(109.9 5)
602	Fired	0.270	14.0	831	4.00	166.6	0.0166 53692	2650	1.29	1.5	9.81	5.570	0.0002 95384	110.26	175.24	33.12	134.33	10.47	46.75	489.29	605.8 2	(116.5 3)
603	Fired	0.270	15.0	843	4.00	157.1	0.0148 15189	2650	1.29	1.5	9.81	4.674	0.0003 13176	101.00	170.19	33.12	126.70	10.16	45.40	461.49	571.4 0	(109.9 1)
604	Fired	0.270	15.5	882	4.00	157.3	0.0148 43329	2650	1.29	1.5	9.81	4.687	0.0003 12879	101.09	170.27	33.12	126.82	10.17	45.42	461.92	571.9 4	(110.0 2)
605	Fired	0.270	15.0	843	4.00	157.2	0.0148 26755	2650	1.29	1.5	9.81	4.679	0.0003 13054	101.01	170.22	33.12	126.75	10.17	45.41	461.67	571.6 2	(109.9 6)
606	Fired	0.270	15.0	831	4.00	155.6	0.0145 22815	2650	1.29	1.5	9.81	4.536	0.0003 16312	99.45	169.34	33.12	125.44	10.11	45.17	456.91	565.7 3	(108.8 2)
607	Fired	0.270	15.0	833	4.00	155.8	0.0145 61969	2650	1.29	1.5	9.81	4.554	0.0003 15887	99.70	169.45	33.12	125.61	10.12	45.20	457.53	566.5 0	(108.9 7)
608	Fired	0.270	14.2	770	4.00	155.4	0.0144 96154	2650	1.29	1.5	9.81	4.524	0.0003 16603	99.36	169.26	33.12	125.33	10.11	45.15	456.49	565.2 1	(108.7 2)
609	Fired	0.270	12.0	605	4.00	155.6	0.0145 33566	2650	1.29	1.5	9.81	4.541	0.0003 16195	99.55	169.37	33.12	125.49	10.12	45.18	457.08	565.9 4	(108.8 6)
610	Fired	0.270	14.0	767	4.00	157.3	0.0148 44544	2650	1.29	1.5	9.81	4.688	0.0003 12866	101.10	170.27	33.12	126.83	10.17	45.42	461.94	571.9 7	(110.0 2)

611	Fired	0.270	9.0	383	4.00	157.1	0.0148 16592	2650	1.29	1.5	9.81	4.674	0.0003 13161	100.96	170.19	33.12	126.71	10.17	45.40	461.51	571.4 3	(109.9 2)
612	Fired	0.270	13.8	781	4.00	161.7	0.0156 88849	2650	1.29	1.5	9.81	5.093	0.0003 04331	105.38	172.64	33.12	130.38	10.31	46.06	474.90	588.0 1	(113.1 1)
613	Fired	0.270	12.7	667	4.00	157.2	0.0148 35225	2650	1.29	1.5	9.81	4.683	0.0003 12964	101.05	170.24	33.12	126.79	10.17	45.42	461.80	571.7 9	(109.9 9)
614	Fired	0.270	14.0	767	4.00	157.3	0.0148 44544	2650	1.29	1.5	9.81	4.688	0.0003 12866	101.10	170.27	33.12	126.83	10.17	45.42	461.94	571.9 7	(110.0 2)
615	Fired	0.270	14.2	782	4.00	157.2	0.0148 35225	2650	1.29	1.5	9.81	4.683	0.0003 12964	101.05	170.24	33.12	126.79	10.17	45.42	461.80	571.7 9	(109.9 9)
616	Fired	0.270	14.5	805	4.00	157.2	0.0148 35225	2650	1.29	1.5	9.81	4.683	0.0003 12964	101.05	170.24	33.12	126.79	10.17	45.42	461.80	571.7 9	(109.9 9)
617	Fired	0.270	13.8	751	4.00	157.2	0.0148 25718	2650	1.29	1.5	9.81	4.679	0.0003 13065	101.00	170.22	33.12	126.75	10.17	45.41	461.65	571.6 0	(109.9 5)
618	Fired	0.270	14.0	767	4.00	157.3	0.0148 44544	2650	1.29	1.5	9.81	4.688	0.0003 12866	101.10	170.27	33.12	126.83	10.17	45.42	461.94	571.9 7	(110.0 2)
619	Fired	0.270	13.3	713	4.00	157.2	0.0148 35225	2650	1.29	1.5	9.81	4.683	0.0003 12964	101.05	170.24	33.12	126.79	10.17	45.42	461.80	571.7 9	(109.9 9)
620	Fired	0.270	14.0	767	4.00	157.3	0.0148 44544	2650	1.29	1.5	9.81	4.688	0.0003 12866	101.10	170.27	33.12	126.83	10.17	45.42	461.94	571.9 7	(110.0 2)

621	Fired	0.270	14.0	767	4.00	157.3	0.0148 44544	2650	1.29	1.5	9.81	4.688	0.0003 12866	101.10	170.27	33.12	126.83	10.17	45.42	461.94	571.9 7	(110.0 2)
622	Fired	0.270	13.4	720	4.00	157.1	0.0148 15403	2650	1.29	1.5	9.81	4.674	0.0003 13173	100.95	170.19	33.12	126.70	10.16	45.40	461.49	571.4 0	(109.9 1)
623	Fired	0.270	13.6	736	4.00	157.2	0.0148 35225	2650	1.29	1.5	9.81	4.683	0.0003 12964	101.05	170.24	33.12	126.79	10.17	45.42	461.80	571.7 9	(109.9 9)
651	Fired	0.270	17.0	997	4.00	157.3	0.0148 42394	2650	1.29	1.5	9.81	4.687	0.0003 12889	101.09	170.26	33.12	126.82	10.17	45.42	461.91	571.9 2	(110.0 1)
652	Fired	0.270	14.0	767	4.00	157.3	0.0148 44544	2650	1.29	1.5	9.81	4.688	0.0003 12866	101.10	170.27	33.12	126.83	10.17	45.42	461.94	571.9 7	(110.0 2)
653	Fired	0.270	15.0	843	4.00	157.2	0.0148 26755	2650	1.29	1.5	9.81	4.679	0.0003 13054	101.01	170.22	33.12	126.75	10.17	45.41	461.67	571.6 2	(109.9 6)
654	Fired	0.270	13.0	690	4.00	157.2	0.0148 23653	2650	1.29	1.5	9.81	4.678	0.0003 13086	101.04	170.21	33.12	126.74	10.17	45.41	461.62	571.5 6	(109.9 5)
655	Fired	0.270	15.0	843	4.00	157.1	0.0148 15189	2650	1.29	1.5	9.81	4.674	0.0003 13176	101.00	170.19	33.12	126.70	10.16	45.40	461.49	571.4 0	(109.9 1)
656	Fired	0.270	14.0	767	4.00	157.2	0.0148 32964	2650	1.29	1.5	9.81	4.682	0.0003 12988	101.09	170.24	33.12	126.78	10.17	45.41	461.76	571.7 4	(109.9 8)
657	Fired	0.270	12.0	605	4.00	155.7	0.0145 44912	2650	1.29	1.5	9.81	4.546	0.0003 16072	99.57	169.40	33.12	125.54	10.12	45.19	457.26	566.1 6	(108.9 1)

658	Fired	0.270	14.0	756	4.00	155.7	0.0145 37966	2650	1.29	1.5	9.81	4.543	0.0003 16148	99.53	169.38	33.12	125.51	10.12	45.19	457.15	566.0 3	(108.8 8)
659	Fired	0.270	10.0	460	4.00	157.2	0.0148 35225	2650	1.29	1.5	9.81	4.683	0.0003 12964	101.05	170.24	33.12	126.79	10.17	45.42	461.80	571.7 9	(109.9 9)
660	Fired	0.270	12.0	605	4.00	155.7	0.0145 44912	2650	1.29	1.5	9.81	4.546	0.0003 16072	99.57	169.40	33.12	125.54	10.12	45.19	457.26	566.1 6	(108.9 1)
661	Fired	0.270	10.0	460	4.00	157.2	0.0148 35225	2650	1.29	1.5	9.81	4.683	0.0003 12964	101.05	170.24	33.12	126.79	10.17	45.42	461.80	571.7 9	(109.9 9)
662	Fired	0.270	13.0	751	4.00	167.2	0.0167 66586	2650	1.29	1.5	9.81	5.627	0.0002 94388	110.77	175.54	33.12	134.79	10.48	46.83	490.94	607.8 7	(116.9 3)
663	Fired	0.270	14.0	767	4.00	157.3	0.0148 44544	2650	1.29	1.5	9.81	4.688	0.0003 12866	101.10	170.27	33.12	126.83	10.17	45.42	461.94	571.9 7	(110.0 2)
664	Fired	0.270	14.5	805	4.00	157.2	0.0148 35225	2650	1.29	1.5	9.81	4.683	0.0003 12964	101.05	170.24	33.12	126.79	10.17	45.42	461.80	571.7 9	(109.9 9)
665	Fired	0.270	15.0	843	4.00	157.2	0.0148 26755	2650	1.29	1.5	9.81	4.679	0.0003 13054	101.01	170.22	33.12	126.75	10.17	45.41	461.67	571.6 2	(109.9 6)
666	Fired	0.270	14.5	805	4.00	157.2	0.0148 35225	2650	1.29	1.5	9.81	4.683	0.0003 12964	101.05	170.24	33.12	126.79	10.17	45.42	461.80	571.7 9	(109.9 9)
667	Fired	0.270	14.0	767	4.00	157.3	0.0148 44544	2650	1.29	1.5	9.81	4.688	0.0003 12866	101.10	170.27	33.12	126.83	10.17	45.42	461.94	571.9 7	(110.0 2)

668	Fired	0.270	14.5	805	4.00	157.2	0.0148 35225	2650	1.29	1.5	9.81	4.683	0.0003 12964	101.05	170.24	33.12	126.79	10.17	45.42	461.80	571.7 9	(109.9 9)
669	Fired	0.270	14.0	767	4.00	157.3	0.0148 44544	2650	1.29	1.5	9.81	4.688	0.0003 12866	101.10	170.27	33.12	126.83	10.17	45.42	461.94	571.9 7	(110.0 2)
670	Fired	0.270	13.5	743	4.00	159.5	0.0152 68732	2650	1.29	1.5	9.81	4.890	0.0003 08489	103.26	171.47	33.12	128.63	10.24	45.74	468.50	580.0 8	(111.5 8)
671	Fired	0.270	14.0	767	4.00	157.3	0.0148 44544	2650	1.29	1.5	9.81	4.688	0.0003 12866	101.10	170.27	33.12	126.83	10.17	45.42	461.94	571.9 7	(110.0 2)
672	Fired	0.270	14.0	767	4.00	157.3	0.0148 44544	2650	1.29	1.5	9.81	4.688	0.0003 12866	101.10	170.27	33.12	126.83	10.17	45.42	461.94	571.9 7	(110.0 2)
701	Fired	0.270	14.3	368	4.00	90.5	0.0049 19371	2650	1.29	1.5	9.81	0.894	0.0005 43484	44.17	129.17	33.12	73.00	7.72	34.46	265.91	329.2 6	(63.35)
702	Fired	0.270	16.5	532	9.50	33.7	0.0006 8312	2650	1.29	1.5	9.81	0.046	0.0014 58456	10.05	78.83	33.12	27.20	4.71	21.04	99.08	122.7 0	(23.62)
703	Fired	0.270	16.0	491	9.50	33.6	0.0006 77135	2650	1.29	1.5	9.81	0.046	0.0014 64887	9.98	78.66	33.12	27.08	4.70	20.99	98.65	122.1 6	(23.51)
704	Fired	0.270	14.5	381	9.50	33.8	0.0006 85718	2650	1.29	1.5	9.81	0.047	0.0014 5569	10.07	78.91	33.12	27.25	4.71	21.06	99.27	122.9 3	(23.66)
705	Fired	0.270	15.0	415	9.50	33.6	0.0006 76048	2650	1.29	1.5	9.81	0.046	0.0014 66064	9.97	78.63	33.12	27.06	4.70	20.98	98.57	122.0 6	(23.49)

706	Fired	0.270	12.4	567	9.50	66.8	0.0026 75143	2650	1.29	1.5	9.81	0.359	0.0007 37001	27.97	110.92	33.12	53.83	6.63	29.59	196.09	242.8 1	(46.72)
707	Fired	0.270	14.0	340	9.50	33.6	0.0006 77356	2650	1.29	1.5	9.81	0.046	0.0014 64648	9.98	78.67	33.12	27.09	4.70	20.99	98.66	122.1 8	(23.52)
708	Fired	0.270	15.5	455	9.50	33.7	0.0006 80957	2650	1.29	1.5	9.81	0.046	0.0014 6077	10.02	78.77	33.12	27.16	4.71	21.02	98.92	122.5 0	(23.58)
709	Fired	0.270	15.5	453	9.50	33.6	0.0006 76637	2650	1.29	1.5	9.81	0.046	0.0014 65426	9.97	78.65	33.12	27.07	4.70	20.99	98.61	122.1 1	(23.50)
710	Fired	0.270	17.0	568	9.50	33.7	0.0006 7966	2650	1.29	1.5	9.81	0.046	0.0014 62163	10.01	78.73	33.12	27.13	4.70	21.01	98.83	122.3 9	(23.56)
711	Fired	0.270	14.5	378	9.50	33.6	0.0006 77932	2650	1.29	1.5	9.81	0.046	0.0014 64026	9.99	78.68	33.12	27.10	4.70	21.00	98.70	122.2 3	(23.53)
712	Fired	0.270	14.5	378	9.50	33.6	0.0006 77932	2650	1.29	1.5	9.81	0.046	0.0014 64026	9.99	78.68	33.12	27.10	4.70	21.00	98.70	122.2 3	(23.53)
713	Fired	0.270	15.2	432	9.50	33.7	0.0006 80388	2650	1.29	1.5	9.81	0.046	0.0014 61381	10.02	78.76	33.12	27.15	4.71	21.02	98.88	122.4 5	(23.57)
714	Fired	0.270	14.0	342	9.50	33.7	0.0006 8312	2650	1.29	1.5	9.81	0.046	0.0014 58456	10.05	78.83	33.12	27.20	4.71	21.04	99.08	122.7 0	(23.62)
715	Fired	0.270	16.0	495	9.50	33.8	0.0006 85119	2650	1.29	1.5	9.81	0.046	0.0014 56327	10.07	78.89	33.12	27.24	4.71	21.05	99.23	122.8 8	(23.65)

716	Fired	0.270	15.0	415	9.50	33.6	0.0006 76048	2650	1.29	1.5	9.81	0.046	0.0014 66064	9.97	78.63	33.12	27.06	4.70	20.98	98.57	122.0 6	(23.49)
717	Fired	0.270	14.0	345	9.50	34.0	0.0006 92511	2650	1.29	1.5	9.81	0.047	0.0014 48532	10.14	79.10	33.12	27.39	4.73	21.11	99.76	123.5 4	(23.78)
718	Fired	0.270	15.3	421	9.50	32.7	0.0006 39901	2650	1.29	1.5	9.81	0.042	0.0015 06903	9.56	77.56	33.12	26.33	4.63	20.70	95.90	118.7 5	(22.86)
719	Fired	0.270	14.0	345	9.50	34.0	0.0006 92511	2650	1.29	1.5	9.81	0.047	0.0014 48532	10.14	79.10	33.12	27.39	4.73	21.11	99.76	123.5 4	(23.78)
720	Aband oned	0.270	0.5	0	9.50			2650	1.29	1.5	9.81											
721	Fired	0.270	15.0	421	4.00	95.2	0.0054 37677	2650	1.29	1.5	9.81	1.039	0.0005 16934	47.60	132.45	33.12	76.75	7.91	35.34	279.57	346.1 7	(66.60)
722	Fired	0.270	13.5	302	4.00	83.2	0.0041 55522	2650	1.29	1.5	9.81	0.694	0.0005 91329	38.92	123.83	33.12	67.10	7.40	33.04	244.40	302.6 2	(58.23)
723	Fired	0.270	15.5	453	9.50	33.6	0.0006 76637	2650	1.29	1.5	9.81	0.046	0.0014 65426	9.97	78.65	33.12	27.07	4.70	20.99	98.61	122.1 1	(23.50)
724	Fired	0.270	13.0	264	9.50	33.6	0.0006 75712	2650	1.29	1.5	9.81	0.046	0.0014 66428	9.96	78.62	33.12	27.05	4.70	20.98	98.54	122.0 3	(23.49)
725	Fired	0.270	15.0	415	9.50	33.6	0.0006 76048	2650	1.29	1.5	9.81	0.046	0.0014 66064	9.97	78.63	33.12	27.06	4.70	20.98	98.57	122.0 6	(23.49)

726	Fired	0.270	14.0	340	9.50	33.6	0.000677356	2650	1.29	1.5	9.81	0.046	0.001464648	9.98	78.67	33.12	27.09	4.70	20.99	98.66	122.18	(23.52)
751	Fired	0.270	15.0	831	9.50	55.5	0.00184532	2650	1.29	1.5	9.81	0.205	0.000887372	21.16	101.08	33.12	44.71	6.04	26.97	162.85	201.66	(38.81)
752	Fired	0.270	15.5	869	9.50	53.8	0.001735935	2650	1.29	1.5	9.81	0.187	0.000914903	20.21	99.55	33.12	43.36	5.95	26.56	157.95	195.59	(37.64)
753	Fired	0.270	17.0	983	9.50	50.0	0.001502689	2650	1.29	1.5	9.81	0.151	0.000983348	18.14	96.02	33.12	40.35	5.74	25.62	146.96	181.98	(35.02)
754	Fired	0.270	17.0	983	4.00	155.7	0.01454224	2650	1.29	1.5	9.81	4.545	0.000316101	99.55	169.40	33.12	125.53	10.12	45.19	457.22	566.11	(108.90)
755	Fired	0.270	17.0	983	4.00	155.7	0.01454224	2650	1.29	1.5	9.81	4.545	0.000316101	99.55	169.40	33.12	125.53	10.12	45.19	457.22	566.11	(108.90)
756	Fired	0.270	16.0	907	4.00	155.6	0.01453336	2650	1.29	1.5	9.81	4.541	0.000316198	99.51	169.37	33.12	125.49	10.12	45.18	457.08	565.94	(108.86)
756R	Abandoned							2650	1.29	1.5	9.81											
757	Fired	0.270	15.0	821	4.00	154.2	0.01425885	2650	1.29	1.5	9.81	4.413	0.000319215	98.14	168.57	33.12	124.30	10.07	44.97	452.75	560.59	(107.84)
758	Fired	0.270	16.0	908	4.00	155.7	0.01454135	2650	1.29	1.5	9.81	4.546	0.000316107	99.61	169.41	33.12	125.54	10.12	45.19	457.26	566.17	(108.91)

759	Fired	0.270	15.5	874	4.00	156.2	0.0146 37794	2650	1.29	1.5	9.81	4.590	0.0003 15068	100.09	169.67	33.12	125.94	10.13	45.26	458.72	567.9 7	(109.2 5)
760	Fired	0.270	15.5	872	4.00	155.9	0.0145 89428	2650	1.29	1.5	9.81	4.567	0.0003 1559	99.84	169.53	33.12	125.73	10.13	45.23	457.96	567.0 3	(109.0 7)
761	Fired	0.270	15.0	833	4.00	155.8	0.0145 61969	2650	1.29	1.5	9.81	4.554	0.0003 15887	99.70	169.45	33.12	125.61	10.12	45.20	457.53	566.5 0	(108.9 7)
762	Fired	0.270	14.5	795	4.00	155.8	0.0145 58361	2650	1.29	1.5	9.81	4.553	0.0003 15926	99.68	169.44	33.12	125.60	10.12	45.20	457.47	566.4 3	(108.9 6)
763	Fired	0.270	15.6	846	4.00	151.6	0.0137 9159	2650	1.29	1.5	9.81	4.198	0.0003 2459	95.72	167.17	33.12	122.25	9.98	44.59	445.26	551.3 1	(106.0 5)
801	Fired	0.270	16.0	906	4.00	155.5	0.0144 98874	2650	1.29	1.5	9.81	4.525	0.0003 16573	99.38	169.27	33.12	125.34	10.11	45.16	456.53	565.2 7	(108.7 3)
802	Fired	0.270	15.8	891	4.00	155.5	0.0145 01225	2650	1.29	1.5	9.81	4.526	0.0003 16548	99.39	169.28	33.12	125.35	10.11	45.16	456.57	565.3 1	(108.7 4)
803	Fired	0.270	16.2	921	4.00	155.4	0.0144 966	2650	1.29	1.5	9.81	4.524	0.0003 16598	99.36	169.26	33.12	125.33	10.11	45.15	456.50	565.2 2	(108.7 3)
804	Fired	0.270	15.5	868	4.00	155.4	0.0144 92843	2650	1.29	1.5	9.81	4.522	0.0003 16639	99.35	169.25	33.12	125.32	10.11	45.15	456.44	565.1 5	(108.7 1)
805	Fired	0.270	16.0	906	4.00	155.5	0.0144 98874	2650	1.29	1.5	9.81	4.525	0.0003 16573	99.38	169.27	33.12	125.34	10.11	45.16	456.53	565.2 7	(108.7 3)

806	Fired	0.270	16.0	906	4.00	155.5	0.0144 98874	2650	1.29	1.5	9.81	4.525	0.0003 16573	99.38	169.27	33.12	125.34	10.11	45.16	456.53	565.2 7	(108.7 3)
807	Fired	0.270	16.0	906	4.00	155.5	0.0144 98874	2650	1.29	1.5	9.81	4.525	0.0003 16573	99.38	169.27	33.12	125.34	10.11	45.16	456.53	565.2 7	(108.7 3)
808	Fired	0.270	14.6	800	4.00	155.4	0.0144 91023	2650	1.29	1.5	9.81	4.521	0.0003 16659	99.34	169.25	33.12	125.31	10.11	45.15	456.41	565.1 1	(108.7 1)
809	Fired	0.270	14.6	800	4.00	155.4	0.0144 91023	2650	1.29	1.5	9.81	4.521	0.0003 16659	99.34	169.25	33.12	125.31	10.11	45.15	456.41	565.1 1	(108.7 1)
810	Fired	0.270	16.0	906	4.00	155.5	0.0144 98874	2650	1.29	1.5	9.81	4.525	0.0003 16573	99.38	169.27	33.12	125.34	10.11	45.16	456.53	565.2 7	(108.7 3)
811	Fired	0.270	15.8	891	4.00	155.5	0.0145 01225	2650	1.29	1.5	9.81	4.526	0.0003 16548	99.39	169.28	33.12	125.35	10.11	45.16	456.57	565.3 1	(108.7 4)
812	Fired	0.270	16.0	906	4.00	155.5	0.0144 98874	2650	1.29	1.5	9.81	4.525	0.0003 16573	99.38	169.27	33.12	125.34	10.11	45.16	456.53	565.2 7	(108.7 3)
813	Fired	0.270	15.6	876	4.00	155.5	0.0145 03658	2650	1.29	1.5	9.81	4.527	0.0003 16521	99.40	169.28	33.12	125.36	10.11	45.16	456.61	565.3 6	(108.7 5)
851	Fired	0.165	18.0	229	4.00	32.5	0.0006 34126	2650	1.29	1.5	9.81	0.041	0.0015 13749	15.54	77.41	33.12	26.21	4.62	20.65	95.47	118.2 3	(22.76)
852	Fired	0.165	15.5	155	4.00	28.3	0.0004 79421	2650	1.29	1.5	9.81	0.027	0.0017 40937	12.60	72.18	33.12	22.79	4.31	19.26	83.01	102.8 1	(19.79)

853	Fired	0.165	15.0	142	4.00	27.4	0.00045045	2650	1.29	1.5	9.81	0.025	0.001796049	12.03	71.06	33.12	22.09	4.24	18.96	80.47	99.65	(19.18)
854	Fired	0.165	17.0	200	10.00	8.4	4.27736E-05	2650	1.29	1.5	9.81	0.001	0.005828457	2.06	39.44	33.12	6.81	2.36	10.52	24.79	30.71	(5.91)
855	Fired	0.165	18.0	228	10.00	8.4	4.26192E-05	2650	1.29	1.5	9.81	0.001	0.005839005	2.05	39.40	33.12	6.79	2.35	10.51	24.75	30.65	(5.90)
856	Fired	0.165	17.5	212	10.00	8.4	4.21161E-05	2650	1.29	1.5	9.81	0.001	0.005873781	2.03	39.28	33.12	6.75	2.35	10.48	24.60	30.47	(5.87)
857	Fired	0.165	17.6	216	10.00	8.4	4.24488E-05	2650	1.29	1.5	9.81	0.001	0.005850716	2.05	39.36	33.12	6.78	2.35	10.50	24.70	30.59	(5.89)
858	Fired	0.165	17.8	222	10.00	8.4	4.25362E-05	2650	1.29	1.5	9.81	0.001	0.005844703	2.05	39.38	33.12	6.79	2.35	10.51	24.72	30.62	(5.90)
859	Fired	0.165	18.0	226	10.00	8.4	4.20802E-05	2650	1.29	1.5	9.81	0.001	0.005876284	2.03	39.27	33.12	6.75	2.35	10.48	24.59	30.46	(5.87)
860	Fired	0.165	18.0	227	10.00	8.4	4.23495E-05	2650	1.29	1.5	9.81	0.001	0.005857574	2.04	39.34	33.12	6.77	2.35	10.50	24.67	30.55	(5.88)
861	Fired	0.165	16.0	169	10.00	8.4	4.1901E-05	2650	1.29	1.5	9.81	0.001	0.005888837	2.03	39.23	33.12	6.74	2.34	10.47	24.54	30.39	(5.85)
862	Fired	0.165	18.0	227	10.00	8.4	4.23495E-05	2650	1.29	1.5	9.81	0.001	0.005857574	2.04	39.34	33.12	6.77	2.35	10.50	24.67	30.55	(5.88)
863	Fired	0.165	17.0	199	10.00	8.4	4.2465E-05	2650	1.29	1.5	9.81	0.001	0.005849598	2.05	39.36	33.12	6.78	2.35	10.50	24.70	30.60	(5.89)
864	Fired	0.165	17.6	217	10.00	8.4	4.2733E-05	2650	1.29	1.5	9.81	0.001	0.005831228	2.06	39.43	33.12	6.80	2.36	10.52	24.78	30.69	(5.91)

865	Fired	0.165	18.0	226	10.00	8.4	4.20802E-05	2650	1.29	1.5	9.81	0.001	0.005876284	2.03	39.27	33.12	6.75	2.35	10.48	24.59	30.46	(5.87)
866	Fired	0.165	18.0	228	10.00	8.4	4.26192E-05	2650	1.29	1.5	9.81	0.001	0.005839005	2.05	39.40	33.12	6.79	2.35	10.51	24.75	30.65	(5.90)
867	Fired	0.165	18.0	227	10.00	8.4	4.23495E-05	2650	1.29	1.5	9.81	0.001	0.005857574	2.04	39.34	33.12	6.77	2.35	10.50	24.67	30.55	(5.88)
868	Abandoned	0.165	0.5	0	10.00			2650	1.29	1.5	9.81											
869	Fired	0.165	14.0	113	10.00	8.4	4.20802E-05	2650	1.29	1.5	9.81	0.001	0.005876284	2.03	39.27	33.12	6.75	2.35	10.48	24.59	30.46	(5.87)
870	Fired	0.165	17.4	211	10.00	8.4	4.26484E-05	2650	1.29	1.5	9.81	0.001	0.005837006	2.05	39.41	33.12	6.80	2.35	10.52	24.76	30.66	(5.91)
871	Fired	0.165	18.0	226	10.00	8.4	4.20802E-05	2650	1.29	1.5	9.81	0.001	0.005876284	2.03	39.27	33.12	6.75	2.35	10.48	24.59	30.46	(5.87)
872	Fired	0.165	18.0	186	10.00	7.3	3.17589E-05	2650	1.29	1.5	9.81	0.000	0.006764083	1.65	36.61	33.12	5.86	2.19	9.77	21.36	26.46	(5.10)
873	Fired	0.165	16.5	186	10.00	8.5	4.28687E-05	2650	1.29	1.5	9.81	0.001	0.005821988	2.06	39.46	33.12	6.81	2.36	10.53	24.82	30.74	(5.92)
874	Fired	0.165	5.0	143	10.00	41.7	0.001042522	2650	1.29	1.5	9.81	0.087	0.001118059	22.57	87.65	33.12	33.61	5.24	23.38	122.42	151.60	(29.18)
875	Fired	0.165	17.0	200	10.00	8.4	4.27736E-05	2650	1.29	1.5	9.81	0.001	0.005828457	2.06	39.44	33.12	6.81	2.36	10.52	24.79	30.71	(5.91)
876	Fired	0.165	17.0	200	10.00	8.4	4.27736E-05	2650	1.29	1.5	9.81	0.001	0.005828457	2.06	39.44	33.12	6.81	2.36	10.52	24.79	30.71	(5.91)

877	Fired	0.165	17.0	200	10.00	8.4	4.27736E-05	2650	1.29	1.5	9.81	0.001	0.005828457	2.06	39.44	33.12	6.81	2.36	10.52	24.79	30.71	(5.91)
879	Abandoned	0.165	0.5	0	10.00			2650	1.29	1.5	9.81											
880	Fired	0.165	16.5	183	10.00	8.4	4.18734E-05	2650	1.29	1.5	9.81	0.001	0.005890774	2.02	39.23	33.12	6.73	2.34	10.47	24.53	30.38	(5.85)
881	Fired	0.165	16.0	169	10.00	8.4	4.1901E-05	2650	1.29	1.5	9.81	0.001	0.005888837	2.03	39.23	33.12	6.74	2.34	10.47	24.54	30.39	(5.85)
882	Fired	0.165	16.3	178	10.00	8.4	4.20887E-05	2650	1.29	1.5	9.81	0.001	0.005875688	2.03	39.28	33.12	6.75	2.35	10.48	24.59	30.46	(5.87)
883	Fired	0.165	13.7	104	10.00	8.3	4.17752E-05	2650	1.29	1.5	9.81	0.001	0.005897696	2.02	39.20	33.12	6.73	2.34	10.46	24.50	30.35	(5.84)
884	Fired	0.165	13.7	104.43196	10.00	8.4	4.20261E-05	2650	1.29	1.5	9.81	0.001	0.005880065	2.03	39.26	33.12	6.75	2.35	10.48	24.58	30.44	(5.86)
885	Fired	0.165	15.3	150	10.00	8.4	4.21919E-05	2650	1.29	1.5	9.81	0.001	0.005868 5	2.04	39.30	33.12	6.76	2.35	10.49	24.62	30.50	(5.87)
886	Fired	0.165	16.0	169	10.00	8.4	4.1901E-05	2650	1.29	1.5	9.81	0.001	0.005888837	2.03	39.23	33.12	6.74	2.34	10.47	24.54	30.39	(5.85)
887	Fired	0.165	16.3	178	10.00	8.4	4.20887E-05	2650	1.29	1.5	9.81	0.001	0.005875688	2.03	39.28	33.12	6.75	2.35	10.48	24.59	30.46	(5.87)
901	Fired	0.165	16.4	384	10.00	14.4	0.000124933	2650	1.29	1.5	9.81	0.004	0.003410388	4.60	51.56	33.12	11.63	3.08	13.76	42.37	52.48	(10.11)

902	Fired	0.165	7.0	113	10.00	26.8	0.0004 31292	2650	1.29	1.5	9.81	0.023	0.0018 35508	11.64	70.29	33.12	21.62	4.20	18.75	78.74	97.51	(18.77)
903	Fired	0.165	8.0	143	10.00	28.1	0.0004 73057	2650	1.29	1.5	9.81	0.027	0.0017 52608	12.48	71.94	33.12	22.64	4.30	19.19	82.46	102.1 2	(19.66)
904	Fired	0.165	7.0	85	10.00	21.8	0.0002 85841	2650	1.29	1.5	9.81	0.013	0.0022 54652	8.55	63.42	33.12	17.60	3.79	16.92	64.10	79.38	(15.28)
905	Fired	0.165	7.0	113	3.00	79.8	0.0038 20883	2650	1.29	1.5	9.81	0.612	0.0006 1668	59.79	121.30	33.12	64.35	7.24	32.35	234.38	290.2 3	(55.85)
906	Fired	0.165	6.0	85	3.00	80.0	0.0038 37176	2650	1.29	1.5	9.81	0.616	0.0006 15369	59.98	121.43	33.12	64.49	7.25	32.39	234.88	290.8 5	(55.97)
907	Fired	0.165	6.0	86	3.00	80.6	0.0039 02564	2650	1.29	1.5	9.81	0.632	0.0006 10192	60.75	121.94	33.12	65.03	7.28	32.53	236.87	293.3 1	(56.44)
908	Fired	0.165	6.0	86	3.00	80.6	0.0039 02564	2650	1.29	1.5	9.81	0.632	0.0006 10192	60.75	121.94	33.12	65.03	7.28	32.53	236.87	293.3 1	(56.44)
909	Fired	0.165	4.5	45	3.00	81.2	0.0039 56836	2650	1.29	1.5	9.81	0.645	0.0006 05993	61.38	122.37	33.12	65.49	7.31	32.64	238.51	295.3 5	(56.84)
910	Fired	0.165	6.0	230	3.00	164.1	0.0161 64194	2650	1.29	1.5	9.81	5.326	0.0002 99823	176.41	173.99	33.12	132.37	10.39	46.40	482.10	596.9 5	(114.8 4)
911	Fired	0.165	6.0	86	3.00	80.6	0.0039 02564	2650	1.29	1.5	9.81	0.632	0.0006 10192	60.75	121.94	33.12	65.03	7.28	32.53	236.87	293.3 1	(56.44)

951	Fired	0.165	17.0	395	3.00	79.7	0.0038 13906	2650	1.29	1.5	9.81	0.610	0.0006 17244	59.71	121.24	33.12	64.29	7.24	32.34	234.16	289.9 6	(55.80)
952	Fired	0.165	16.5	387	3.00	80.6	0.0039 02564	2650	1.29	1.5	9.81	0.632	0.0006 10192	60.75	121.94	33.12	65.03	7.28	32.53	236.87	293.3 1	(56.44)
953	Fired	0.165	15.5	358	3.00	80.6	0.0038 9732	2650	1.29	1.5	9.81	0.631	0.0006 10603	60.69	121.90	33.12	64.99	7.28	32.51	236.71	293.1 2	(56.41)
954	Fired	0.165	16.0	373	3.00	80.7	0.0039 07608	2650	1.29	1.5	9.81	0.633	0.0006 09798	60.81	121.98	33.12	65.08	7.28	32.54	237.02	293.5 0	(56.48)
955	Fired	0.165	15.0	339	3.00	79.8	0.0038 20883	2650	1.29	1.5	9.81	0.612	0.0006 1668	59.79	121.30	33.12	64.35	7.24	32.35	234.38	290.2 3	(55.85)
956	Aband oned	0.165	0.5	0	3.00																	

APPENDIX B. Data for Graph 35 (Modified Flyrock Footprint Calculation)

Table 14: Adjusted flyrock footprint calculation data

Hole ID	Hole Status	Hole diameter (m)	Hole depth (m)	Explosives (kg)	Stemming (m)	SF	Xf (mm)	sa(m^2)	pr(kg/m³)	pa(kg/m³)	cd	g	m(kg)	k	Kv	Vo(m/s)	Launch Angle (θo)	H(m)	T(sec)	Va(m/s)	Range (m) (Chudinov)	Range (m) (McKenzie 2009)	Variance (m)
101	Fired	0.270	15.2	770	5.00	1.3	107.2	0.006897348	2650	1.29	1.5	9.81	1.485	0.000353067	56.92	140.57	33.12	103.45	9.19	42.12	386.90	389.88	(2.98)
102	Fired	0.270	15.0	755	5.00	1.3	107.2	0.006898642	2650	1.29	1.5	9.81	1.485	0.000353034	56.93	140.57	33.12	103.46	9.19	42.12	386.93	389.91	(2.98)
103	Fired	0.270	14.3	702	5.00	1.3	107.2	0.006896513	2650	1.29	1.5	9.81	1.484	0.000353088	56.91	140.56	33.12	103.45	9.18	42.12	386.87	389.85	(2.98)
104	Fired	0.270	13.5	645	5.00	1.3	107.6	0.006949171	2650	1.29	1.5	9.81	1.501	0.000351748	57.24	140.83	33.12	103.84	9.20	42.20	388.35	391.34	(2.99)
105	Fired	0.270	14.0	680	5.00	1.3	107.3	0.006905977	2650	1.29	1.5	9.81	1.487	0.000352846	56.97	140.61	33.12	103.52	9.19	42.14	387.14	390.12	(2.98)
106	Fired	0.270	14.0	684	5.00	1.3	107.7	0.006964741	2650	1.29	1.5	9.81	1.506	0.000351355	57.34	140.91	33.12	103.96	9.21	42.22	388.78	391.78	(3.00)
107	Fired	0.270	15.5	795	5.00	1.3	107.4	0.006926946	2650	1.29	1.5	9.81	1.494	0.000352312	57.10	140.72	33.12	103.68	9.19	42.17	387.73	390.71	(2.99)

108	Fired	0.270	14.0	684	5.00	1.3	107.7	0.006964741	2650	1.29	1.5	9.81	1.506	0.000351355	57.34	140.91	33.12	103.96	9.21	42.22	388.78	391.78	(3.00)
109	Fired	0.270	13.0	613	5.00	1.3	108.4	0.007047636	2650	1.29	1.5	9.81	1.533	0.000349282	57.85	141.33	33.12	104.58	9.23	42.35	391.09	394.10	(3.01)
110	Fired	0.270	15.0	843	5.00	1.3	116.2	0.008096712	2650	1.29	1.5	9.81	1.888	0.00032587	64.16	146.32	33.12	112.09	9.56	43.84	419.19	422.42	(3.23)
111	Fired	0.270	15.0	831	4.00	1.3	155.5	0.014511486	2650	1.29	1.5	9.81	4.531	0.000243412	99.44	169.31	33.12	150.07	11.06	50.73	561.21	565.51	(4.30)
112	Fired	0.270	15.0	767	4.00	1.3	146.8	0.012935054	2650	1.29	1.5	9.81	3.813	0.000257819	91.18	164.51	33.12	141.68	10.75	49.29	529.85	533.91	(4.06)
113	Fired	0.270	13.0	613	4.00	1.3	144.4	0.012504166	2650	1.29	1.5	9.81	3.624	0.000262223	88.89	163.12	33.12	139.30	10.66	48.88	520.95	524.95	(4.00)
114	Fired	0.270	16.0	843	5.00	1.3	108.4	0.007055212	2650	1.29	1.5	9.81	1.536	0.000349095	57.87	141.36	33.12	104.63	9.24	42.36	391.30	394.31	(3.01)
115	Fired	0.270	15.7	220	4.00	1.3	57.0	0.001947661	2650	1.29	1.5	9.81	0.223	0.000664418	22.04	102.45	33.12	54.97	6.70	30.70	205.58	207.18	(1.60)
116	Fired	0.270	10.5	421	4.00	1.3	139.2	0.011627594	2650	1.29	1.5	9.81	3.250	0.000271928	84.18	160.18	33.12	134.33	10.47	48.00	502.36	506.21	(3.86)
117	Abandoned	0.270	0.5	0	-				2650	1.29	1.5	9.81											

118	Fired	0.270	12.0	529	5.00	1.3	107.3	0.006914017	2650	1.29	1.5	9.81	1.490	0.000352641	57.00	140.65	33.12	103.58	9.19	42.15	387.36	390.35	(2.98)
119	Abandoned	0.270	0.5	0	-				2650	1.29	1.5	9.81											
121	Fired	0.270	15.0	843	4.00	1.3	157.2	0.014826755	2650	1.29	1.5	9.81	4.679	0.00024081	101.01	170.22	33.12	151.69	11.12	51.00	567.28	571.62	(4.35)
122	Fired	0.270	15.5	805	5.00	1.3	108.5	0.007059243	2650	1.29	1.5	9.81	1.537	0.000348995	57.89	141.38	33.12	104.66	9.24	42.37	391.41	394.43	(3.02)
123	Fired	0.270	10.5	498	4.00	1.3	157.2	0.014820891	2650	1.29	1.5	9.81	4.676	0.000240858	100.98	170.20	33.12	151.66	11.12	51.00	567.16	571.51	(4.35)
124	Fired	0.270	15.0	882	4.00	1.3	162.4	0.01582781	2650	1.29	1.5	9.81	5.161	0.000233071	106.08	173.02	33.12	156.73	11.31	51.84	586.12	590.61	(4.49)
125	Fired	0.270	15.0	843	4.00	1.3	157.2	0.014826755	2650	1.29	1.5	9.81	4.679	0.00024081	101.01	170.22	33.12	151.69	11.12	51.00	567.28	571.62	(4.35)
126	Fired	0.270	14.0	690	5.00	1.3	108.5	0.007059243	2650	1.29	1.5	9.81	1.537	0.000348995	57.89	141.38	33.12	104.66	9.24	42.37	391.41	394.43	(3.02)
127	Fired	0.270	13.0	613	5.00	1.3	108.4	0.007053701	2650	1.29	1.5	9.81	1.535	0.000349132	57.86	141.36	33.12	104.62	9.24	42.36	391.26	394.27	(3.01)
128	Fired	0.270	16.0	820	4.00	1.3	144.7	0.012563146	2650	1.29	1.5	9.81	3.650	0.000261607	89.21	163.31	33.12	139.63	10.67	48.93	522.18	526.18	(4.01)

129	Fired	0.270	16.0	843	5.00	1.3	108.4	0.007055212	2650	1.29	1.5	9.81	1.536	0.000349095	57.87	141.36	33.12	104.63	9.24	42.36	391.30	394.31	(3.01)
130	Fired	0.270	16.2	859	5.00	1.3	108.5	0.007063202	2650	1.29	1.5	9.81	1.539	0.000348897	57.92	141.40	33.12	104.69	9.24	42.37	391.52	394.54	(3.02)
201	Fired	0.270	15.6	889	5.00	1.3	115.7	0.008036828	2650	1.29	1.5	9.81	1.867	0.000327082	63.81	146.05	33.12	111.68	9.54	43.76	417.64	420.85	(3.21)
202	Fired	0.270	15.8	905	4.00	1.3	157.3	0.014843123	2650	1.29	1.5	9.81	4.687	0.000240678	101.09	170.27	33.12	151.77	11.13	51.02	567.59	571.94	(4.35)
203	Fired	0.270	15.2	860	4.00	1.3	157.4	0.014868516	2650	1.29	1.5	9.81	4.699	0.000240472	101.22	170.34	33.12	151.90	11.13	51.04	568.08	572.43	(4.35)
204	Fired	0.270	14.9	836	4.00	1.3	157.3	0.014843775	2650	1.29	1.5	9.81	4.687	0.000240672	101.10	170.27	33.12	151.78	11.13	51.02	567.60	571.95	(4.35)
205	Fired	0.270	15.0	843	4.00	1.3	157.2	0.014826755	2650	1.29	1.5	9.81	4.679	0.00024081	101.01	170.22	33.12	151.69	11.12	51.00	567.28	571.62	(4.35)
206	Fired	0.270	16.6	966	4.00	1.3	157.2	0.014835225	2650	1.29	1.5	9.81	4.683	0.000240742	101.05	170.24	33.12	151.73	11.12	51.01	567.44	571.79	(4.35)
207	Fired	0.270	15.2	860	4.00	1.3	157.4	0.014868516	2650	1.29	1.5	9.81	4.699	0.000240472	101.22	170.34	33.12	151.90	11.13	51.04	568.08	572.43	(4.35)
208	Fired	0.270	15.8	906	4.00	1.3	157.4	0.014866823	2650	1.29	1.5	9.81	4.698	0.000240486	101.21	170.33	33.12	151.90	11.13	51.04	568.04	572.40	(4.35)

209	Fired	0.270	15.4	864	4.00	1.3	155.9	0.014590633	2650	1.29	1.5	9.81	4.568	0.000242751	99.80	169.54	33.12	150.48	11.08	50.80	562.74	567.05	(4.31)
210	Fired	0.270	15.5	882	4.00	1.3	157.3	0.014843329	2650	1.29	1.5	9.81	4.687	0.000240676	101.09	170.27	33.12	151.78	11.13	51.02	567.59	571.94	(4.35)
211	Fired	0.270	18.0	1073	4.00	1.3	157.2	0.01482857	2650	1.29	1.5	9.81	4.680	0.000240796	101.02	170.22	33.12	151.70	11.12	51.01	567.31	571.66	(4.35)
212	Fired	0.270	18.0	1073	4.00	1.3	157.2	0.01482857	2650	1.29	1.5	9.81	4.680	0.000240796	101.02	170.22	33.12	151.70	11.12	51.01	567.31	571.66	(4.35)
213	Fired	0.270	18.0	1073	4.00	1.3	157.2	0.01482857	2650	1.29	1.5	9.81	4.680	0.000240796	101.02	170.22	33.12	151.70	11.12	51.01	567.31	571.66	(4.35)
214	Fired	0.270	15.5	882	4.00	1.3	157.3	0.014843329	2650	1.29	1.5	9.81	4.687	0.000240676	101.09	170.27	33.12	151.78	11.13	51.02	567.59	571.94	(4.35)
215	Fired	0.270	15.8	905	4.00	1.3	157.3	0.014843123	2650	1.29	1.5	9.81	4.687	0.000240678	101.09	170.27	33.12	151.77	11.13	51.02	567.59	571.94	(4.35)
216	Fired	0.270	15.0	843	4.00	1.3	157.2	0.014826755	2650	1.29	1.5	9.81	4.679	0.00024081	101.01	170.22	33.12	151.69	11.12	51.00	567.28	571.62	(4.35)
217	Fired	0.270	13.8	751	4.00	1.3	157.2	0.014825718	2650	1.29	1.5	9.81	4.679	0.000240819	101.00	170.22	33.12	151.69	11.12	51.00	567.26	571.60	(4.35)
218	Fired	0.270	14.0	767	4.00	1.3	157.3	0.014844544	2650	1.29	1.5	9.81	4.688	0.000240666	101.10	170.27	33.12	151.78	11.13	51.02	567.62	571.97	(4.35)

219	Fired	0.270	16.5	958	4.00	1.3	157.2	0.014827771	2650	1.29	1.5	9.81	4.680	0.000240802	101.02	170.22	33.12	151.70	11.12	51.00	567.30	571.64	(4.35)
220	Fired	0.270	18.0	1073	4.00	1.3	157.2	0.01482857	2650	1.29	1.5	9.81	4.680	0.000240796	101.02	170.22	33.12	151.70	11.12	51.01	567.31	571.66	(4.35)
221	Fired	0.270	17.0	997	4.00	1.3	157.3	0.014842394	2650	1.29	1.5	9.81	4.687	0.000240684	101.09	170.26	33.12	151.77	11.13	51.02	567.58	571.92	(4.35)
222	Fired	0.270	18.0	1073	4.00	1.3	157.2	0.01482857	2650	1.29	1.5	9.81	4.680	0.000240796	101.02	170.22	33.12	151.70	11.12	51.01	567.31	571.66	(4.35)
223	Fired	0.270	18.0	1073	4.00	1.3	157.2	0.01482857	2650	1.29	1.5	9.81	4.680	0.000240796	101.02	170.22	33.12	151.70	11.12	51.01	567.31	571.66	(4.35)
224	Fired	0.270	17.5	1035	4.00	1.3	157.2	0.014835225	2650	1.29	1.5	9.81	4.683	0.000240742	101.05	170.24	33.12	151.73	11.12	51.01	567.44	571.79	(4.35)
225	Fired	0.270	18.0	1073	4.00	1.3	157.2	0.01482857	2650	1.29	1.5	9.81	4.680	0.000240796	101.02	170.22	33.12	151.70	11.12	51.01	567.31	571.66	(4.35)
226	Fired	0.270	16.5	958	4.00	1.3	157.2	0.014827771	2650	1.29	1.5	9.81	4.680	0.000240802	101.02	170.22	33.12	151.70	11.12	51.00	567.30	571.64	(4.35)
227	Fired	0.270	16.0	907	4.00	1.3	155.6	0.014533336	2650	1.29	1.5	9.81	4.541	0.000243229	99.51	169.37	33.12	150.18	11.07	50.75	561.63	565.94	(4.30)
228	Fired	0.270	17.0	983	4.00	1.3	155.7	0.01454224	2650	1.29	1.5	9.81	4.545	0.000243155	99.55	169.40	33.12	150.23	11.07	50.76	561.81	566.11	(4.31)

229	Fired	0.270	17.0	983	4.00	1.3	155.7	0.014542244	2650	1.29	1.5	9.81	4.545	0.000243155	99.55	169.40	33.12	150.23	11.07	50.76	561.81	566.11	(4.31)
230	Fired	0.270	15.5	869	4.00	1.3	155.6	0.014528304	2650	1.29	1.5	9.81	4.539	0.000243271	99.48	169.36	33.12	150.16	11.07	50.75	561.54	565.84	(4.30)
231	Fired	0.270	18.0	1058	4.00	1.3	155.6	0.014530029	2650	1.29	1.5	9.81	4.539	0.000243257	99.49	169.36	33.12	150.17	11.07	50.75	561.57	565.87	(4.30)
232	Fired	0.270	18.0	1058	4.00	1.3	155.6	0.014530029	2650	1.29	1.5	9.81	4.539	0.000243257	99.49	169.36	33.12	150.17	11.07	50.75	561.57	565.87	(4.30)
233	Fired	0.270	16.5	945	4.00	1.3	155.7	0.014537966	2650	1.29	1.5	9.81	4.543	0.00024319	99.53	169.38	33.12	150.21	11.07	50.75	561.72	566.03	(4.30)
234	Fired	0.270	17.0	983	4.00	1.3	155.7	0.014542244	2650	1.29	1.5	9.81	4.545	0.000243155	99.55	169.40	33.12	150.23	11.07	50.76	561.81	566.11	(4.31)
235	Fired	0.270	15.5	869	4.00	1.3	155.6	0.014528304	2650	1.29	1.5	9.81	4.539	0.000243271	99.48	169.36	33.12	150.16	11.07	50.75	561.54	565.84	(4.30)
236	Fired	0.270	17.0	983	4.00	1.3	155.7	0.014542244	2650	1.29	1.5	9.81	4.545	0.000243155	99.55	169.40	33.12	150.23	11.07	50.76	561.81	566.11	(4.31)
237	Fired	0.270	17.5	1035	4.00	1.3	157.2	0.014835225	2650	1.29	1.5	9.81	4.683	0.000240742	101.05	170.24	33.12	151.73	11.12	51.01	567.44	571.79	(4.35)
238	Fired	0.270	14.0	767	4.00	1.3	157.3	0.014844544	2650	1.29	1.5	9.81	4.688	0.000240666	101.10	170.27	33.12	151.78	11.13	51.02	567.62	571.97	(4.35)

239	Abandoned	0.270	0.5	0	4.00				2650	1.29	1.5	9.81										
240	Fired	0.270	12.0	613	4.00	1.3	157.2	0.014823579	2650	1.29	1.5	9.81	4.678	0.000240836	100.99	170.21	33.12	151.67	11.12	51.00	567.22	571.56	(4.35)
301	Fired	0.270	17.0	997	4.00	1.3	157.3	0.014842394	2650	1.29	1.5	9.81	4.687	0.000240684	101.09	170.26	33.12	151.77	11.13	51.02	567.58	571.92	(4.35)
302	Fired	0.270	16.4	951	4.00	1.3	157.3	0.01484274	2650	1.29	1.5	9.81	4.687	0.000240681	101.09	170.27	33.12	151.77	11.13	51.02	567.58	571.93	(4.35)
303	Fired	0.270	14.0	767	4.00	1.3	157.3	0.014844544	2650	1.29	1.5	9.81	4.688	0.000240666	101.10	170.27	33.12	151.78	11.13	51.02	567.62	571.97	(4.35)
304	Fired	0.270	14.5	805	4.00	1.3	157.2	0.014835225	2650	1.29	1.5	9.81	4.683	0.000240742	101.05	170.24	33.12	151.73	11.12	51.01	567.44	571.79	(4.35)
305	Fired	0.270	13.5	728	4.00	1.3	157.2	0.014825417	2650	1.29	1.5	9.81	4.679	0.000240821	101.00	170.22	33.12	151.68	11.12	51.00	567.25	571.60	(4.35)
306	Fired	0.270	12.0	605	4.00	1.3	155.7	0.014544912	2650	1.29	1.5	9.81	4.546	0.000243132	99.57	169.40	33.12	150.24	11.07	50.76	561.86	566.16	(4.31)
307	Fired	0.270	15.5	882	4.00	1.3	157.3	0.014843329	2650	1.29	1.5	9.81	4.687	0.000240676	101.09	170.27	33.12	151.78	11.13	51.02	567.59	571.94	(4.35)
308	Fired	0.270	16.2	935	4.00	1.3	157.2	0.014827588	2650	1.29	1.5	9.81	4.680	0.000240804	101.01	170.22	33.12	151.70	11.12	51.00	567.29	571.64	(4.35)

601	Fired	0.270	14.5	805	4.00	1.3	157.2	0.014823653	2650	1.29	1.5	9.81	4.678	0.000240836	101.04	170.21	33.12	151.68	11.12	51.00	567.22	571.56	(4.35)
602	Fired	0.270	14.0	831	4.00	1.3	166.6	0.016653692	2650	1.29	1.5	9.81	5.570	0.000227218	110.26	175.24	33.12	160.77	11.45	52.51	601.22	605.82	(4.60)
603	Fired	0.270	15.0	843	4.00	1.3	157.1	0.014815189	2650	1.29	1.5	9.81	4.674	0.000240904	101.00	170.19	33.12	151.63	11.12	50.99	567.06	571.40	(4.35)
604	Fired	0.270	15.5	882	4.00	1.3	157.3	0.014843329	2650	1.29	1.5	9.81	4.687	0.000240676	101.09	170.27	33.12	151.78	11.13	51.02	567.59	571.94	(4.35)
605	Fired	0.270	15.0	843	4.00	1.3	157.2	0.014826755	2650	1.29	1.5	9.81	4.679	0.00024081	101.01	170.22	33.12	151.69	11.12	51.00	567.28	571.62	(4.35)
606	Fired	0.270	15.0	831	4.00	1.3	155.6	0.014522815	2650	1.29	1.5	9.81	4.536	0.000243317	99.45	169.34	33.12	150.13	11.06	50.74	561.43	565.73	(4.30)
607	Fired	0.270	15.0	833	4.00	1.3	155.8	0.014561969	2650	1.29	1.5	9.81	4.554	0.00024299	99.70	169.45	33.12	150.33	11.07	50.77	562.19	566.50	(4.31)
608	Fired	0.270	14.2	770	4.00	1.3	155.4	0.014496154	2650	1.29	1.5	9.81	4.524	0.000243541	99.36	169.26	33.12	149.99	11.06	50.72	560.92	565.21	(4.30)
609	Fired	0.270	12.0	605	4.00	1.3	155.6	0.014533566	2650	1.29	1.5	9.81	4.541	0.000243227	99.55	169.37	33.12	150.18	11.07	50.75	561.64	565.94	(4.30)
610	Fired	0.270	14.0	767	4.00	1.3	157.3	0.014844544	2650	1.29	1.5	9.81	4.688	0.000240666	101.10	170.27	33.12	151.78	11.13	51.02	567.62	571.97	(4.35)

611	Fired	0.270	9.0	383	4.00	1.3	157.1	0.014816592	2650	1.29	1.5	9.81	4.674	0.000240893	100.96	170.19	33.12	151.64	11.12	51.00	567.08	571.43	(4.35)
612	Fired	0.270	13.8	781	4.00	1.3	161.7	0.015688849	2650	1.29	1.5	9.81	5.093	0.000234101	105.38	172.64	33.12	156.04	11.28	51.73	583.54	588.01	(4.47)
613	Fired	0.270	12.7	667	4.00	1.3	157.2	0.014835225	2650	1.29	1.5	9.81	4.683	0.000240742	101.05	170.24	33.12	151.73	11.12	51.01	567.44	571.79	(4.35)
614	Fired	0.270	14.0	767	4.00	1.3	157.3	0.014844544	2650	1.29	1.5	9.81	4.688	0.000240666	101.10	170.27	33.12	151.78	11.13	51.02	567.62	571.97	(4.35)
615	Fired	0.270	14.2	782	4.00	1.3	157.2	0.014835225	2650	1.29	1.5	9.81	4.683	0.000240742	101.05	170.24	33.12	151.73	11.12	51.01	567.44	571.79	(4.35)
616	Fired	0.270	14.5	805	4.00	1.3	157.2	0.014835225	2650	1.29	1.5	9.81	4.683	0.000240742	101.05	170.24	33.12	151.73	11.12	51.01	567.44	571.79	(4.35)
617	Fired	0.270	13.8	751	4.00	1.3	157.2	0.014825718	2650	1.29	1.5	9.81	4.679	0.000240819	101.00	170.22	33.12	151.69	11.12	51.00	567.26	571.60	(4.35)
618	Fired	0.270	14.0	767	4.00	1.3	157.3	0.014844544	2650	1.29	1.5	9.81	4.688	0.000240666	101.10	170.27	33.12	151.78	11.13	51.02	567.62	571.97	(4.35)
619	Fired	0.270	13.3	713	4.00	1.3	157.2	0.014835225	2650	1.29	1.5	9.81	4.683	0.000240742	101.05	170.24	33.12	151.73	11.12	51.01	567.44	571.79	(4.35)
620	Fired	0.270	14.0	767	4.00	1.3	157.3	0.014844544	2650	1.29	1.5	9.81	4.688	0.000240666	101.10	170.27	33.12	151.78	11.13	51.02	567.62	571.97	(4.35)

621	Fired	0.270	14.0	767	4.00	1.3	157.3	0.014844544	2650	1.29	1.5	9.81	4.688	0.000240666	101.10	170.27	33.12	151.78	11.13	51.02	567.62	571.97	(4.35)
622	Fired	0.270	13.4	720	4.00	1.3	157.1	0.014815403	2650	1.29	1.5	9.81	4.674	0.000240903	100.95	170.19	33.12	151.63	11.12	50.99	567.06	571.40	(4.35)
623	Fired	0.270	13.6	736	4.00	1.3	157.2	0.014835225	2650	1.29	1.5	9.81	4.683	0.000240742	101.05	170.24	33.12	151.73	11.12	51.01	567.44	571.79	(4.35)
651	Fired	0.270	17.0	997	4.00	1.3	157.3	0.014842394	2650	1.29	1.5	9.81	4.687	0.000240684	101.09	170.26	33.12	151.77	11.13	51.02	567.58	571.92	(4.35)
652	Fired	0.270	14.0	767	4.00	1.3	157.3	0.014844544	2650	1.29	1.5	9.81	4.688	0.000240666	101.10	170.27	33.12	151.78	11.13	51.02	567.62	571.97	(4.35)
653	Fired	0.270	15.0	843	4.00	1.3	157.2	0.014826755	2650	1.29	1.5	9.81	4.679	0.00024081	101.01	170.22	33.12	151.69	11.12	51.00	567.28	571.62	(4.35)
654	Fired	0.270	13.0	690	4.00	1.3	157.2	0.014823653	2650	1.29	1.5	9.81	4.678	0.000240836	101.04	170.21	33.12	151.68	11.12	51.00	567.22	571.56	(4.35)
655	Fired	0.270	15.0	843	4.00	1.3	157.1	0.014815189	2650	1.29	1.5	9.81	4.674	0.000240904	101.00	170.19	33.12	151.63	11.12	50.99	567.06	571.40	(4.35)
656	Fired	0.270	14.0	767	4.00	1.3	157.2	0.014832964	2650	1.29	1.5	9.81	4.682	0.00024076	101.09	170.24	33.12	151.72	11.12	51.01	567.40	571.74	(4.35)
657	Fired	0.270	12.0	605	4.00	1.3	155.7	0.014544912	2650	1.29	1.5	9.81	4.546	0.000243132	99.57	169.40	33.12	150.24	11.07	50.76	561.86	566.16	(4.31)

658	Fired	0.270	14.0	756	4.00	1.3	155.7	0.014537966	2650	1.29	1.5	9.81	4.543	0.00024319	99.53	169.38	33.12	150.21	11.07	50.75	561.72	566.03	(4.30)
659	Fired	0.270	10.0	460	4.00	1.3	157.2	0.014835225	2650	1.29	1.5	9.81	4.683	0.000240742	101.05	170.24	33.12	151.73	11.12	51.01	567.44	571.79	(4.35)
660	Fired	0.270	12.0	605	4.00	1.3	155.7	0.014544912	2650	1.29	1.5	9.81	4.546	0.000243132	99.57	169.40	33.12	150.24	11.07	50.76	561.86	566.16	(4.31)
661	Fired	0.270	10.0	460	4.00	1.3	157.2	0.014835225	2650	1.29	1.5	9.81	4.683	0.000240742	101.05	170.24	33.12	151.73	11.12	51.01	567.44	571.79	(4.35)
662	Fired	0.270	13.0	751	4.00	1.3	167.2	0.016766586	2650	1.29	1.5	9.81	5.627	0.000226452	110.77	175.54	33.12	161.31	11.47	52.60	603.25	607.87	(4.62)
663	Fired	0.270	14.0	767	4.00	1.3	157.3	0.014844544	2650	1.29	1.5	9.81	4.688	0.000240666	101.10	170.27	33.12	151.78	11.13	51.02	567.62	571.97	(4.35)
664	Fired	0.270	14.5	805	4.00	1.3	157.2	0.014835225	2650	1.29	1.5	9.81	4.683	0.000240742	101.05	170.24	33.12	151.73	11.12	51.01	567.44	571.79	(4.35)
665	Fired	0.270	15.0	843	4.00	1.3	157.2	0.014826755	2650	1.29	1.5	9.81	4.679	0.00024081	101.01	170.22	33.12	151.69	11.12	51.00	567.28	571.62	(4.35)
666	Fired	0.270	14.5	805	4.00	1.3	157.2	0.014835225	2650	1.29	1.5	9.81	4.683	0.000240742	101.05	170.24	33.12	151.73	11.12	51.01	567.44	571.79	(4.35)
667	Fired	0.270	14.0	767	4.00	1.3	157.3	0.014844544	2650	1.29	1.5	9.81	4.688	0.000240666	101.10	170.27	33.12	151.78	11.13	51.02	567.62	571.97	(4.35)

668	Fired	0.270	14.5	805	4.00	1.3	157.2	0.014835225	2650	1.29	1.5	9.81	4.683	0.000240742	101.05	170.24	33.12	151.73	11.12	51.01	567.44	571.79	(4.35)
669	Fired	0.270	14.0	767	4.00	1.3	157.3	0.014844544	2650	1.29	1.5	9.81	4.688	0.000240666	101.10	170.27	33.12	151.78	11.13	51.02	567.62	571.97	(4.35)
670	Fired	0.270	13.5	743	4.00	1.3	159.5	0.015268732	2650	1.29	1.5	9.81	4.890	0.0002373	103.26	171.47	33.12	153.94	11.20	51.38	575.67	580.08	(4.41)
671	Fired	0.270	14.0	767	4.00	1.3	157.3	0.014844544	2650	1.29	1.5	9.81	4.688	0.000240666	101.10	170.27	33.12	151.78	11.13	51.02	567.62	571.97	(4.35)
672	Fired	0.270	14.0	767	4.00	1.3	157.3	0.014844544	2650	1.29	1.5	9.81	4.688	0.000240666	101.10	170.27	33.12	151.78	11.13	51.02	567.62	571.97	(4.35)
701	Fired	0.270	14.3	368	4.00	1.3	90.5	0.004919371	2650	1.29	1.5	9.81	0.894	0.000418065	44.17	129.17	33.12	87.37	8.44	38.71	326.74	329.26	(2.52)
702	Fired	0.270	16.5	532	9.50	1.3	33.7	0.00068312	2650	1.29	1.5	9.81	0.046	0.001121889	10.05	78.83	33.12	32.55	5.15	23.63	121.74	122.70	(0.95)
703	Fired	0.270	16.0	491	9.50	1.3	33.6	0.000677135	2650	1.29	1.5	9.81	0.046	0.001126836	9.98	78.66	33.12	32.41	5.14	23.58	121.21	122.16	(0.95)
704	Fired	0.270	14.5	381	9.50	1.3	33.8	0.000685718	2650	1.29	1.5	9.81	0.047	0.001119761	10.07	78.91	33.12	32.61	5.16	23.65	121.98	122.93	(0.96)
705	Fired	0.270	15.0	415	9.50	1.3	33.6	0.000676048	2650	1.29	1.5	9.81	0.046	0.001127741	9.97	78.63	33.12	32.38	5.14	23.57	121.11	122.06	(0.95)

706	Fired	0.270	12.4	567	9.50	1.3	66.8	0.002675143	2650	1.29	1.5	9.81	0.359	0.000569244	27.97	110.92	33.12	64.42	7.25	33.24	240.94	242.81	(1.87)
707	Fired	0.270	14.0	340	9.50	1.3	33.6	0.000677356	2650	1.29	1.5	9.81	0.046	0.001126652	9.98	78.67	33.12	32.41	5.14	23.58	121.23	122.18	(0.95)
708	Fired	0.270	15.5	455	9.50	1.3	33.7	0.000680957	2650	1.29	1.5	9.81	0.046	0.001123669	10.02	78.77	33.12	32.50	5.15	23.61	121.55	122.50	(0.95)
709	Fired	0.270	15.5	453	9.50	1.3	33.6	0.000676637	2650	1.29	1.5	9.81	0.046	0.001127251	9.97	78.65	33.12	32.40	5.14	23.57	121.16	122.11	(0.95)
710	Fired	0.270	17.0	568	9.50	1.3	33.7	0.00067966	2650	1.29	1.5	9.81	0.046	0.001124741	10.01	78.73	33.12	32.47	5.15	23.60	121.44	122.39	(0.95)
711	Fired	0.270	14.5	378	9.50	1.3	33.6	0.000677932	2650	1.29	1.5	9.81	0.046	0.001126173	9.99	78.68	33.12	32.43	5.14	23.58	121.28	122.23	(0.95)
712	Fired	0.270	14.5	378	9.50	1.3	33.6	0.000677932	2650	1.29	1.5	9.81	0.046	0.001126173	9.99	78.68	33.12	32.43	5.14	23.58	121.28	122.23	(0.95)
713	Fired	0.270	15.2	432	9.50	1.3	33.7	0.000680388	2650	1.29	1.5	9.81	0.046	0.001124139	10.02	78.76	33.12	32.49	5.15	23.61	121.50	122.45	(0.95)
714	Fired	0.270	14.0	342	9.50	1.3	33.7	0.00068312	2650	1.29	1.5	9.81	0.046	0.001121889	10.05	78.83	33.12	32.55	5.15	23.63	121.74	122.70	(0.95)
715	Fired	0.270	16.0	495	9.50	1.3	33.8	0.000685119	2650	1.29	1.5	9.81	0.046	0.001120251	10.07	78.89	33.12	32.60	5.16	23.65	121.92	122.88	(0.95)

716	Fired	0.270	15.0	415	9.50	1.3	33.6	0.000676048	2650	1.29	1.5	9.81	0.046	0.001127741	9.97	78.63	33.12	32.38	5.14	23.57	121.11	122.06	(0.95)
717	Fired	0.270	14.0	345	9.50	1.3	34.0	0.000692511	2650	1.29	1.5	9.81	0.047	0.001114256	10.14	79.10	33.12	32.78	5.17	23.71	122.58	123.54	(0.96)
718	Fired	0.270	15.3	421	9.50	1.3	32.7	0.000639901	2650	1.29	1.5	9.81	0.042	0.001159156	9.56	77.56	33.12	31.51	5.07	23.25	117.83	118.75	(0.92)
719	Fired	0.270	14.0	345	9.50	1.3	34.0	0.000692511	2650	1.29	1.5	9.81	0.047	0.001114256	10.14	79.10	33.12	32.78	5.17	23.71	122.58	123.54	(0.96)
720	Abandoned	0.270	0.5	0	9.50				2650	1.29	1.5	9.81											
721	Fired	0.270	15.0	421	4.00	1.3	95.2	0.005437677	2650	1.29	1.5	9.81	1.039	0.000397641	47.60	132.45	33.12	91.86	8.65	39.69	343.52	346.17	(2.65)
722	Fired	0.270	13.5	302	4.00	1.3	83.2	0.004155522	2650	1.29	1.5	9.81	0.694	0.000454868	38.92	123.83	33.12	80.30	8.09	37.11	300.30	302.62	(2.32)
723	Fired	0.270	15.5	453	9.50	1.3	33.6	0.000676637	2650	1.29	1.5	9.81	0.046	0.001127251	9.97	78.65	33.12	32.40	5.14	23.57	121.16	122.11	(0.95)
724	Fired	0.270	13.0	264	9.50	1.3	33.6	0.000675712	2650	1.29	1.5	9.81	0.046	0.001128022	9.96	78.62	33.12	32.38	5.14	23.56	121.08	122.03	(0.95)
725	Fired	0.270	15.0	415	9.50	1.3	33.6	0.000676048	2650	1.29	1.5	9.81	0.046	0.001127741	9.97	78.63	33.12	32.38	5.14	23.57	121.11	122.06	(0.95)

726	Fired	0.270	14.0	340	9.50	1.3	33.6	0.000677356	2650	1.29	1.5	9.81	0.046	0.001126652	9.98	78.67	33.12	32.41	5.14	23.58	121.23	122.18	(0.95)
751	Fired	0.270	15.0	831	9.50	1.3	55.5	0.00184532	2650	1.29	1.5	9.81	0.205	0.000682594	21.16	101.08	33.12	53.51	6.61	30.29	200.11	201.66	(1.56)
752	Fired	0.270	15.5	869	9.50	1.3	53.8	0.001735935	2650	1.29	1.5	9.81	0.187	0.000703771	20.21	99.55	33.12	51.90	6.51	29.83	194.08	195.59	(1.51)
753	Fired	0.270	17.0	983	9.50	1.3	50.0	0.001502689	2650	1.29	1.5	9.81	0.151	0.000756421	18.14	96.02	33.12	48.28	6.27	28.78	180.57	181.98	(1.41)
754	Fired	0.270	17.0	983	4.00	1.3	155.7	0.01454224	2650	1.29	1.5	9.81	4.545	0.000243155	99.55	169.40	33.12	150.23	11.07	50.76	561.81	566.11	(4.31)
755	Fired	0.270	17.0	983	4.00	1.3	155.7	0.01454224	2650	1.29	1.5	9.81	4.545	0.000243155	99.55	169.40	33.12	150.23	11.07	50.76	561.81	566.11	(4.31)
756	Fired	0.270	16.0	907	4.00	1.3	155.6	0.014533336	2650	1.29	1.5	9.81	4.541	0.000243229	99.51	169.37	33.12	150.18	11.07	50.75	561.63	565.94	(4.30)
756R	Abandoned								2650	1.29	1.5	9.81											
757	Fired	0.270	15.0	821	4.00	1.3	154.2	0.014259885	2650	1.29	1.5	9.81	4.413	0.00024555	98.14	168.57	33.12	148.76	11.01	50.51	556.33	560.59	(4.26)
758	Fired	0.270	16.0	908	4.00	1.3	155.7	0.014545135	2650	1.29	1.5	9.81	4.546	0.000243131	99.61	169.41	33.12	150.24	11.07	50.76	561.86	566.17	(4.31)

759	Fired	0.270	15.5	874	4.00	1.3	156.2	0.014637794	2650	1.29	1.5	9.81	4.590	0.00024236	100.09	169.67	33.12	150.72	11.09	50.84	563.65	567.97	(4.32)
760	Fired	0.270	15.5	872	4.00	1.3	155.9	0.014589428	2650	1.29	1.5	9.81	4.567	0.000242761	99.84	169.53	33.12	150.47	11.08	50.80	562.72	567.03	(4.31)
761	Fired	0.270	15.0	833	4.00	1.3	155.8	0.014561969	2650	1.29	1.5	9.81	4.554	0.00024299	99.70	169.45	33.12	150.33	11.07	50.77	562.19	566.50	(4.31)
762	Fired	0.270	14.5	795	4.00	1.3	155.8	0.014558361	2650	1.29	1.5	9.81	4.553	0.00024302	99.68	169.44	33.12	150.31	11.07	50.77	562.12	566.43	(4.31)
763	Fired	0.270	15.6	846	4.00	1.3	151.6	0.01379159	2650	1.29	1.5	9.81	4.198	0.000249684	95.72	167.17	33.12	146.30	10.92	50.09	547.11	551.31	(4.19)
801	Fired	0.270	16.0	906	4.00	1.3	155.5	0.014498874	2650	1.29	1.5	9.81	4.525	0.000243518	99.38	169.27	33.12	150.00	11.06	50.72	560.97	565.27	(4.30)
802	Fired	0.270	15.8	891	4.00	1.3	155.5	0.014501225	2650	1.29	1.5	9.81	4.526	0.000243498	99.39	169.28	33.12	150.02	11.06	50.72	561.01	565.31	(4.30)
803	Fired	0.270	16.2	921	4.00	1.3	155.4	0.0144966	2650	1.29	1.5	9.81	4.524	0.000243537	99.36	169.26	33.12	149.99	11.06	50.72	560.92	565.22	(4.30)
804	Fired	0.270	15.5	868	4.00	1.3	155.4	0.014492843	2650	1.29	1.5	9.81	4.522	0.000243569	99.35	169.25	33.12	149.97	11.06	50.71	560.85	565.15	(4.30)
805	Fired	0.270	16.0	906	4.00	1.3	155.5	0.014498874	2650	1.29	1.5	9.81	4.525	0.000243518	99.38	169.27	33.12	150.00	11.06	50.72	560.97	565.27	(4.30)

806	Fired	0.270	16.0	906	4.00	1.3	155.5	0.014498874	2650	1.29	1.5	9.81	4.525	0.000243518	99.38	169.27	33.12	150.00	11.06	50.72	560.97	565.27	(4.30)
807	Fired	0.270	16.0	906	4.00	1.3	155.5	0.014498874	2650	1.29	1.5	9.81	4.525	0.000243518	99.38	169.27	33.12	150.00	11.06	50.72	560.97	565.27	(4.30)
808	Fired	0.270	14.6	800	4.00	1.3	155.4	0.014491023	2650	1.29	1.5	9.81	4.521	0.000243584	99.34	169.25	33.12	149.96	11.06	50.71	560.82	565.11	(4.30)
809	Fired	0.270	14.6	800	4.00	1.3	155.4	0.014491023	2650	1.29	1.5	9.81	4.521	0.000243584	99.34	169.25	33.12	149.96	11.06	50.71	560.82	565.11	(4.30)
810	Fired	0.270	16.0	906	4.00	1.3	155.5	0.014498874	2650	1.29	1.5	9.81	4.525	0.000243518	99.38	169.27	33.12	150.00	11.06	50.72	560.97	565.27	(4.30)
811	Fired	0.270	15.8	891	4.00	1.3	155.5	0.014501225	2650	1.29	1.5	9.81	4.526	0.000243498	99.39	169.28	33.12	150.02	11.06	50.72	561.01	565.31	(4.30)
812	Fired	0.270	16.0	906	4.00	1.3	155.5	0.014498874	2650	1.29	1.5	9.81	4.525	0.000243518	99.38	169.27	33.12	150.00	11.06	50.72	560.97	565.27	(4.30)
813	Fired	0.270	15.6	876	4.00	1.3	155.5	0.014503658	2650	1.29	1.5	9.81	4.527	0.000243478	99.40	169.28	33.12	150.03	11.06	50.72	561.06	565.36	(4.30)
851	Fired	0.165	18.0	229	4.00	1.3	32.5	0.000634126	2650	1.29	1.5	9.81	0.041	0.001164422	15.54	77.41	33.12	31.37	5.06	23.19	117.31	118.23	(0.92)
852	Fired	0.165	15.5	155	4.00	1.3	28.3	0.000479421	2650	1.29	1.5	9.81	0.027	0.001339182	12.60	72.18	33.12	27.28	4.72	21.63	102.00	102.81	(0.80)

853	Fired	0.165	15.0	142	4.00	1.3	27.4	0.00045045	2650	1.29	1.5	9.81	0.025	0.001381576	12.03	71.06	33.12	26.44	4.64	21.29	98.87	99.65	(0.78)
854	Fired	0.165	17.0	200	10.00	1.3	8.4	4.27736E-05	2650	1.29	1.5	9.81	0.001	0.004483428	2.06	39.44	33.12	8.15	2.58	11.82	30.46	30.71	(0.24)
855	Fired	0.165	18.0	228	10.00	1.3	8.4	4.26192E-05	2650	1.29	1.5	9.81	0.001	0.004491542	2.05	39.40	33.12	8.13	2.58	11.81	30.41	30.65	(0.24)
856	Fired	0.165	17.5	212	10.00	1.3	8.4	4.21161E-05	2650	1.29	1.5	9.81	0.001	0.004518293	2.03	39.28	33.12	8.08	2.57	11.77	30.23	30.47	(0.24)
857	Fired	0.165	17.6	216	10.00	1.3	8.4	4.24488E-05	2650	1.29	1.5	9.81	0.001	0.004500551	2.05	39.36	33.12	8.11	2.57	11.80	30.35	30.59	(0.24)
858	Fired	0.165	17.8	222	10.00	1.3	8.4	4.25362E-05	2650	1.29	1.5	9.81	0.001	0.004495926	2.05	39.38	33.12	8.12	2.57	11.80	30.38	30.62	(0.24)
859	Fired	0.165	18.0	226	10.00	1.3	8.4	4.20802E-05	2650	1.29	1.5	9.81	0.001	0.004520218	2.03	39.27	33.12	8.08	2.57	11.77	30.22	30.46	(0.24)
860	Fired	0.165	18.0	227	10.00	1.3	8.4	4.23495E-05	2650	1.29	1.5	9.81	0.001	0.004505826	2.04	39.34	33.12	8.11	2.57	11.79	30.31	30.55	(0.24)
861	Fired	0.165	16.0	169	10.00	1.3	8.4	4.1901E-05	2650	1.29	1.5	9.81	0.001	0.004529874	2.03	39.23	33.12	8.06	2.56	11.76	30.15	30.39	(0.24)
862	Fired	0.165	18.0	227	10.00	1.3	8.4	4.23495E-05	2650	1.29	1.5	9.81	0.001	0.004505826	2.04	39.34	33.12	8.11	2.57	11.79	30.31	30.55	(0.24)

863	Fired	0.165	17.0	199	10.00	1.3	8.4	4.2465E-05	2650	1.29	1.5	9.81	0.001	0.004499691	2.05	39.36	33.12	8.12	2.57	11.80	30.35	30.60	(0.24)
864	Fired	0.165	17.6	217	10.00	1.3	8.4	4.2733E-05	2650	1.29	1.5	9.81	0.001	0.00448556	2.06	39.43	33.12	8.14	2.58	11.82	30.45	30.69	(0.24)
865	Fired	0.165	18.0	226	10.00	1.3	8.4	4.20802E-05	2650	1.29	1.5	9.81	0.001	0.004520218	2.03	39.27	33.12	8.08	2.57	11.77	30.22	30.46	(0.24)
866	Fired	0.165	18.0	228	10.00	1.3	8.4	4.26192E-05	2650	1.29	1.5	9.81	0.001	0.004491542	2.05	39.40	33.12	8.13	2.58	11.81	30.41	30.65	(0.24)
867	Fired	0.165	18.0	227	10.00	1.3	8.4	4.23495E-05	2650	1.29	1.5	9.81	0.001	0.004505826	2.04	39.34	33.12	8.11	2.57	11.79	30.31	30.55	(0.24)
868	Abandoned	0.165	0.5	0	10.00				2650	1.29	1.5	9.81											
869	Fired	0.165	14.0	113	10.00	1.3	8.4	4.20802E-05	2650	1.29	1.5	9.81	0.001	0.004520218	2.03	39.27	33.12	8.08	2.57	11.77	30.22	30.46	(0.24)
870	Fired	0.165	17.4	211	10.00	1.3	8.4	4.26484E-05	2650	1.29	1.5	9.81	0.001	0.004490004	2.05	39.41	33.12	8.13	2.58	11.81	30.42	30.66	(0.24)
871	Fired	0.165	18.0	226	10.00	1.3	8.4	4.20802E-05	2650	1.29	1.5	9.81	0.001	0.004520218	2.03	39.27	33.12	8.08	2.57	11.77	30.22	30.46	(0.24)
872	Fired	0.165	18.0	186	10.00	1.3	7.3	3.17589E-05	2650	1.29	1.5	9.81	0.000	0.005203141	1.65	36.61	33.12	7.02	2.39	10.97	26.25	26.46	(0.21)

873	Fired	0.165	16.5	186	10.00	1.3	8.5	4.28687E-05	2650	1.29	1.5	9.81	0.001	0.004478453	2.06	39.46	33.12	8.15	2.58	11.83	30.50	30.74	(0.24)
874	Fired	0.165	5.0	143	10.00	1.3	41.7	0.001042522	2650	1.29	1.5	9.81	0.087	0.000908146	22.57	87.65	33.12	40.22	5.73	26.26	150.42	151.60	(1.18)
875	Fired	0.165	17.0	200	10.00	1.3	8.4	4.27736E-05	2650	1.29	1.5	9.81	0.001	0.004483428	2.06	39.44	33.12	8.15	2.58	11.82	30.46	30.71	(0.24)
876	Fired	0.165	17.0	200	10.00	1.3	8.4	4.27736E-05	2650	1.29	1.5	9.81	0.001	0.004483428	2.06	39.44	33.12	8.15	2.58	11.82	30.46	30.71	(0.24)
877	Fired	0.165	17.0	200	10.00	1.3	8.4	4.27736E-05	2650	1.29	1.5	9.81	0.001	0.004483428	2.06	39.44	33.12	8.15	2.58	11.82	30.46	30.71	(0.24)
879	Abandoned	0.165	0.5	0	10.00				2650	1.29	1.5	9.81											
880	Fired	0.165	16.5	183	10.00	1.3	8.4	4.18734E-05	2650	1.29	1.5	9.81	0.001	0.004531364	2.02	39.23	33.12	8.06	2.56	11.76	30.14	30.38	(0.24)
881	Fired	0.165	16.0	169	10.00	1.3	8.4	4.1901E-05	2650	1.29	1.5	9.81	0.001	0.004529874	2.03	39.23	33.12	8.06	2.56	11.76	30.15	30.39	(0.24)
882	Fired	0.165	16.3	178	10.00	1.3	8.4	4.20887E-05	2650	1.29	1.5	9.81	0.001	0.00451976	2.03	39.28	33.12	8.08	2.57	11.77	30.22	30.46	(0.24)
883	Fired	0.165	13.7	104	10.00	1.3	8.3	4.17752E-05	2650	1.29	1.5	9.81	0.001	0.004536689	2.02	39.20	33.12	8.05	2.56	11.75	30.11	30.35	(0.24)

884	Fired	0.165	13.7	104.43196	10.00	1.3	8.4	4.20261E-05	2650	1.29	1.5	9.81	0.001	0.004523127	2.03	39.26	33.12	8.07	2.57	11.77	30.20	30.44	(0.24)
885	Fired	0.165	15.3	150	10.00	1.3	8.4	4.21919E-05	2650	1.29	1.5	9.81	0.001	0.004514231	2.04	39.30	33.12	8.09	2.57	11.78	30.26	30.50	(0.24)
886	Fired	0.165	16.0	169	10.00	1.3	8.4	4.1901E-05	2650	1.29	1.5	9.81	0.001	0.004529874	2.03	39.23	33.12	8.06	2.56	11.76	30.15	30.39	(0.24)
887	Fired	0.165	16.3	178	10.00	1.3	8.4	4.20887E-05	2650	1.29	1.5	9.81	0.001	0.00451976	2.03	39.28	33.12	8.08	2.57	11.77	30.22	30.46	(0.24)
901	Fired	0.165	16.4	384	10.00	1.3	14.4	0.000124933	2650	1.29	1.5	9.81	0.004	0.002623376	4.60	51.56	33.12	13.92	3.37	15.45	52.07	52.48	(0.41)
902	Fired	0.165	7.0	113	10.00	1.3	26.8	0.000431292	2650	1.29	1.5	9.81	0.023	0.001411929	11.64	70.29	33.12	25.87	4.59	21.06	96.75	97.51	(0.76)
903	Fired	0.165	8.0	143	10.00	1.3	28.1	0.000473057	2650	1.29	1.5	9.81	0.027	0.00134816	12.48	71.94	33.12	27.09	4.70	21.56	101.32	102.12	(0.80)
904	Fired	0.165	7.0	85	10.00	1.3	21.8	0.000285841	2650	1.29	1.5	9.81	0.013	0.001734348	8.55	63.42	33.12	21.06	4.14	19.00	78.76	79.38	(0.62)
905	Fired	0.165	7.0	113	3.00	1.3	79.8	0.003820883	2650	1.29	1.5	9.81	0.612	0.000474369	59.79	121.30	33.12	77.01	7.92	36.34	288.00	290.23	(2.23)
906	Fired	0.165	6.0	85	3.00	1.3	80.0	0.003837176	2650	1.29	1.5	9.81	0.616	0.000473361	59.98	121.43	33.12	77.18	7.93	36.38	288.61	290.85	(2.24)

907	Fired	0.165	6.0	86	3.00	1.3	80.6	0.003902564	2650	1.29	1.5	9.81	0.632	0.000469379	60.75	121.94	33.12	77.83	7.97	36.53	291.06	293.31	(2.26)
908	Fired	0.165	6.0	86	3.00	1.3	80.6	0.003902564	2650	1.29	1.5	9.81	0.632	0.000469379	60.75	121.94	33.12	77.83	7.97	36.53	291.06	293.31	(2.26)
909	Fired	0.165	4.5	45	3.00	1.3	81.2	0.003956836	2650	1.29	1.5	9.81	0.645	0.000466149	61.38	122.37	33.12	78.37	7.99	36.66	293.08	295.35	(2.27)
910	Fired	0.165	6.0	230	3.00	1.3	164.1	0.016164194	2650	1.29	1.5	9.81	5.326	0.000230633	176.41	173.99	33.12	158.42	11.37	52.12	592.40	596.95	(4.54)
911	Fired	0.165	6.0	86	3.00	1.3	80.6	0.003902564	2650	1.29	1.5	9.81	0.632	0.000469379	60.75	121.94	33.12	77.83	7.97	36.53	291.06	293.31	(2.26)
951	Fired	0.165	17.0	395	3.00	1.3	79.7	0.003813906	2650	1.29	1.5	9.81	0.610	0.000474803	59.71	121.24	33.12	76.94	7.92	36.32	287.73	289.96	(2.23)
952	Fired	0.165	16.5	387	3.00	1.3	80.6	0.003902564	2650	1.29	1.5	9.81	0.632	0.000469379	60.75	121.94	33.12	77.83	7.97	36.53	291.06	293.31	(2.26)
953	Fired	0.165	15.5	358	3.00	1.3	80.6	0.00389732	2650	1.29	1.5	9.81	0.631	0.000469694	60.69	121.90	33.12	77.78	7.96	36.52	290.86	293.12	(2.25)
954	Fired	0.165	16.0	373	3.00	1.3	80.7	0.003907608	2650	1.29	1.5	9.81	0.633	0.000469076	60.81	121.98	33.12	77.88	7.97	36.55	291.25	293.50	(2.26)
955	Fired	0.165	15.0	339	3.00	1.3	79.8	0.003820883	2650	1.29	1.5	9.81	0.612	0.000474369	59.79	121.30	33.12	77.01	7.92	36.34	288.00	290.23	(2.23)

956	Abandoned	0.165	0.5	0	3.00																		

APPENDIX C. Flyrock Calculator

As part of the study to verify the predictive model in BlastLogic, as well as having a tool to use in trajectory estimations for use in the video analysis, a Microsoft Excel™ based flyrock calculator was created. Figure 68 is a snapshot highlighting the components of the flyrock calculator created in this study.

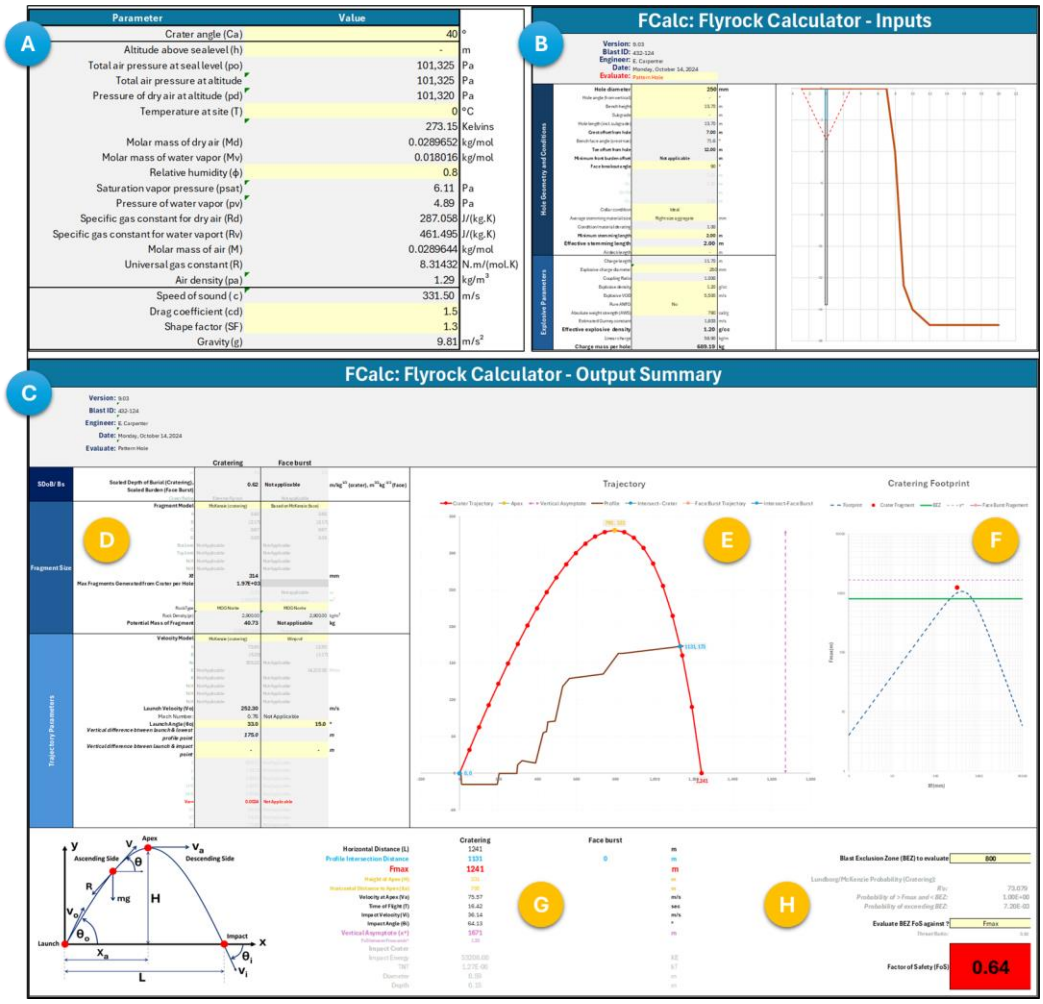

Figure 68: Snapshot of the input and output sheets of the flyrock calculator

The components labelled in Figure 68 are:

A. The model settings input area.
B. Hole detail input screen where the geometry of the blast hole, as well as the explosive information is entered.
C. The main output screen components covered in D to H.
D. Information on the confinement, fragment size and trajectory parameters.

E. Graphic with the trajectory and surface profile.
F. Applicable flyrock footprint.
G. Trajectory calculation output; and
H. Clearance criteria evaluation covering risk probability and effective factor of safety.

APPENDIX D. Flyrock Risk Reporting Dashboard

Figure 69 is a snapshot of the initial flyrock risk dashboard created in Microsoft's Excel™. This initial dashboard was created to establish the concept and currently this is being converted into a Microsoft PowerBI™ dashboard by the company's mining applications team.

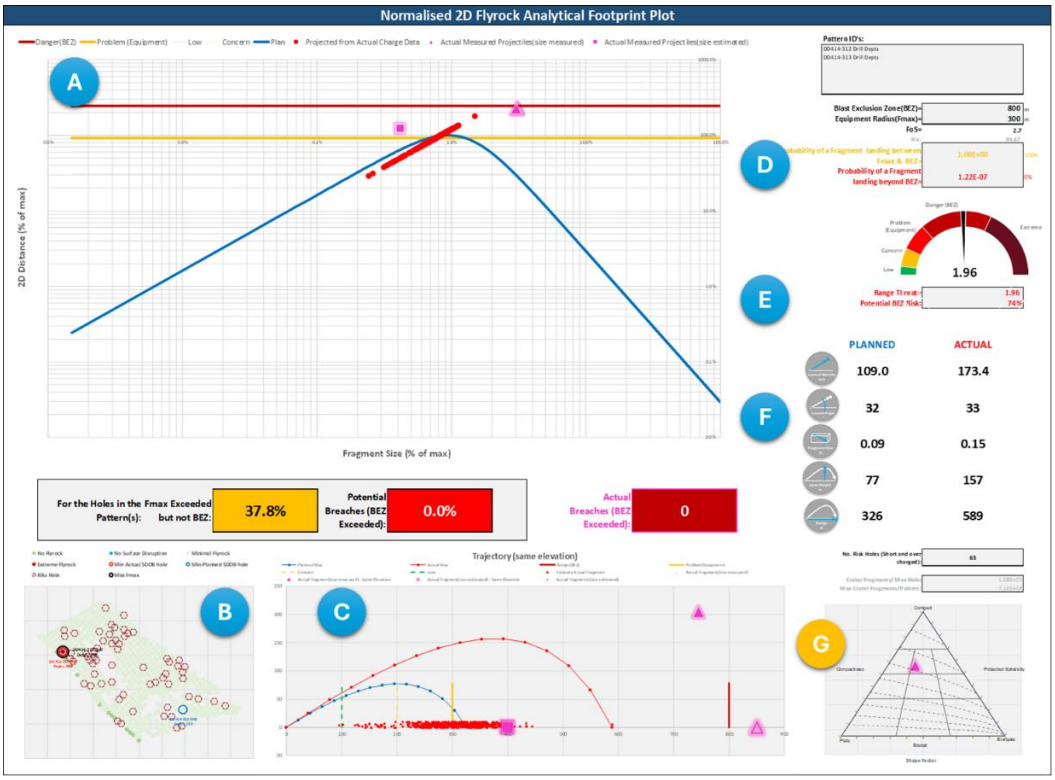

Figure 69: Example of flyrock risk reporting dashboard

The components labelled in Figure 69 are:

A. The normalised flyrock footprint depicting the estimated flyrock footprint line (distance vs fragment size) from the designed data as well as the estimated actual points based on the actual data from BlastLogic. If actual flyrock was measured in the field or on the video analysis it is also plotted on this footprint.

B. SDOB plot highlighting the holes according to the SDOB categories. It also displays the potential source holes and risk holes.

C. This is a 2D side view showing the trajectory of the planning and estimated actual maximum range. Each hole's range is also plotted as a red dot on the x- axis. The Fmax and BEZ set for the blast are also indicated. If actual

flyrock was measured in field or with video analysis it is plotted on this view as well (solid purple triangle is the position given the range and vertical difference between the launch point and the impact position measured, while the hollow purple triangle is the projection onto the same elevation as the launch point). Figure 70 is another view available for the trajectory plot.

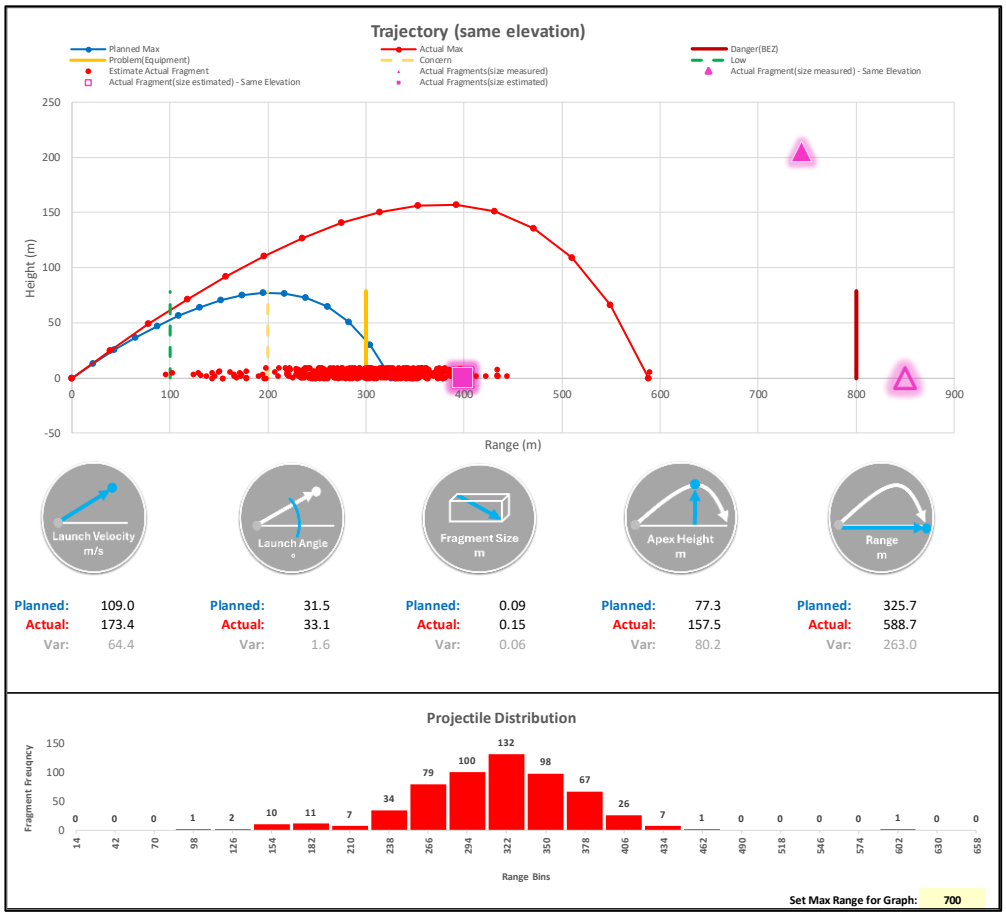

Figure 70: Alternative view of the trajectory plot

D. Probability statistics based on the work by McKenzie (2022).
E. Risk rating based on the work by Raina, et al. (2011).
F. Full numerical output of the trajectory calculations for both the planned and estimated actual data; and
G. Implementation of a Sneed and Folk diagram for representing actual measured fragment shape on a diagram (Graham & Midgley, 2000).